ALS Linked Mutations in Matrin 3 Alter Protein-Protein Interactions and Impede mRNA Nuclear Export

by

Ashley Boehringer

A Dissertation Presented in Partial Fulfillment
of the Requirements for the Degree
Doctor of Philosophy

Approved February 2018 by the
Graduate Supervisory Committee:

Robert Bowser, Co-Chair
Julie Liss, Co-Chair
Kendall Jensen
Shafeeq Ladha

ARIZONA STATE UNIVERSITY

May 2018

ABSTRACT

Exome sequencing was used to identify novel variants linked to amyotrophic lateral sclerosis (ALS), in a family without mutations in genes previously linked to ALS. A F115C mutation in the gene MATR3 was identified, and further examination of other ALS kindreds identified an additional three mutations in MATR3; S85C, P154S and T622A. Matrin 3 is an RNA/DNA binding protein as well as part of the nuclear matrix. Matrin 3 interacts with TDP-43, a protein that is both mutated in some forms of ALS, and found in pathological inclusions in most ALS patients. Matrin 3 pathology, including mislocalization and rare cytoplasmic inclusions, was identified in spinal cord tissue from a patient carrying a mutation in Matrin 3, as well as sporadic ALS patients. In an effort to determine the mechanism of Matrin 3 linked ALS, the protein interactome of wild-type and ALS-linked MATR3 mutations was examined. Immunoprecipitation followed by mass spectrometry experiments were performed using NSC-34 cells expressing human wild-type or mutant Matrin 3. Gene ontology analysis identified a novel role for Matrin 3 in mRNA transport centered on proteins in the TRanscription and EXport (TREX) complex, known to function in mRNA biogenesis and nuclear export. ALS-linked mutations in Matrin 3 led to its re-distribution within the nucleus, decreased co-localization with endogenous Matrin 3 and increased co-localization with specific TREX components. Expression of disease-causing Matrin 3 mutations led to nuclear mRNA export defects of both global mRNA and more specifically the mRNA of TDP-43 and FUS. Our findings identify ALS-causing mutations in the gene MATR3, as well as a potential pathogenic mechanism attributable to MATR3 mutations and further link cellular transport defects to ALS.

TABLE OF CONTENTS

Page

CHAPTER Page

CHAPTER Page

LIST OF TABLES

LIST OF FIGURES

Figure Page

CHAPTER 1

INTRODUCTION

1.1 INTRODUCTION TO ALS

Amyotrophic lateral sclerosis (ALS) is a fatal neurodegenerative disorder first described by Charcot in 1874 (Charcot 1874). ALS is characterized by the loss of upper motor neurons, located in the cortex and projecting to the brainstem and spinal cord, and lower motor neurons which are found in the brainstem and spinal cord and project to muscles. This loss of motor neurons leads to progressive paralysis characterized by spasticity and muscle stiffness due to the loss of upper motor neurons, as well as fasciculations and muscle atrophy due to the loss of lower motor neurons (Brown and Al-Chalabi 2017). In Europe and the United States, the incidence of ALS is approximately 2 per 100,000 individuals with a prevalence of 5 per 100,000 people (Chio, Logroscino et al. 2013). The mean age of symptom onset is 62 years and the mean age of diagnosis is 64 years. In approximately two thirds of ALS cases symptom onset is in the limbs, with approximately one third of patients presenting with bulbar symptoms first (Brown and Al-Chalabi 2017).

The diagnosis of ALS is made clinically, often with the aid of electromyography (EMG) along with investigations to exclude ALS mimics (Lenglet and Camdessanché 2017). Most studies report a diagnostic delay of approximately 1 year, suggesting that there is still a significant delay between symptom onset and a diagnosis of ALS (Chio, Logroscino et al. 2013). After diagnosis, the average survival of patients is approximately 3-5 years with most patients succumbing to respiratory failure. Survival is very heterogenous however, with approximately 5-10% of patients surviving 10 years or

longer (Chio, Logroscino et al. 2009). In addition to motor symptoms, approximately 13% of patients are also diagnosed with behavioral variant FTD (frontotemporal dementia), and as many as 50% of ALS patients exhibit some degree of cognitive or behavioral abnormalities (Lomen-Hoerth, Murphy et al. 2003).

Currently there are two FDA approved drugs to treat ALS: Riluzole and Edaravone. Riluzole was approved in 1995 after clinical trials suggested that treatment extended survival and slowed deterioration of muscle strength (Bensimon, Lacomblez et al. 1994). Since its initial approval, studies suggest that Riluzole can extend survival by only three months on average (Traynor, Alexander et al. 2003, Miller, Mitchell et al. 2012). Edaravone was approved in May 2017 after clinical trials performed in Japan suggested that it could slow the decline of ALSFRS-R scores in a subset of patients that were early in the disease process with a fast disease progression (Writing and Edaravone 2017).

Approximately 5-10% of ALS cases are considered familial, which while well not formally defined, is generally considered patients who have at least one first or second degree relative with ALS or FTD (Boylan 2015). Mutations in over 30 genes have been implicated in ALS to date, beginning with the discovery of mutations in SOD1 in 1993 (Rosen, Siddique et al. 1993, Renton, Chio et al. 2014). Proteins implicated in ALS tend to fall into three categories; RNA binding proteins and proteins involved in RNA processing, proteins involved in cytoskeletal dynamics and proteins involved in proteostasis. The most common genetic cause of ALS is a hexanucleotide repeat expansion in the chromosome 9 open reading frame 72 (C9orf72) which does not appear to fall into these common categories (DeJesus-Hernandez, Mackenzie et al. 2011,

Renton, Majounie et al. 2011). Overall, in 2014 it was estimated that the genetic etiology of approximately two thirds of familial and 11% of sporadic ALS was known (Renton, Chio et al. 2014).

While the genetic causes of ALS are diverse there are some pathologies connecting them. The most common pathology in the neurons of ALS patients is the mislocalization and/or aggregation of proteins. The most commonly aggregated protein is TDP-43 (TAR DNA Binding Protein 43) which is mutated in approximately 4% of familial ALS cases and 1% of sporadic ALS cases, and yet is mislocalized from the nucleus, where it is normally found, to the cytoplasm and aggregated in an estimated 97% of ALS patients (Neumann, Sampathu et al. 2006, Kabashi, Valdmanis et al. 2008, Sreedharan, Blair et al. 2008, Ling, Polymenidou et al. 2013). Patients carrying mutations in SOD1 or FUS generally do not have TDP-43 pathology and instead present with aggregates containing SOD1 and FUS respectively (Bruijn, Houseweart et al. 1997, Hewitt, Kirby et al. 2010). Patients carrying the C9orf72 repeat expansion generally have both TDP-43 pathology as well as pathology unique to C9orf72 including both RNA foci created from the repeat in the nucleus as well as peptides created from an alternative form of translation. These DPR (Di-Peptide Repeat) products are created from RAN (Repeat Associated Non-ATG) translation and can be made in any reading frame in both the sense and antisense direction (Mackenzie, Frick et al. 2014).

1.2 LITERATURE REVIEW OF MATRIN 3

1.2.1 Cellular Roles of Matrin 3

Mutations in Matrin 3 were linked to ALS in 2014 after the discovery of Matrin 3 mutations in four families with ALS. Matrin 3 is an RNA binding protein and like many

proteins involved in ALS has roles in RNA processing and biogenesis. Matrin 3 was first identified in 1991 as an "acidic internal matrix protein." Matrin 3 is a part of the nuclear matrix which is defined as the "salt-resistant proteinaceous nuclear structure that is isolated from the interphase cell," and thought to have roles in RNA processing, chromatin organization and DNA replication (Belgrader, Dey et al. 1991).

After the initial identification of Matrin 3, another group cloned a protein they termed P130, which was later determined to be Matrin 3. They discovered that Matrin 3 binds to repetitive DNA sequences as well as matrix attachment regions (MARs), which are defined as genomic DNA sequences at the boundaries of chromatin loops. MARs are thought to function in chromatin folding and unfolding and transcriptional regulation via an ATATAT sequence (Hibino 2000). It was also shown that the association of Matrin 3 with chromosomes requires the presence of both of its zinc-finger domains (Hibino, Usui et al. 2006).

When dsRNA (double-stranded RNA) is found in the nucleus, especially when the double stranded portion is longer than 15 base pairs, it is often edited by the ADAR (Adenosine Deaminase Acting on RNA) family of proteins (Nishikura 1992). This editing takes the form of the hydrolytic deamination of adenosine to inosine (A-to-I). Inosine base pairs with cytosine which results in it being read as a guanine by the cell's translational machinery. Selective A-to-I editing is required for the proper function of some transcripts, most notably glutamate receptor subunits and subtypes of the serotonin receptor, but extensive editing, often referred to as promiscuous editing, can be detrimental (Higuchi, Single et al. 1993, Burns, Chu et al. 1997). After the discovery that extensively edited RNAs are retained within the nucleus (Kumar and Carmichael 1997),

the authors sought to identify proteins that preferentially bound inosine containing RNA. The protein $p54^{nrb}$ (NonO) was identified as preferentially binding to inosine containing RNA and it was found that this binding occurred as a complex along with the proteins PSF (SPPQ, the protein originally named Matrin 4 was later positively identified as PSF) and Matrin 3 which were found in a 1:1:1 ratio. Matrin 3 does not appear to bind directly to inosine containing RNA, and the authors speculate both that Matrin 3 interacts with this complex via protein-protein interactions with PSF and $p54^{nrb}$, and that Matrin 3 may confer the cooperative binding properties of the complex (Zhang and Carmichael 2001).

Matrin 3 was identified as the predominant protein phosphorylated by the kinase PKA after the addition of N-methyl-D-aspartate (NMDA) to cultures of rat cerebellar neurons. It was further shown that Matrin 3 is both phosphorylated and degraded after treatment with NMDA. Using a model of NMDA receptor activation in which rats are injected intraperitoneally with ammonium acetate, Matrin 3 was shown to be phosphorylated and degraded *in vivo* as well. PKA inhibition prevented the phosphorylation and degradation of Matrin 3, as well as rescued cell death (Giordano, Sanchez-Perez et al. 2005).

The location of Matrin 3 within the nucleus, as compared to other nuclear factors such as RNA polymerase II (Pol II), euchromatin and heterochromatin (as defined by the intensity of DAPI staining), SAF-A (hnRNPU), TS (nascent transcript sites) and PCNA (active DNA replication sites) was studied by immunofluorescence. Matrin 3 was found in a punctate staining pattern with most puncta approximately 0.2-0.4μm in diameter throughout the extranucleolar space and was suggested to form a network-like structure. Matrin 3 was highly co-localized with SAF-A, as well as Pol II and PCNA

(Malyavantham, Bhattacharya et al. 2008). In a later study Matrin 3 was found in both gene poor and gene rich chromosomal regions, though it appeared to be excluded from heterochromatin as well as the Barr body (Zeitz, Malyavantham et al. 2009).

As part of cells' normal response to double stranded DNA breaks the kinase ATM is activated. Matrin 3 was identified as a potential target of ATM (at amino acid 208) and its role in response to DNA damage was further supported by the identification of two of its binding partners PSF (SFPQ) and p54 (NONO) as binding DNA end-rejoining proteins. Matrin 3 was further shown to immunoprecipitate the Ku heterodimer Ku70/Ku80 which is an integral part of the non-homologous end rejoining (NHEJ) DNA repair process. When the recruitment of these proteins to sites of DNA damage was investigated it was shown that while both PSF and p54 are recruited to sites of DNA damage, Matrin 3 was not, and knockdown of Matrin 3 did not affect the recruitment of PSF or p54. Interestingly, knockdown of Matrin 3 did affect the retention of PSF and p54 at the site of DNA damage, causing them to remain at the site for approximately 30 minutes longer. The knockdown of Matrin 3 also led to both increased radiosensitivity and increased the proportion of cells in S phase after damage induction, suggesting that Matrin 3 has a role in the cellular response to double stranded DNA damage by altering the kinetics of other proteins involved in the response (Salton, Lerenthal et al. 2010).

Matrin 3 has been identified as interacting with a host of different proteins including PKCε after it has been induced to translocate to the nucleus (Xu and Rumsby 2004). It also exhibits calcium dependent binding to CaM and is susceptible to cleavage by caspases 3 and 8(Valencia, Ju et al. 2007). Heat shock proteins GRP78, GRP75 and GSTπ2 were identified by others as Matrin 3 interacting proteins (Osman and van

Loveren 2014). Immunoprecipitation followed by mass spectrometry was performed by two groups. The first identified 8 Matrin 3 binding partners; DHX9, PABPC1, DDX17, DDX5, hnRNPL, hnRNPK, PTBP1, and ILF2. Matrin 3 was also identified as binding to the non-coding RNAs; U4, SNORA73A, 7SK, and RMRP. Knockdown of Matrin 3 also resulted in decreased levels of 77 genes by microarray analysis (Salton, Elkon et al. 2011). Matrin 3 has been shown to decrease in protein level after treatment of SH-SY5y cells with the neurotrophic factors GDNF and Artemin (Park and Lee 2011). Matrin 3 was identified as a binding partner of the Y RNA, pY RNA1-s2 which has increased expression in retinal cells though its function in unknown (Yamazaki, Kim et al. 2014).

Matrin 3 was identified as a binding partner of PABPN1 (poly(A) binding protein), in skeletal muscle tissue lysates from mice overexpressing PABPN1. Skeletal muscle was studied due to the role of mutations in PABPN1 in OPMD (OculoPharyngeal Muscular Dystrophy). Matrin 3 was also found to bind to myogenic transcripts in primary myoblasts and depletion of Matrin 3 led to a decrease in proliferation and differentiation of the myoblasts. Matrin 3 depletion was also found to alter poly adenylation site selection and intron retention of PABPN1 targets. Matrin 3 was found to interact with the lncRNA *Neat1*, a major component of the nuclear structure paraspeckles. Depletion of either PABPN1 or Matrin 3 was found to increase *Neat1* levels, increased numbers of paraspeckles, increased editing of the transcript *Ctn* which is normally adenosine to inosine (A-to-I) edited in paraspeckles(Banerjee, Vest et al. 2017).

A role for Matrin 3 in insulator complexes has been shown using iChIP (insertional chromatin immunoprecipitation) which involves the isolation of a genomic region of interest prior to ChIP. Insulators are a part of the complex epigenetic regulation

that occurs, and function as boundaries to chromatin domains, protecting the genes they flank from trans elements and chromatin silencing. Matrin 3 was identified as part of the chicken insulator complex HS4 which regulates expression of β-globin genes. Matrin 3 was not found to bind directly to the DNA but rather to other protein components of the insulator complex, and the authors suggest a possible role for Matrin 3 in tethering these complexes to the nuclear matrix (Fujita and Fujii 2011).

Matrin 3 also appears to have a role in gene regulation via the homeodomain transcription factor Pit1. After identifying the proteins Matrin 3, β-catenin, and Satb1, as a Pit1 binding proteins, ChIP was performed with a Matrin 3 antibody, and it was determined that more than half of Matrin 3 binding sites co-localized with H3K4me2 peaks. Of the sites where the two co-localized, over 80% of them were elements distal to transcription start sites, suggesting an association between Matrin 3 and DNA regulatory elements. It was further noted that these Matrin 3 sites often co-localized with Pit1 enhancers. When cells were depleted of β-catenin or Satb1, the levels of Pit1 bound enhancers co-localizing with Matrin 3 decreased, suggesting β-catenin and Satb1 are required for this interaction. A dominant negative mutation in Pit1 causes combined pituitary hormone deficiency as well as the loss of the interaction with β-catenin and Satb1, and therefore Matrin 3. Loss of Pit1 resulted in the loss of both co-localization of Pit1 bound enhancers with Matrin 3, as well as decreased expression of Pit1 dependent genes. Both phenotypes could be rescued by expression of Pit1 but not by expression of dominant negative Pit1. Interestingly, attaching a SAF/SAP domain (matrix attachment region) from rat HNRNPU, to the dominant negative form of Pit1 restored its ability to

rescue both phenotypes, suggesting that tethering of Pit1 bound enhancers by Matrin 3 are required for their function (Skowronska-Krawczyk, Ma et al. 2014).

An example of Matrin 3 functioning with an enhancer was recently investigated after the discovery of the lncRNA (long non-coding RNA) PINCR (p53 induced non-coding RNA) identified in a microarray performed in colorectal cancer cell lines after induction of p53. Matrin 3 was found to mediate the association between PINCR and p53 allowing PINCR to associate with enhancer regions (Chaudhary, Gryder et al. 2017).

Matrin 3 has been identified as a nesprin-1 binding partner by immunoprecipitation followed by mass spectrometry experiments. Nesprin-1 functions in connecting the nucleoskeleton and cytoskeleton, and a short isoform generated by alternative transcription has been identified in p-bodies (mRNA processing bodies). After mapping the interaction between Matrin 3 and Nesprin-1 to two Nesprin-1 domains that are known to function in miRISC (micro RNA Induced Silencing Complex) function, and due to the fact that Matrin 3 had been previously identified in Argonaute protein complexes, a role for Matrin 3 in miRISC function was assessed. Using a Let-7a miRISC reporter assay it was determined that knockdown of Matrin 3 resulted in enhanced luciferase activity suggesting a role for Matrin 3 in miRNA-mediated gene silencing. A 50kD N-terminal Matrin 3 isoform was identified, which seems to be associated with p-bodies. Truncating mutations in Matrin 3 form cytoplasmic foci that seem to transition to stress granules upon heat shock, though this did not occur using full length Matrin 3. Additionally, no known clones seem to represent this potential short isoform of Matrin 3 (Rajgor, Hanley et al. 2016).

Matrin 3 was shown to have a role in splicing after it was identified in a proteomics screen as the strongest interactor of the splicing regulator PTB (polypyrimidine tract binding protein). Knockdown of Matrin 3 was found to cause over 600 alterative splicing events, half of which were cassette exons. Of the cassette exons the majority were inclusion events suggesting that Matrin 3 represses inclusion of these exons. To determine the relationship between Matrin 3 binding and splicing regulation iCLIP (individual-nucleotide resolution Cross-Linking and ImmunoPrecipitation) was performed and Matrin 3 was found to bind uniformly with no peaks at long intronic regions within 500 nucleotides of the repressed exon. The role for Matrin 3 in splicing regulation seems to require its RRM (RNA Recognition Motifs) but not its zinc-finger domains (Coelho, Attig et al. 2015).

Murine Matrin 3 protein expression was investigated and Matrin 3 was found to be expressed ubiquitously in all tissues tested. Expression was highest in reproductive organs and lowest in muscle. Within the CNS Matrin 3 expression was variable across different brain regions, but as a whole higher in the brain than in the spinal cord. Matrin 3 was also found to be expressed within the nucleus of all cell types examined though staining intensity was variable, particularly within the Purkinje cells of the cerebellum. When Matrin 3 expression was measured on the scale of a whole tissue (whole brain lysate, whole spinal cord lysate) during development, expression was found to decrease postnatally by 2.5 fold in brain and 11 fold in spinal cord over the first 37 days of life. This reduction in Matrin 3 levels seems to occur during development, while there was a decrease in Matrin 3 expression between 1 and 4 months there was no difference between 4 and 21 months (Rayaprolu, D'Alton et al. 2016).

A mouse model which was initially published as overexpressing full length wild-type Matrin 3 was created with expression driven by the mouse prion promoter. Since the time of publication this work has been retracted as it is believed that constucts were mislabeled and the mice examined in the study actually expressed mutant Matrin 3. Three founder lines were created that all produced progeny with hindlimb paresis and paralysis though the age at which these different lines began to show a phenotype ranged from approximately one month of age to one year of age. In addition to paralysis all lines of mice had decreased body weight compared to their nontransgenic littermates, rounded muscle fibers of variable size, subsarcolemmal vacuoles, internal nuclei and nuclear chains in myofibers and increased nuclear size. Matrin 3 immunoreactivity was increased in the nucleus though staining was variable between nuclei, and rare cytoplasmic Matrin 3 staining was seen. Neuromuscular junctions were also altered with a collapsed morphology, decreased post-synaptic junction size, and a reduction in the overlap between pre- and post-synaptic junction markers. In the spinal cord increased nuclear immunoreactivity for Matrin 3 was seen along with occasional cytoplasmic staining as well as gliosis (Moloney, Rayaprolu et al. 2016).

1.2.2 Matrin 3 Alterations in Disease

Matrin 3 has also been found to be altered in diseases apart from those caused by mutations in Matrin 3. A group performing quantitative proteomics analyses on fetal cortex tissue from controls and Down's syndrome identified Matrin 3 as one of three proteins with altered expression early in development in Down's syndrome. Matrin 3 protein expression was approximately four-fold higher in control brains as compared to Down's syndrome though it is not clear what if any significance this downregulation may

have to Down's syndrome pathogenesis (Bernert, Fountoulakis et al. 2002). Matrin 3 expression level affects both cell viability and proliferation. Treatment with siRNA against Matrin 3 in cultured cells led increased cell death, decreased proliferation, decreased size, and a shift to cells in G_0 (Przygodzka, Boncela et al. 2011).

Matrin 3 was identified as a binding partner of Lamin A after a protein domain found within Lamin A, the Lamin A tail domain was expressed, purified and crosslinked to a sepharose column which was then incubated with the nuclear lamina protein extract isolated from differentiated C2C12 myotubes. The binding between Matrin 3 and Lamin A was further characterized and found to occur between the IgG fold tail region of Lamin A and the carboxy terminus of Matrin 3. Interestingly the LMNA R453W mutation which is causative of Emery Dreifuss Muscular Dystrophy, but not R527P mutations, increase the binding between Matrin 3 and Lamin A. Immunocytochemistry performed on differentiating myotubes suggests that Matrin 3 expression is found near the nuclear membrane within myotubes that have begun differentiating which is a similar to the staining pattern of Lamin A. In fibroblasts heterozygous for a truncating mutation in Lamin A, Δ303, which causes cardiomyopathy and muscular dystrophy, the level of co-localization between Matrin 3 and Lamin A is decreased (Depreux, Puckelwartz et al. 2015).

A number of groups have also implicated Matrin 3 in viral pathogenesis. It was first identified as a target of the US3 family of kinases found in alphaherpes viruses where it is phosphorylated at T150 upon infection. It was suggested that this phosphorylation led to a more diffuse nuclear staining of Matrin 3 (Erazo, Yee et al. 2011). Matrin 3 is also involved in HIV pathogenesis through its role in viral RNA

export. Unspliced and partially spliced transcripts require the HIV protein Rev for export to the cytoplasm. Matrin 3 was initially identified as an HIV RNA binding protein, it was then shown that knockdown of Matrin 3 affected the cytoplasmic levels of transcripts requiring Rev for export (Kula, Guerra et al. 2011). Overexpression of Matrin 3 can both stabilize and increase the levels of these transcripts (Yedavalli and Jeang 2011). The role of Matrin 3 in viral Rev dependent RNA export was shown to be after the release of RNA from the site of transcription, and unspliced HIV RNA was shown to associated with Matrin 3 in the insoluble nuclear matrix fraction (Kula, Gharu et al. 2013). Matrin 3 has also been shown to regulate viral transcripts via its interaction with the protein ZAP (CCCH-type Zinc-Finger Antiviral protein), which acts as a restriction factor that binds viral RNA and recruits the RNA processing exosome leading to RNA degradation. Matrin 3 was identified by performing immunoprecipitation followed by mass spectrometry using antibodies against Matrin 3 in CHME3 cells that were either uninfected or infected with HIV-1. Two proteins intricately involved in the RNA processing exosome DDX17 and EXOSC3 were both identified as binding Matrin 3 only in infected cells. The role of Matrin 3 in ZAP mediated HIV-1 restriction was tested in a series of knockdown experiments in cells infected with HIV-1. Overexpression of ZAP alone led to a 6 fold restriction of HIV-1 expression and knockdown of Matrin 3 alone led to a four-fold decrease inhibition of HIV-1 expression, but overexpression of ZAP and in the context of Matrin 3 knockdown led to a 35-fold restriction of HIV-1 suggesting a role for Matrin 3 as a negative regulator of ZAP-mediated viral restriction (Erazo and Goff 2015).

Alterations in Matrin 3 have been linked to congenital heart defects including bicuspid aortic valve, coarctation of the aorta, and patent ductus arteriosus in a patient with a balanced translocation 46,XY,t(1;5)(p36.11;q31.2)dn. The breakpoints of this translocation disrupted two genes AHDC1 and MATR3. In addition to heart defects this patient exhibited global developmental delays including speech delays and was diagnosed with Noonan-like syndrome. Loss of function of AHDC1 has been shown to cause cognitive abnormalities and developmental delays suggesting that this part of the phenotype may be due to the loss of AHDC1. The breakpoint within MATR3 is found 667 bp downstream of the stop codon, in the 3' UTR of MATR3 exon 15. 3' RACE (Rapid Amplification of cDNA Ends), a technique that utilizes a sequence specific primer as well as an adaptor primer against the poly (A) tail, performed on adult tissue from various organs showed that there are two different MATR3 RACE products created through the use of an alternative polyadenylation site. In all tested tissues, with the exception of skeletal muscle and cardiac muscle, the product is 1589 bp whereas in skeletal muscle and cardiac muscle a band of 963 bp predominates. The location of the translocation suggests that it would disrupt the creation of the longer transcript that utilizes the distal polyadenylation site. In patient lymphoblasts, the longer transcript from the distal polyadenylation site is lost which seems to result in an upregulation of the shorter transcript from the proximal polyadenylation site. Interestingly, this alteration in polyadenylation seems to lead to an increase in Matrin 3 protein, which was found to be increased by 2.7 fold in patient lymphoblasts compared to controls. A gene trap mouse model in which the MATR3 gene is interrupted in exon 13, is homozygous embryonic

lethal and heterozygotes have cardiac defects similar to patients (Quintero-Rivera, Xi et al. 2015)

1.2.3 Ser85Cys Matrin 3 Mutations in VCPDM

Before mutations in Matrin 3 were identified in ALS patients, a Ser85Cys mutation was identified as the cause of a form of distal myopathy known as vocal cord and pharyngeal weakness with distal myopathy (VCPDM). Patients with VCPDM are described as having an average age of onset of 35-57 years, and commonly exhibit the initial symptom of foot drop and ankle dorsiflexion weakness. These patients then went on to develop progressive weakness including vocal cord and/or swallowing dysfunction in some but not all patients. EMG and nerve conduction studies were reported to suggest a myopathy and muscle biopsies showed variations in muscle fiber size, fiber splitting, and subsarcolemmal rimmed vacuoles (Feit, Silbergleit et al. 1998). The chromosomal location of the causative mutation was narrowed to a region of the 5^{th} chromosome but mutations in Matrin 3 were not identified until additional family members were diagnosed with the disease (Senderek, Garvey et al. 2009).

While Ser85Cys mutations in Matrin 3 are associated with distal myopathy a common phenotype in these patients is respiratory dysfunction. When eight patients were studied 6 reported exertional dyspnea and all 8 had respiratory symptoms of some form including diaphragm dysfunction, weak expiratory muscles, and reduced airway clearance. Two patients progressed to the point where they required mechanical ventilation and one experienced sudden respiratory failure (Kraya, Schmidt et al. 2015).

The clinical phenotype of patients with Ser85Cys mutations in Matrin 3 has been assessed by other groups who support the diagnosis of distal myopathy. An additional

American family in which Ser85Cys mutations were identified had 6 affected individuals over two generations. The age of onset ranged from 31-48 years and initially manifested as limb weakness. Two of the family members developed hypophonia and dysphagia and two family members developed respiratory symptoms. A muscle biopsy was performed and showed rimmed-vacuolated fibers, accumulation of TDP-43 and p62 in rimmed-vacuolar fibers, and a staining for Matrin 3 at the membrane of myonuclei but absent from the center of the nucleus. Electron microscopy also showed highly convoluted myonuclei. Matrin 3 protein levels were reported to be the same as in controls (Palmio, Evilä et al. 2016).

The Ser85Cys mutation in Matrin 3 was also found in a Japanese family consisting of a father who developed gait disturbance and respiratory failure as well as his daughters, two half sisters. One of the two sisters first presented with difficulty in ambulation and then went on to develop dysphagia and dysarthria. The second sister first experienced dysphagia and dysarthria and then went on to develop muscle wasting. Both of the two sisters were examined and were found to lack upper motor neuron signs, preventing a diagnosis of ALS, and instead suggesting VCPDM. Both sisters underwent muscle biopsies and which showed myopathic changes and internal nuclei were found within the myofibers. One of the two sisters had autophagic vacuoles in degenerating myofibers and an increase in type I fibers, whereas her sister was found to have an increase in type II fibers. Their muscle fibers also contained p62 positive sarcoplasmic aggregates, and had variable nuclear immunoreactivity for Matrin 3. Matrin 3 staining patterns were also explored in other types of myopathies and sarcoplasmic granular staining for Matrin 3 was present in p62 positive degenerating fibers in tissue from

patients with sIBM (sporadic Inclusion Body Myositis), OPMD, as well as myopathies with mutations in the genes GNE and VCP. TDP-43 aggregates were present in one of the cases with decreased nuclear immunoreactivity for both TDP-43 and Matrin 3 in the myofibers with aggregates and diffuse sarcoplasmic immunoreactivity for TDP-43 was found in the other case (Yamashita, Mori et al. 2015).

1.2.4 Matrin 3 Mutations in ALS

Mutational analysis was performed on 169 Taiwanese ALS patients that did not have mutations in any other genes linked to ALS and an Ala72Thr (c.214G>A) mutation in Matrin 3 was found. This mutation was identified in an apparently sporadic ALS patient with bulbar onset disease who initially presented with slurred speech at age 53. She progressed to dysphagia and progressive muscle weakness and atrophy within 3 years and died 11 years after symptom onset. Amino acid 72 in Matrin 3 is well conserved across a host of different species and this alteration was not found in controls from the Exome Aggregation Consortium, dbSNP, or the 1000 genomes project (Lin, Tsai et al. 2015).

The frequency of Matrin 3 mutations was assessed in a French-Canadian population resulting in the identification of one missense mutation and two splicing variations in sporadic ALS patients. The authors reported the mutational frequency in their cohort of sporadic ALS patients was 1.8%. The missense mutation V394M, is in a highly conserved region but was not predicted to be pathogenic by Polyphen-2, SIFT or Provean. Of the two splicing variations c.48+1G>T alters a splice site resulting in a 24 amino acid longer protein. The second splicing variation (c.-339+2T>A) is within the 5' UTR. None of the three variations were found in the control databases NHLBI Exome

Sequencing Project, 1000 Genomes Project, dbSNP or internal control samples. However, the c.48+1G>T variation was reported in 1 individual from ExAc database (Leblond, Gan-Or et al. 2016).

Matrin 3 mutations were also assessed in a cohort of two hundred Italian ALS patients leading to the discovery of a p.Arg147Trp mutation in Matrin 3. This mutation was identified in a sporadic ALS patient. The patient presented with progressive weakness predominantly in the lower limbs at age 43 and followed a slow disease course. At the time of publication the patient was still living, 9 years after diagnosis with tetraparesis and severe muscle atrophy, though without dementia, dysarthria or dysphagia. This variant was not present in the Human Gene Diversity Panel or 500 unrelated Italian controls (Origone, Verdiani et al. 2015).

A cohort of 322 Italian ALS patients were examined for Matrin 3 mutations and 5 missense variants were identified in 6 individuals (mutational frequency of 1.9%). The variants identified were p.Q66K, p.G153C (twice), p.E664A, p.S707L, and p.N787S. These patients had an age of onset ranging from 48 to 64 years and 2 (S707L and E664A) presented with bulbar onset, one presented with respiratory symptoms first (Q66K), the patient carrying the N787S and one of the patients carrying the G153C mutations presented with lower limb onset, and the second G153C presented with upper limb onset. Two patients underwent muscle biopsies which showed neurogenic changes including atrophic angulated or round fibers, pyknotic nuclear clumps, abnormal checkerboard staining of type 1 fibers and internal nuclei. One patient (S707L) also developed FTD (Marangi, Lattante et al. 2017).

Matrin 3 mutations were not found in ALS patients studied in France (153 patients) (Millecamps, Septenville et al. 2014), or Australia (106 patients) (Fifita, Williams et al. 2015).

Expression of the ALS associated mutations in Matrin 3 (Ser85Cys, Phe115Cys, Pro154Ser, Thr622Ala) was studied in CHO and H4 cell lines. The expression of both wild-type and mutant Matrin 3 was predominantly nuclear. While there was occasional cytoplasmic staining, there was no statistical difference in the number of cells with cytoplasmic staining in mutant as compared to wild-type. Treatment of cells with arsenite induced cytoplasmic stress granules but Matrin 3 remained nuclear. Expression of a mCherry-tagged stress granule component G3BP1 led to the occasional accumulation of Matrin 3 within cytoplasmic puncta but only in cells that were not treated with arsenite; in cells treated with arsenite Matrin 3 again remained nuclear. The authors suggest that this phenomenon could be the consequence of Matrin 3 interacting with G3BP1 outside of stress granules (Gallego-Iradi, Clare et al. 2015).

Matrin 3 staining patterns were explored by another group studying an ALS linked mutation in Sigma Receptor-1. Expression of mutant Sigma Receptor-1 in immortalized cells as well as patient lympoblastoid cells, led to the cytoplasmic accumulation of TDP-43, FUS and Matrin 3. Immunohistochemistry was performed on spinal cord tissue from sporadic and familial ALS patients to explore Matrin 3 pathology. Nuclear Matrin 3 immunoreactivity was increased in sporadic ALS patients as compared to controls and Matrin 3 positive inclusions and cytoplasmic accumulation was found in familial ALS patients carrying mutations in either FUS or carrying the C9orf72 repeat expansion (Dreser, Vollrath et al. 2017).

Immunohistochemistry using four different antibodies against Matrin 3 was performed on spinal cord tissue from controls and sporadic ALS patients. Matrin 3 immunoreactivity was classified into two categories; mild and strong. The percentage of cells in control cases and ALS cases with mild versus strong Matrin 3 staining was similar. Of the four antibodies one showed Matrin 3 positive cytoplasmic inclusions in 9 out of 15 sporadic ALS cases in 2-9% of motor neurons. The majority of Matrin 3 positive inclusions were described as round in shape with very few showing a skein-like morphology. Immunohistochemistry with an antibody against TDP-43 was also performed and it was noted that cells containing either a Matrin 3 positive inclusion or a TDP-43 positive inclusion tended to have mild nuclear staining for Matrin 3. Matrin 3 inclusions were also suggested to co-localize with TDP-43 inclusions in all cases though not all TDP-43 positive inclusions co-localized with Matrin 3. It was also noted that the patients that did have Matrin 3 positive inclusions in some of their cells had a shorter disease span than those that did not have Matrin 3 positive inclusions (Tada, Doi et al. 2017).

1.3 RNA EXPORT IN NEURODEGENERATIVE DISEASE

1.3.1 RNA Export Under Normal Conditions

In eukaryotic cells, transcription and translation are compartmentalized by the nuclear membrane, or nuclear envelope. The nuclear membrane separates the nucleus, where transcription takes place, from the cytoplasm, where translation occurs. Transport between the two compartments is tightly regulated via trafficking through nuclear pores that are contained within the nuclear membrane. While molecules, including both proteins and nucleic acids, with a molecular mass below 40kDa may diffuse freely

through the pores, most larger molecules are actively transported using numerous carrier proteins (Paine 1975, De Robertis, Longthorne et al. 1978, Dingwall, Sharnick et al. 1982). RNA transport is predominantly mediated by either NXF1 (Nuclear RNA Export Factor 1), also known as TAP, or members of the exportin family of proteins. The export adaptor used is largely dependent on the type of RNA, with mRNA predominantly relying on NXF1 (Segref, Sharma et al. 1997, Herold, Klymenko et al. 2001). All other types of RNA require a member of the exportin family as an adaptor, along with a gradient of the GTPase Ran. rRNA (Thomas and Kutay 2003, Rouquette, Choesmel et al. 2005, Wild, Horvath et al. 2010), snRNA and some mRNAs utilize CRM1 (exportin-1, XPO1) (Fornerod, Ohno et al. 1997, Watanabe, Fukuda et al. 1999), and tRNA and miRNA require exportin-t and exportin-5 respectively (Arts, Fornerod et al. 1998, Kutay, Lipowsky et al. 1998, Bohnsack, Czaplinski et al. 2004, Lund, Guttinger et al. 2004). In each case, the transport carrier protein is required to move the RNA, in the form of a ribonucleoprotein particle (RNP), through the nuclear pore and release it on the cytoplasmic side. In this chapter, we will review the canonical pathways for transport of RNA from the nucleus to the cytoplasm under normal conditions, as well as explore the alterations in RNA transport that have been identified in neurodegenerative diseases. These alterations predominantly fall into three categories; alterations in the nuclear envelope as well as mislocalization of the proteins making up the nuclear pore, alterations in the Ran gradient, and deficits in the export of mRNA, identified in both models of neurodegenerative disease and tissue from patients who suffered from these diseases.

Transport between the nucleoplasm and cytoplasm is controlled by a protein structure called the nuclear pore complex (NPC). The NPC is approximately 125MDa in size in

humans and comprised of a group of proteins known as nucleoporins (Reichelt, Holzenburg et al. 1990). The geometric structure of the nuclear pore consists of 8 spokes connecting radially to form concentric rings and exhibits an eight-fold symmetry, formed from over 500 copies of up to 30 different nucleoporins (Reichelt, Holzenburg et al. 1990, Cronshaw, Krutchinsky et al. 2002). The NPC can be broken into three regions; the central channel, nuclear basket and cytoplasmic filaments. The central channel which is embedded within the nuclear envelope allows cargoes to move in and out of the nucleus. The nuclear basket is found on the nuclear side of the pore, and functions to bind transport competent mRNPs (messenger ribonucleoprotein particles) and direct them to the pore. Cytoplasmic filaments guide both proteins into the nuclear pore, and RNA cargoes which are exiting the pore, toward the translational machinery. The pore forms a central channel approximately 50-100kDa/40nm in size and is lined with nucleoporins containing phenylalanine-glycine (FG) repeat domains. These FG repeats both fill the channel of the pore as well as comprise both the cytoplasmic filaments and nuclear basket. An estimated 6MDa of FG repeats are found in a single pore and these domains provide both a barrier to diffusion, as well as docking sites for transport factors as they are trafficked through the pore (Frey and Gorlich 2007).

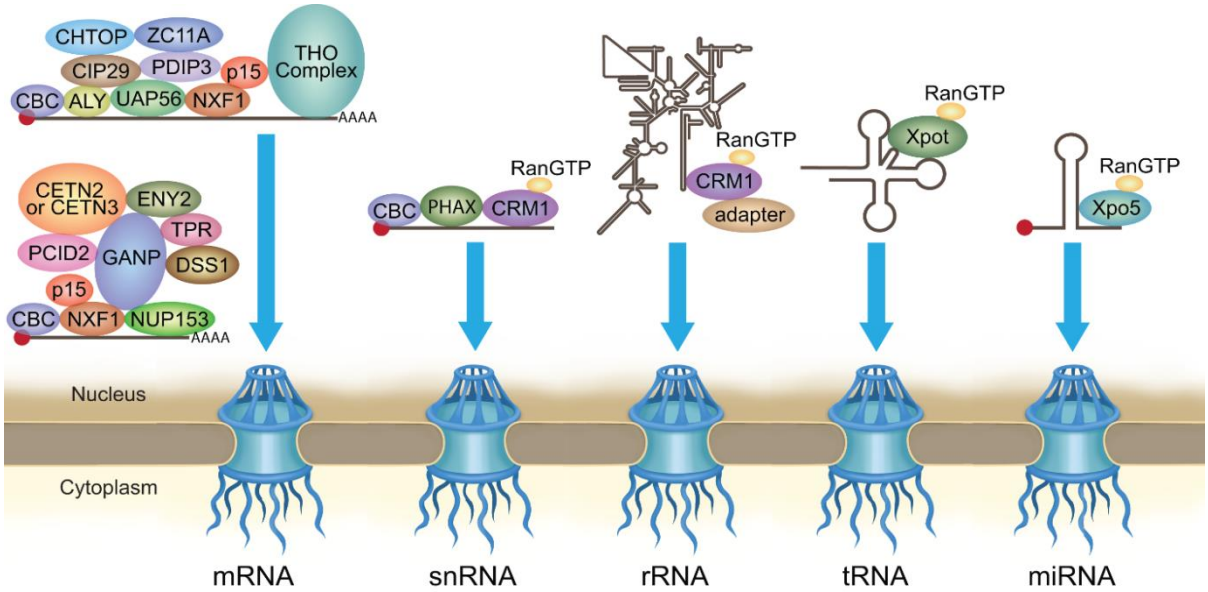

Figure 1.1 Canonical RNA Export Pathways

Export of mRNA predominantly requires the TREX and TREX-2 pathways. snRNA and rRNA export requires the exportin CRM1 bound to RanGTP along with the adaptor PHAX for snRNA and as well as specific adaptors for different subunits of rRNA. Export of tRNA and miRNA require the exportins XPOt and XPO5 respectively, bound to RanGTP.

Different types of molecules (proteins, mRNA, rRNA, tRNA, miRNA) rely on a host of different transport factors to transverse through the nuclear pore. Some mRNA as well as most other types of RNA, including rRNA, tRNA, and miRNA, require a member of the exportin family to facilitate their export (Fukuda, Asano et al. 1997). Exportins are a family of 7 proteins including CRM1 (XPO1), CSE1L (XPO2), XPOt (XPO3), XPO4, XPO5, XPO6, XPO7 which function in export from the nucleus (Figure 1.1). Much like the nuclear import transporters importins, exportins require the small GTPase Ran to function. Export via exportins requires a gradient of Ran to exist in which GTP bound Ran (RanGTP) is concentrated in the nucleus, and both GDP bound Ran (RanGDP) and its GTPase activator RanGAP1 are concentrated in the cytoplasm (Bischoff and Ponstingl 1991). Of the 7 known exportins, CRM1 is required for the export of some mRNAs as well as rRNA, in addition to being a primary transporter of proteins (Fukuda, Asano et al. 1997). CRM1 does not bind RNA itself but instead relies on a series of RNA binding adaptor proteins which bind RNA and then CRM1 for RNA export (Figure 1.1) (Brennan, Gallouzi et al. 2000, Yang, Bogerd et al. 2001, Topisirovic, Siddiqui et al. 2009). These adaptor proteins requires a NES (Nuclear Export Sequence) which for CRM1 is HX2–3HX2–3HXH, where H is a hydrophobic amino acid (i.e.,isoleucine, leucine, methionine, phenylalanine, or valine) X is any amino acid (Kalderon, Roberts et al. 1984, Henderson and Eleftheriou 2000). The binding of CRM1 to an NES containing protein is cooperative with its binding to RanGTP (Petosa, Schoehn et al. 2004). After transport through the nuclear pore, GTP hydrolysis occurs which helps to dissociate its cargoes. In addition to a small subset of mRNAs, CRM1 is necessary for the export of rRNAs. Both the pre-60S subunit and the pre-40S subunit can be exported via CRM1 and

an adaptor (Nmd3 or Lvt1 respectively). The pre-60S can also be exported by exportin-5 while the pre-40S subunit seems to rely solely on CRM1 (Thomas and Kutay 2003, Wild, Horvath et al. 2010). Other types of RNAs are also exported in a similar Ran dependent process using other exportins, with export of tRNA requiring exportin-t (XPOt) and export of miRNA requiring exportin-5 (XPO5) (Arts, Fornerod et al. 1998, Kutay, Lipowsky et al. 1998, Yi, Qin et al. 2003, Bohnsack, Czaplinski et al. 2004, Lund, Guttinger et al. 2004) (Figure 1.1). Binding between pre-miRNA and XPO5 is mediated by the pre-miRNA structure rather than sequence with the recognition of a two nucleotide 3' end overhang structure and the double stranded stem found in pre-miRNA (Okada, Yamashita et al. 2009). In both cases the RNA is bound by GTP-bound exportin which allows for its trafficking through the pore.

Nucleocytoplasmic trafficking of mRNA through the nuclear pore mainly occurs via the transport factor NXF1. NXF1 is loaded onto mRNA via a series of handoffs involving the TREX (TRanscription and EXport) complex. Transport of mRNA is intricately linked with transcription and all stages of pre-mRNA processing including splicing. The TREX complex is made up of the THO complex containing Thoc1 (Hpr1), Thoc2, Thoc3 (hTEX1), Thoc5, Thoc6 and Thoc7 as well as UAP56 (ddx39b), and Aly (Ref) (Strasser, Masuda et al. 2002) (Figure 1.1). Unlike exportin mediated export, TREX does not rely on a Ran gradient but rather ATP hydrolysis.

The specificity of mRNA to TREX is mediated by its link to RNA polymerase II transcription, as well as a length requirement mediated by hnRNPC. hnRNPC interacts with the 5' end of RNA if it is longer than 300bp, preventing the recruitment of export factors other than TREX to the mRNP (McCloskey, Taniguchi et al. 2012). During

transcription, proteins necessary for capping of the 5' end, splicing, 3' end cleavage, and polyadenylation bind to the nascent RNA. In metazoans, TREX has been shown to be predominantly coupled to splicing, whereas in yeast it has been shown to be more associated with transcription (Reed and Cheng 2005). In human cells, TREX proteins have been shown to be recruited to the 5' end of pre-mRNA near the cap binding complex (CBC) which consists of the proteins CBP80 and CBP20 (Cheng, Dufu et al. 2006). Aly binds closest to the CBC followed by UAP56 which binds downstream of Aly but upstream of the exon junction complex (EJC) (Figure 1.1). This interaction is thought to be mediated by protein-protein interactions between Aly and CBP80 (Cheng, Dufu et al. 2006). Interestingly, binding of mRNA to Aly and TREX complex member Thoc2 has been shown to require capped and spliced mRNA, suggesting that the recruitment of Aly to mRNA requires more than just binding to CBP80 (Cheng, Dufu et al. 2006).

Binding of Aly and RNA to UAP56 has been shown to stimulate the intrinsic ATPase activity of UAP56, which aids in its dissociation from the complex. The dissociation of UAP56 from the mRNP constitutes the handover of the mRNP to Aly. Aly along with a co-activator, Thoc5 or Chtop, are required for the binding of NXF1 to RNA (Viphakone, Hautbergue et al. 2012). NXF1 functions as a heterodimer with p15 (NXT1), and has very little RNA binding activity in its native state. Upon binding with Aly and a co-activator, NXF1 is remodeled to expose its RNA binding domains (Viphakone, Hautbergue et al. 2012). At this stage, the mRNP is turned over to NXF1 for trafficking though the nuclear pore.

Another export complex, TREX-2, also has a role in the export of mRNA via the NXF1 transporter. TREX-2 is built upon a scaffold protein GANP (Germinal-center

associated nuclear protein), which binds ENY2, PCID2 and DSS1 (Wickramasinghe, Stewart et al. 2010) (Figure 1.1). The exact role of TREX-2 is unclear, though in yeast it has been shown to be involved in localizing a subset of actively transcribing genes to the pore (Kohler, Schneider et al. 2008). In metazoans however, it has been shown to be involved in chaperoning mature mRNPs from processing centers to the pore for export (Wickramasinghe, Stewart et al. 2010). It is unclear whether TREX and TREX-2 work cooperatively on the same mRNPs or transport different subsets of mRNPs, though some cooperation between the two complexes is thought to occur in mammalian cells (Wickramasinghe, Stewart et al. 2010). One proposed model suggests that TREX-2 attaches to the mRNP after it is transferred from Aly to NXF1 and mediates its transport to and interaction with the nuclear pore (Wickramasinghe, Stewart et al. 2010).

Many groups, including ours, have recently emphasized the role alterations in nucleocytoplasmic trafficking play in a number of neurodegenerative diseases (Sheffield, Miskiewicz et al. 2006, Freibaum, Lu et al. 2015, Zhang, Donnelly et al. 2015, Gasset-Rosa, Chillon-Marinas et al. 2017, Grima, Daigle et al. 2017, Shang, Yamashita et al. 2017). While initial studies have focused on defects in protein trafficking, likely due to the common pathology of protein aggregation in the cytoplasm observed in many of these diseases, evidence for defects in RNA trafficking has recently come to light (Freibaum, Lu et al. 2015, Boehringer, Garcia-Mansfield et al. 2017). These RNA trafficking alterations in disease states predominantly fall into three categories of defects; alterations in the localization of nucleoporins and abnormal nuclear envelope architecture, defects in the Ran gradient and alterations in the proteins that are responsible for maintaining it, and alterations in TREX proteins as well as mRNA retention within the nucleus. It is

important to note that alterations in protein trafficking are intricately linked to alterations in RNA trafficking due to the use of common regulatory proteins in nuclear export of proteins and RNA. Alterations in nucleoporins and the nuclear envelope as well as loss of the Ran gradient is likely to influence all forms of transport in and out of the nucleus. While export of mRNA via the TREX/NXF1 pathway is Ran independent, it requires members of the export process to be imported back into the nucleus to function, which is a Ran dependent process.

1.3.2 Nuclear Envelope and Nucleoporin Abnormalities

The earliest evidence for RNA transport alterations is the mislocalization of nucleoporins away from the nuclear envelope where they function, as well as abnormal nuclear envelope morphology which is often highlighted by nucleoporin immunostaining. These phenotypes have been identified in both animal models and patient tissue from several different neurodegenerative diseases (Sheffield, Miskiewicz et al. 2006, Freibaum, Lu et al. 2015, Zhang, Donnelly et al. 2015, Gasset-Rosa, Chillon-Marinas et al. 2017, Grima, Daigle et al. 2017).

In Alzheimer's disease tissue, nuclear envelope abnormalities were noted in the hippocampus after staining with Nup62, an FG containing nucleoporin normally localized to the central channel of the nuclear pore (Sheffield, Miskiewicz et al. 2006). In control tissue, Nup62 immunoreactivity forms a smooth circle in the nuclear envelope whereas in Alzheimer's patients forms a tortuous and uneven nuclear envelope. It is important to note that these alterations in the nuclear envelope were not accompanied by positive staining for caspase-3 or TUNEL suggesting that this is not a consequence of cell death (Sheffield, Miskiewicz et al. 2006).

In a mouse model of Huntington's disease, mice expressing physiological levels of ~175 CAG trinucleotide repeat expansion within one or both huntingtin (*Htt)* alleles exhibited a dose and age dependent increase in the number of cells with abnormal nuclear envelopes, as observed using staining against Lamin B1 in the cortex and striatum (Gasset-Rosa, Chillon-Marinas et al. 2017). This phenotype was also present in the cortex of mice expressing a 23kD human exon 1 fragment of *Htt* with a 120-125 repeat polyglutamine expansion (R6/2 mice) (Gasset-Rosa, Chillon-Marinas et al. 2017). This same mouse model of *Htt* was shown by others to exhibit intranuclear inclusions of Nup62 that co-localized with mHtt aggregates in the striatum and cortex (Grima, Daigle et al. 2017). In the zQ175 mouse model of Huntington's disease which contains the human *Htt* exon 1 sequence with a 193 CAG repeat which replaces the mouse *Htt* exon 1 within the mouse *Htt* gene, the nucleoporin Nup88, was identified in intracellular inclusions that co-localized with mHtt aggregates (Grima, Daigle et al. 2017). Abnormal nuclear envelopes were also seen in iPS (induced pluripotent stem cell) derived neural progenitors from Huntington's patients, and in the motor cortex of patient tissue (Gasset-Rosa, Chillon-Marinas et al. 2017). Components of the nuclear pore complex including Dbp5, a protein necessary at the terminal step of mRNA export to remove proteins from mRNAs after they have been transported through the pore, and RanBP3, a Ran binding protein that acts a cofactor for CRM1 mediated export were also identified in the isolated polyglutamine aggregates induced in a cell culture model of Huntington's disease (Suhr, Senut et al. 2001).

In ALS disease models based on expression of mutant SOD1 in mice, alterations of NPC components including increased immunoreactivity of the nucleoporins GP210

and Nup205 (Shang, Yamashita et al. 2017). This staining was reminiscent of staining patterns in sporadic ALS patients which showed increased staining for GP210 in the nuclear envelope and cytoplasm. (Shang, Yamashita et al. 2017). Others have also identified nuclear envelope irregularities as denoted by Nup62, Nup88 and Nup153 immunoreactivity in SOD1 mice which worsened with age as well as in both sporadic ALS (sALS) and familial ALS (fALS) patient tissue (Kinoshita, Ito et al. 2009).

In a genetic screen performed in a *Drosophila* model of C9orf72, loss of function of Nup50 enhanced the phenotype of the C9 repeat, as did a dominant negative form of Ran, whereas loss of function of Nup107 and Nup160 suppressed the phenotype (Freibaum, Lu et al. 2015). These results suggest altered subcellular distribution of nucleoporins may have a functional role in disease pathogenesis rather than being a consequence of the disease pathology, and that these alterations could have both loss of function and toxic gains of function phenotypes. This phenotype was accompanied by nuclear envelope irregularities as well as puncta of Nup107 in the salivary glands of flies (Freibaum, Lu et al. 2015). As Nup107 is both found in aggregates and puncta, and its loss of function suppresses the disease phenotype in flies, it is possible that these aggregates and puncta of NPC can be toxic to cells. The mechanism by which these alterations in the nuclear envelope and mislocalization of NPC proteins induce disease is unknown, but a number of hypotheses have been proposed. PR dipeptides, formed from RAN (repeat associated non-ATG) translation of the C9orf72 repeat expansion (DPRs) were found to bind to the FG repeat of the central channel of the nuclear pore complex and keep them in a polymerized state, possibly physically blocking movement through the nuclear pore (Shi, Mori et al. 2017). Nuclear transport proteins including nuclear pore

complex components and transport proteins such as CRM1 were found to interact with the DPRs PR and GR, produced from the C9orf72 repeat expansion, and CRM1 was also found to be an enhancer of a GR viability phenotype in *Drosophila* (Lee, Zhang et al. 2016). Another group suggests that cytoplasmic protein aggregates lead to the mislocalization of NPC proteins (Woerner, Frottin et al. 2016). This hypothesis was tested using an artificial, aggregation prone β-sheet protein which led to the accumulation of NPC proteins in the cytoplasm and defects in both protein import and export (Woerner, Frottin et al. 2016).

1.3.3 Alterations in the Ran Gradient

Another common theme amongst neurodegenerative diseases is alterations in the Ran gradient or its binding partners and regulators. A high nuclear to cytoplasmic ratio of RanGTP is required for nuclear export where RanGTP is needed to bind to the exportin family of proteins within the nucleus.

In mice expressing mutant *Htt*, Gle1, part of the terminal step of mRNA export, as well as RanGAP1 are found co-aggregated with *Htt* (Gasset-Rosa, Chillon-Marinas et al. 2017). RanGAP1, (Ran GTPase Activating Protein) which is necessary for activating the GTPase function of Ran leading to its conversion to a GDP bound state, and Nup62 were found in inclusions in Htt R6/2 mice and RanGAP1 and Nup88 were found in mHtt inclusions in zQ175 Htt mice (Grima, Daigle et al. 2017). RanGAP1 was also mislocalized and concentrated in perinuclear puncta, and Nup62 was mislocalized in the frontal cortex and striatum of Huntington's patients (Grima, Daigle et al. 2017). Higher levels of RanGTP are required in the nucleus compared to the cytoplasm to fuel active transport via exportins. In iPS derived neurons from Huntington's patients, the nuclear to

cytoplasmic ratio of Ran is decreased (Grima, Daigle et al. 2017). Interestingly, expression of either RanGAP1 or Ran ameliorated cell death in cells expressing mutant Huntingtin, suggesting that at least part of the mechanism of action may be a loss of function of these proteins (Grima, Daigle et al. 2017).

In Alzheimer's disease, cytoplasmic aggregates of NTF2, part of the import pathway required for importing Ran into the nucleus, were found in patient tissue (Sheffield, Miskiewicz et al. 2006). Nuclear levels of Ran were also found to be decreased both in a mouse model of FTD based on mutations in progranulin, and in tissue from patients carrying that mutation (Chen-Plotkin, Geser et al. 2008, Ward, Taubes et al. 2014).

In a model of Parkinson's disease based on administration of the drug 1-methyl-4-phenyl-1,2,3,6-tetrahydropyridine (MPTP), mice that lacked one copy of the Ran binding protein, Ranbp2, had a more severe disease course and slower recovery (Cho, Searle et al. 2012). Interestingly, in mice lacking any other genetic modifications, knock down of Ranbp2 in Thy1 positive motor neurons led to motor deficits, respiratory distress and premature death (Cho, Yoon et al. 2017).

Many models of ALS also exhibit similar defects in either the Ran gradient or in Ran binding proteins. TDP-43 is a protein mutated in rare forms of ALS as well as present in pathological aggregates in most ALS, FTD and subsets of a number of other neurodegenerative diseases, and has been shown to bind the 3' UTR of Ran mRNA and regulate its levels (Ward, Taubes et al. 2014). Loss of nuclear TDP-43 correlated with loss of Ran in the frontal gyrus of patients with FTD caused by mutations in progranulin (GRN) and led to overall decreased levels of Ran in the cortex (Ward, Taubes et al.

2014). In addition, knockdown of TDP-43 in SH-SY5Y cells leads to decreased levels of RanBP1 (Stalekar, Yin et al. 2015). In mice expressing mutant SOD1 an upregulation and nucleoplasmic mislocalization of RanGAP1 were observed (Shang, Yamashita et al. 2017). A similar increase in RanGAP1 staining was seen in tissue from sALS patients (Shang, Yamashita et al. 2017).

The RanGAP1 protein has also been shown to bind to the G-quadruplex structure formed by the RNA of the C9orf72 repeat expansion, and there is a reduced nuclear to cytoplasmic ratio of Ran in iPS motor neurons derived from C9-ALS patients as well as in immortalized cell lines expressing the repeat (Freibaum, Lu et al. 2015). Both iPS derived motor neurons and motor cortex tissue from ALS patients carrying the C9orf72 expansion exhibited discontinuous nuclear envelope staining for RanGAP1 as well as mislocalization and puncta that occasionally co-localized with Nup107 and Nup205 (Zhang, Donnelly et al. 2015). In a mouse model of C9orf72 expressing the GA DPR, both RanGAP and Pom121, a transmembrane nucleoporin involved in anchoring the NPC to the membrane, were found in nuclear and cytoplasmic puncta which often co-localized with the poly(GA) aggregates (Zhang, Gendron et al. 2016). Interestingly, in a D*rosophila* model of C9orf72, a genetic screen found that RanGAP suppressed the toxicity accompanied by the repeat, whereas RanGEF enhanced the toxicity (Zhang, Donnelly et al. 2015). Importantly, in this model system the phenotype of the altered Ran gradient (which likely inhibits the export of both proteins and RNA) could be partially rescued by a variety of treatments. The Ran gradient phenotype was rescued with antisense oligonucleotides against the C9orf72 repeat, by destabilizing the G quadruplex structure the repeat forms, or by inhibiting CRM1, suggesting both that these defects are

may be induced by the repeat, and that drug strategies currently being employed for the repeat might modulate these defects (Zhang, Donnelly et al. 2015).

1.3.4 Defects in mRNA Export

While mislocalization of nucleoporins and defects in the Ran gradient and Ran binding proteins are likely to cause alterations in the nuclear export of RNA, recent studies have identified deficits in the export of mRNA in models of neurodegenerative disease.

In Huntington R6/2 mice, the TREX complex component Thoc2, is mislocalized and found in inclusions, and mRNA was found to be retained within the nucleus of these cells (Woerner, Frottin et al. 2016, Gasset-Rosa, Chillon-Marinas et al. 2017). The same phenotypes of Thoc2 aggregation and nuclear mRNA retention were found in cells expressing Htt86Q as well as c-terminal fragments of TDP-43 or even an artificial aggregation prone β-sheet construct (Woerner, Frottin et al. 2016). In mice expressing a ~175 CAG trinucleotide repeat of *Htt* (Htt^{Q165}), mRNA accumulated within nuclei by RNA-FISH (fluorescence *in situ* hybridization) using an oligo dT probe, in a dose dependent manner (Gasset-Rosa, Chillon-Marinas et al. 2017). In addition to phenotypes in models of neurodegenerative disease, this phenotype of mRNA nuclear accumulation has been identified in the cortex in tissue from Huntington's patients (Gasset-Rosa, Chillon-Marinas et al. 2017).

Some rare forms of fALS are caused by mutations in Gle1 which is an integral component of the release of mRNA from transport machinery in the cytoplasm. While the mechanism by which these mutations cause disease is not completely understood it has

been suggested that haploinsufficiency of Gle1 is to blame, suggesting a role for mRNA transport defects in this disease (Kaneb, Folkmann et al. 2015).

Expression of an ALS causing variant of SOD1 (G93A) in NSC-34 cells causes retention of RNA within the nucleus, as measured by an increased nuclear to cytoplasmic ratio of RNA transcripts identified using RNA-seq (Kim, Hong et al. 2017). This retention was not accompanied by an increase in transcripts containing introns suggesting that the nuclear retention was not linked to defects in splicing but rather likely due to defects in nuclear trafficking (Kim, Hong et al. 2017).

Recently, multiple groups have shown interactions between the C9orf72 repeat or its products with proteins involved in mRNA nuclear export. Multiple nucleoporins as well as CRM1 and SRSF7 have been identified as protein interactors of the dipeptide repeats PR and GR (Lee, Zhang et al. 2016). In a genetic screen in *Drosophila* aimed at discovering modifiers of the C9orf72 phenotype, proteins involved in mRNA export were identified. The strongest suppressor was found to be Aly, with partial loss of function of NXF1, CHTOP, NCBP2, ARS2, Gle1 and CRM1 enhancing the phenotype. Importantly, expression of the repeat in cells led to an accumulation of poly (A)+ mRNA within the nucleus, which can be decreased with Aly knockdown (Freibaum, Lu et al. 2015). Others have also shown the accumulation of poly (A)+ mRNA within the nucleus of cells transfected with the C9orf72 repeat accompanied by the nuclear accumulation of PABPc with binds to the C9orf72 RNA. PABPc accumulation is a phenomenon reminiscent of viral infection where nuclear PABPc nuclear accumulation is sufficient to cause nuclear mRNA retention (Rossi, Serrano et al. 2015).

Recently we have shown that Matrin 3, a nuclear matrix protein mutated in rare forms of ALS, binds to many TREX components and proteins involved in nuclear RNA export including, Aly, UAP56 and Sarnp in cell culture as well as nuclear spinal cord lysates (Boehringer, Garcia-Mansfield et al. 2017). The expression of ALS linked mutations in Matrin 3 in cell lines also causes the accumulation of poly (A)+ mRNA within the nucleus. These mutations also caused nuclear accumulation of mRNAs of ALS-relevant proteins TDP-43 and FUS linking mRNA nuclear retention to disease pathology (Boehringer, Garcia-Mansfield et al. 2017).

Alterations in nucleocytoplasmic transport have been identified by numerous groups in a wide range of neurodegenerative disorders including Alzheimer's disease, Huntington's disease, FTD and ALS. The identification of these alterations in such a wide span of neurodegenerative diseases suggests neuronal survival depends upon proper regulation of trafficking to and from the nucleus. While altered protein nucleocytoplasmic transport has been well documented in many neurodegenerative diseases, the only direct evidence for defective RNA transport has been the accumulation of poly (A)+ mRNA within the nucleus in patient derived tissue and various disease models. However, the alterations in both the localization and levels of nucleoporins and the loss of the Ran gradient and mislocalization of Ran binding proteins strongly suggests defects occur in the transport of all RNA subtypes. Further studies are necessary to explore how other RNA subtypes are mislocalized in neurodegenerative diseases. While it is unclear why defects in nucleocytoplasmic trafficking preferentially affect neurons, there is evidence to suggest that post-mitotic cells including neurons may be more susceptible to age related defects in nucleocytoplasmic transport. The proteins of the

NPC are normally replaced during cell division where they are disassembled and reassembled with newly synthesized proteins during mitosis (Rabut, Lenart et al. 2004). In post-mitotic cells such as neurons, the NPC is not completely disassembled and proteins such as Nup107 and Nup160 do not appear to turn over, suggesting that they are some of the longest-lived proteins in the body (D'Angelo, Raices et al. 2009, Savas, Toyama et al. 2012). The longevity of the NPC makes it vulnerable to the buildup of damage over time and unsurprisingly is subject to age related dysfunction (D'Angelo, Raices et al. 2009). The susceptibility of neurons as post-mitotic cells to defects in the NPC, as well as the age-related nature of neurodegenerative diseases, could explain the contribution of nucleocytoplasmic trafficking defects in these diseases. While there is clear evidence that these defects are present in neurodegenerative diseases such as Alzheimer's disease, Huntington's disease, FTD and ALS, the mechanism by which these defects occur as well as the role that these defects play in disease onset and pathogenesis remains unknown and merits continued study.

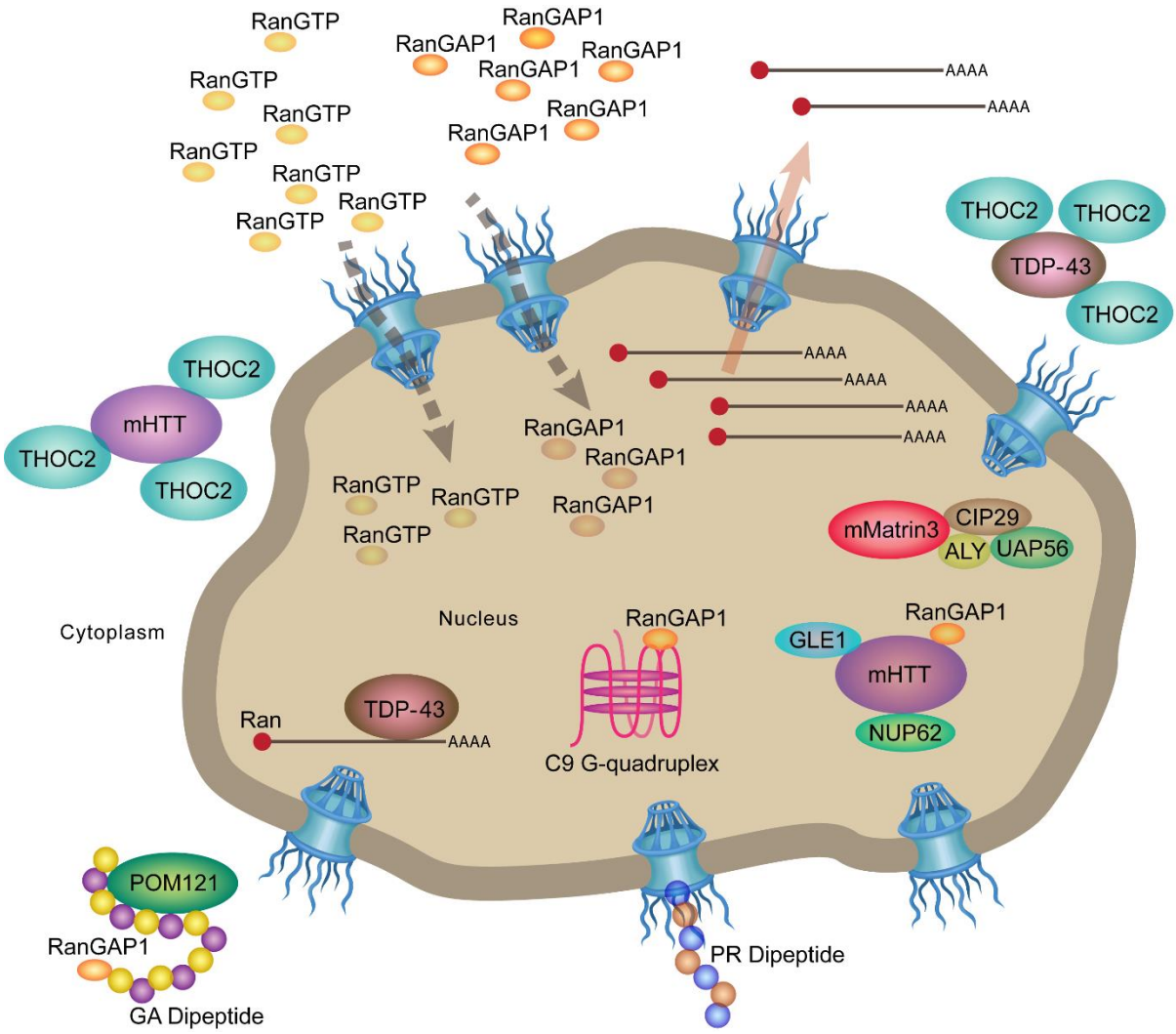

Figure 1.2 RNA export defects identified in neurodegenerative diseases.

Altered nuclear membrane morphology, interactions between DPRs and the nuclear pore, mislocalization and sequestration of export proteins into pathological aggregates, mutant proteins or pathological RNA species, interactions of TDP-43 with Ran mRNA as well as modifications to the Ran and RanGAP1 gradients, and decreased levels of mRNA export are all seen in a host of different neurodegenerative diseases.

CHAPTER 2

MUTATIONS IN THE MATRIN 3 GENE CAUSE FAMILIAL AMYOTROPHIC LATERAL SCLEROSIS

2.1 ABSTRACT

MATR3 is an RNA/DNA binding protein that interacts with TDP-43, a major disease protein linked to amyotrophic lateral sclerosis (ALS) and fronto-temporal dementia. Using exome sequencing, we identified mutations in MATR3 in ALS kindreds. We also observed MATR3 pathology in the spinal cords of ALS cases with and without MATR3 mutations. Our data provide additional evidence supporting the role of aberrant RNA processing in motor neuron degeneration.

2.2 INTRODUCTION

Amyotrophic lateral sclerosis (ALS) is a devastating neurodegenerative disease characterized by progressive paralysis and respiratory failure leading to death, typically within two to three years of symptom onset. Much attention has focused on the discovery of causal genes on the basis that understanding the pathophysiology underlying motor neuron degeneration would provide rational targets for therapeutic development. These efforts have been successful to the point that the genetic etiology of two thirds of the familial form of ALS and 11% of the more common sporadic form of the disease is now known (Renton, Chio et al. 2014). Nevertheless, the discovery of additional genes would allow complete mapping of the cellular pathways underlying this fatal neurological condition.

2.3 METHODS

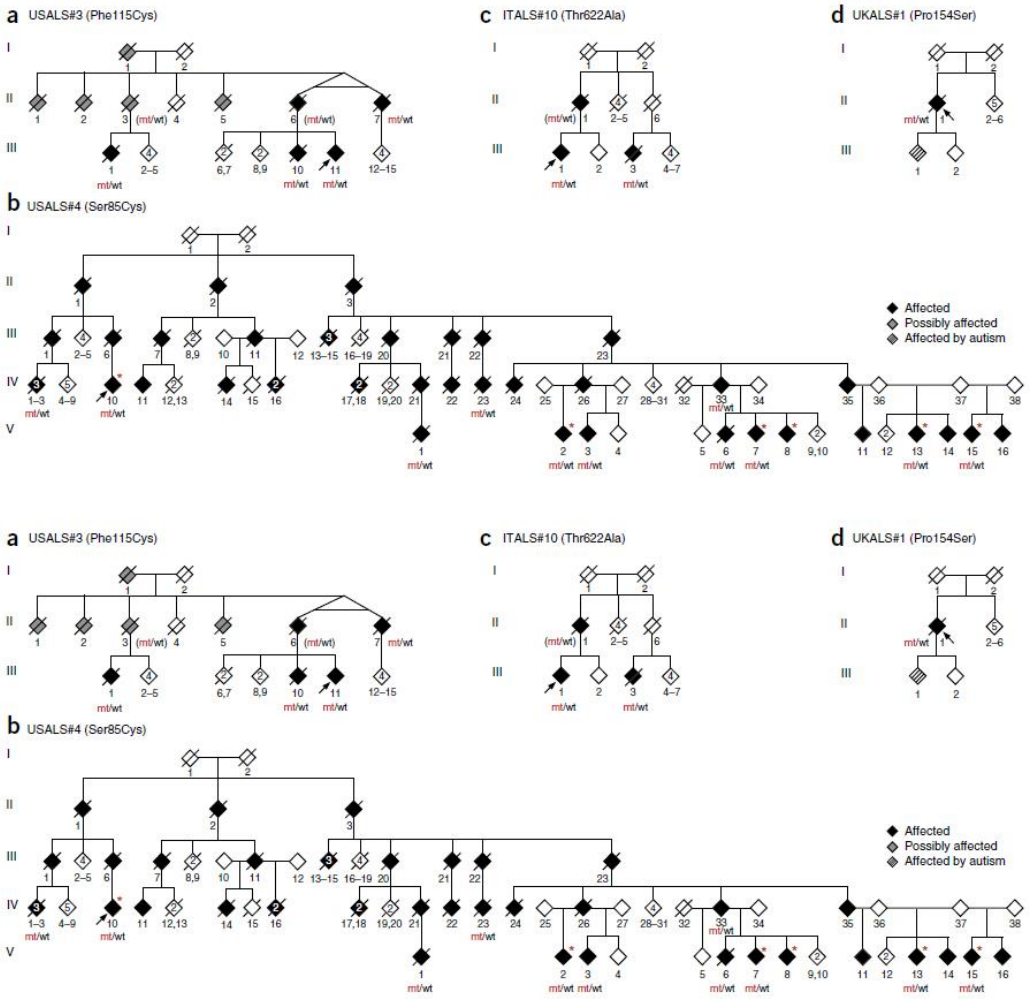

Figure 2.1 Pedigrees of patients with MATR3 mutations.

a) Kindred USALS#3. b) Kindred USALS#4. c) Kindred ITALS#10. d) Kindred UKALS#1. mt, mutant alleles; wt, wild-type alleles. Genotypes of presumed obligate carriers are in brackets. Red asterisks indicate individuals who underwent clinical examination. Arrows denote probands.

2.3.1 Description of Pedigrees

Description of the USALS#3 pedigree (Phe115Cys). The proband (III:11, Fig. 2.1a) developed dysarthria at 50 years of age. He developed gait difficulties because of leg stiffness and cramping in the feet. He began choking on liquids at age 51 and developed pseudobulbar affect but no detectable cognitive impairment. Nocturnal noninvasive ventilation was prescribed for obstructive sleep apnea since age 53. Neurological examination at 52 years revealed mild, predominantly spastic dysarthria; increased jaw jerk; brisk facial reflexes, especially on the right; and slowed lateral tongue movements. Mild muscle atrophy was noted in the right thigh and rare fasciculations were seen in the proximal upper limbs. Tone was mildly spastic in the right arm and lower limbs, with slowed right fine finger movements and right foot tapping. Power in upper and lower limbs was normal. Tendon reflexes were pathologically brisk throughout, with right extensor plantar response. Gait and sensation were normal.

Dysarthria, dysphagia, and distal weakness in upper and lower extremities progressed slowly over 2 years, requiring use of bilateral ankle foot orthoses. Most recent neurologic examination at age 55 revealed mild cognitive impairment with disinhibition and inability to vocalize (anarthria). Vertical saccades were slowed and upgaze was noticeably limited. Jaw jerk was markedly brisk with clonus, as were facial reflexes, and there was a hyperactive gag reflex. The tongue was severely atrophic, fasciculating, and unable to move off the midline or protrude beyond the lower teeth. Muscle atrophy was global, being moderate proximally and severe distally, especially in intrinsic hand muscles and forelegs. Fasciculations were active in both upper limbs and neck regions, and tone was markedly spastic in the arms and legs, particularly over the right side.

Weakness was most prominent distally in hands and feet, with little or no movement of thumb and fingers (0–2/5) and ankle and toes (0–2/5). Proximal upper and lower limb strength was better (4/5), allowing the patient to stand, although shoulder pain from contractions limited useful arm function. Tendon reflexes were pathologically brisk throughout, more marked on the right with ipsilateral extensor plantar response. He was unable to walk because of the weakness and spasticity, and used a wheelchair for mobility.

Patient II:6. The mother of the proband (II:6, Fig. 2.1a) developed bilateral finger and hand weakness at age 70. This was followed a few months later by speech and swallowing problems, and ALS was diagnosed at age 71. Her father had died at 47 years of age after a prolonged course involving leg muscle weakness. Three siblings died in their eighties: one (II:1) died of dementia, another (II:2) developed limb weakness and was unable to walk at the time of death, and a third (II:5) died of dementia and also was reported to be dysarthric and to have upper limb weakness.

Neurological examination at 71 years revealed normal speech and cognition, brisk facial reflexes, mentalis muscle fasciculations and weak (4/5) neck flexors. Fasciculations were seen in both upper extremities and thighs, with moderate atrophy of intrinsic hand muscles. She was weaker distally, with thumb abductors, thumb flexors and intrinsic hand muscles 3/5, shoulder abductors 4/5, ankle dorsiflexors and toe extensors 4/5, and hip flexors 4/5. Tendon reflexes were pathologically brisk, with a right extensor plantar response. Gait was unsteady and partially steppage in nature. Over the next 3 years, her limbs became progressively paralyzed and she developed dysarthria and mild cognitive impairment. She died of respiratory failure at 75 years of age.

Patient II:7. An aunt of the proband (II:7, Fig. 2.1a) and identical twin of the proband's mother developed slowly progressive hand weakness at 57 years of age. Four years later, she began experiencing dysarthria, at which point she was diagnosed with ALS. Her weakness gradually spread to the rest of her limbs and she developed severe cognitive impairment. Currently, at age 82, she is unable to stand or walk and uses a wheelchair for mobility. Her hand weakness has deteriorated to the point that she cannot feed herself or brush her teeth, and she is aphasic. She has respiratory failure (forced vital capacity 49%).

Patient III:10. The proband's older sibling (III:10, Fig. 2.1a) developed right (dominant) hand stiffness and cramping at 52 years of age. At 57 years, he began experiencing progressive weakness of right hand and finger muscles resulting in inability to button or tie shoelaces. Atrophy of intrinsic right hand muscles was also noted. The patient denied leg weakness but would develop cramping of thigh muscles after squatting. About 18 months later the patient noticed worsening left hand weakness. There were no bulbar symptoms or shortness of breath initially.

Neurological examination at age 58 revealed no cognitive or behavioral abnormalities, normal speech, and no bulbar signs except for slightly increased right facial reflex and right palmomental reflex. Upper limbs showed moderate atrophy of distal muscles, especially of the lateral hand in a split hand pattern, with continuous fasciculation of right more than left shoulder and arm muscles. Lower limbs showed no changes. Tone was normal throughout. Weakness was most prominent distally and slightly worse on the right, with thumb abductors and deep finger flexors 3/5, finger abductors and extensors 4/5, wrist flexors and extensors 4+/5, and elbow flexors and

extensors almost 5/5. Tendon reflexes were pathologically brisk throughout, with left extensor plantar response. Over the next 2 years, the patient's condition gradually deteriorated, with progressive limb and respiratory muscle weakness. The patient expired 2 years later from respiratory failure at 60 years of age. Brain and spinal cord were obtained for pathologic analysis.

Patient III:1. A cousin of the proband (III:1, Fig. 2.1a) initially presented with lower limb weakness at 63 years of age. Symptoms progressed to involve the remaining limbs and bulbar musculature. Severe dysphagia necessitated the placement of a gastrostomy tube. The patient's mother (II:3) died of dementia in her eighties. The patient became cognitively impaired several years after the initial presentation and died from respiratory failure at the age of 68. Affected members of the USALS#3 kindred were negative for the pathogenic repeat expansion of C9ORF72.

Description of the USALS#4 pedigree (Ser85Cys). The proband of the USALS#4 family (IV:10, Fig. 2.1b) developed right foot drop at 44 years of age. Muscle weakness spread to the remaining limbs over the next 2 years. A diagnosis of Charcot-Marie-Tooth disease was made at the age 46 on the basis of a neurogenic pattern observed in an electromyogram and nerve conduction studies (EMG/NCS). Reevaluation 2 years later led to the patient's illness being reclassified as non-Scandinavian distal myopathy. The patient's condition progressed, with the development of dysarthria and mild dysphagia by the age of 53 and respiratory failure requiring nocturnal noninvasive ventilation by the age of 56. Currently, at age 65, the subject uses a power wheelchair for mobility.

Neurological examination at age 65 revealed mild dysarthria, perioral fasciculations, a brisk jaw jerk and moderately weak neck extension. There was generalized muscle wasting and pyramidal-distribution weakness in all four limbs. In the upper limbs, shoulder abduction was 3/5 bilaterally, elbow extension was 4/5, wrist extension and finger extension were 1/5, and finger abduction, finger adduction and thumb abduction were 3/5, whereas shoulder adduction, elbow flexion, wrist flexion and abductor digiti minimi were 5/5 bilaterally. In the lower limbs, hip flexion was 4/5 bilaterally; ankle dorsiflexion, ankle plantar flexion and extensor hallucis longus were 0/5, whereas hip abduction, hip adduction, knee flexion and knee extension were 5/5 bilaterally. Tendon reflexes were absent, and toes were mute on Babinski testing. Proprioception and vibration sensation were diminished to the level of the ankles and knees, respectively, bilaterally. The patient was able to stand and walk slowly using a walker and with the assistance of one person.

Patient V:2. A cousin of the proband (V:2, Fig. 2.1b) noticed right foot drop at 42 years of age. Within 5 years, the muscle weakness had spread to involve both hands. The patient developed dysarthria and mild dysphagia at age 47 and respiratory failure requiring supplemental oxygen and noninvasive ventilation at 49. The patient had an episode of aspiration pneumonia at age 55 that required prolonged intubation and ventilation. Currently, at age 57, the patient uses a power wheelchair but can walk slowly using a walker.

Neurological examination at age 57 revealed mild dysarthria, mild facial weakness, poor palate elevation and a brisk jaw jerk. Limb examination showed generalized muscle atrophy and a pyramidal pattern of weakness. In the upper limbs,

shoulder abduction and elbow extension were 4/5 bilaterally, wrist dorsiflexion was 1/5, finger extension and thumb abduction were 3/5, and finger flexion and abductor digiti minimi were 4/5, whereas shoulder adduction, elbow flexion and wrist flexion were 5/5 bilaterally. In the lower limbs, hip flexion was 4/5 bilaterally, and ankle dorsiflexion, ankle plantar flexion, toe flexion and toe extension were 1/5, whereas hip abduction, hip adduction, knee flexion and knee extension were 5/5 bilaterally. Deep tendon reflexes were absent in the upper limbs. The right knee jerk was 2+, and the left knee jerk was brisk (3+). Ankle jerks were absent and toes were mute on Babinski testing. There was loss of pinprick and temperature sensation to the mid-calf level bilaterally.

Patient V:7. A cousin of the proband (V:7, Fig. 2.1b) observed right leg weakness at 33 years of age. Symptoms progressed to the point that the patient has been using a power wheelchair since 57, although continuing to walk slowly using a rollator walker as part of an exercise regimen. Hand weakness developed at age 60, and the subject had an episode of aspiration pneumonia requiring prolonged intubation and hospitalization at age 63. The patient has required nocturnal noninvasive ventilation and daytime oxygen supplementation since that time. Mild dysphagia and occasional choking episodes required changes in food consistency.

Neurological examination at age 65 revealed mild dysarthria, mild facial weakness and a brisk jaw jerk. Generalized limb atrophy and pyramidal-distribution weakness was evident. In the upper limbs, shoulder abduction, elbow flexion and elbow extension were 4/5 bilaterally, wrist extension was 3/5, finger extension was 4/5 and thumb abduction was 3/5, whereas shoulder adduction, wrist flexion and adductor digiti minimi were 5/5 bilaterally. In the lower limbs, hip flexion was 4/5 bilaterally, hip

abduction and hip adduction were 3/5, knee flexion and knee extension were 1/5, ankle dorsiflexion and ankle plantar flexion were 0/5, and toe extension was 1/5 bilaterally. Deep tendon reflexes were absent in all four limbs, and toes were mute on Babinski testing. Temperature sensation was diminished to the mid-calf level bilaterally.

Patient V:8. A cousin of the proband (V:8, Fig. 2.1b) presented with dysarthria and choking at 47 years of age. The patient developed left ankle weakness at age 52. Weakness had spread to both hands by age 58. Currently, at age 63, the patient has difficulty using eating utensils and walks with the aid of a walker.

Neurological examination at age 63 revealed dysarthria with nasal air escape, poor palate elevation, tongue fasciculations and a brisk jaw jerk. There was marked distal atrophy and weakness. In the upper limbs, wrist extension was 4/5 bilaterally, finger extension and thumb abduction were 3/5, and left abductor digiti minimi was 4/5, whereas bilateral shoulder abduction, shoulder adduction, elbow flexion, elbow extension, wrist flexion and right adductor digiti minimi were 5/5. In the lower limbs, ankle dorsiflexion and ankle invertors were 3/5 bilaterally and extensor hallucis longus was 4/5, whereas hip flexion, hip extension, hip abduction, hip adduction, knee flexion, knee extension, ankle plantar flexion and foot evertors were 5/5 bilaterally. Triceps reflexes were brisk (3+) bilaterally, whereas other deep tendon reflexes in the upper limbs were normal (2+). Knee jerks were brisk (3+) bilaterally, ankle jerks were absent, and toes were mute on Babinski testing. Vibration sensation was diminished to the level of the ankles bilaterally.

Patient V:13. A cousin of the proband (V:13, Fig. 2.1b) noticed mild dysarthria and throat-clearing difficulties at 42 years of age. At age 44, the subject developed right leg weakness that spread to involve the left leg and both hands by age 51. The patient occasionally chokes when eating. Currently, at age 58, the patient remains mobile with the aid of bilateral ankle orthotics.

Neurological examination, at age 58, revealed trace dysarthria. There was prominent distal muscle atrophy. In the upper limbs, right shoulder abduction was 4/5 bilaterally and wrist extension and finger extension were 3/5, whereas shoulder adduction, elbow flexion, elbow extension, wrist flexion and finger flexion were 5/5 bilaterally. In the lower limbs, left hip flexion was 4/5, ankle dorsiflexion was 2/5 bilaterally and extensor hallucis longus was 3/5, whereas hip extension, hip abduction, hip adduction, knee flexion, knee extension and ankle plantar flexion were 5/5 bilaterally. In the upper limbs, reflexes were diminished (1+). In the lower limbs, knee jerks were brisk (3+ with crossed adductors), ankle jerks were absent, and the toes were mute on Babinski testing. All sensory modalities were intact.

Patient V:15. A cousin of the proband (V:15, Fig. 2.1b) developed hand weakness at 49 years of age. Currently, at age 50, the patient complains of fatigue, frequent cramping of the right foot, and mild dysarthria when fatigued.

Neurological examination, at age 50, revealed bilateral thenar and first dorsal interossei muscle atrophy. In the upper limbs, wrist extension, finger extension and thumb abduction were 4/5 bilaterally, whereas shoulder abduction, shoulder adduction, elbow flexion, elbow extension, wrist flexion and finger flexion were 5/5 bilaterally. In the lower limbs, extensor hallucis longus was 4/5 bilaterally, whereas all other muscle

groups were 5/5. Reflexes in the upper limbs were 2+ with the exception of the left brachioradialis, which was diminished (1+).

In the lower limbs, knee jerks were brisk (3+ with crossed adductors) bilaterally, ankle jerks were absent, and toes were downgoing on Babinski testing. Vibration sensation was diminished to the level of the ankle bilaterally. The patient had difficulty with heel walking and toe walking.

In summary, the clinical features of patients in the Ser85Cys MATR3 kindred were consistent with a progressive, fatal motor neuron disease with combined upper and lower motor neuron signs, bulbar dysfunction and respiratory failure.

Description of the ITALS#10 pedigree (Thr622Ala). The proband (III:1, Fig. 2.1c) developed spinal ALS presenting with left foot drop at 62 years of age. MRI with diffusion tensor imaging revealed bilateral corticospinal tract damage. The patient was cognitively normal on exam, and [18F]fluorodeoxyglucose PET imaging was also reported to be normal. The patient remains alive 32 months after symptom onset and uses noninvasive ventilation for 12 h per day.

Patient III:3. A cousin of the proband (III:3, Fig. 2.1c) presented with a 5-month history of progressive right arm weakness at 60 years of age. Neurological examination at the time of presentation showed weakness and hypotrophy in upper limbs, more evident on the right side and in distal muscles. Deep tendon reflexes were diffusely brisk, especially on the right. MRIs of the brain and cervical spinal cord were normal. EMG showed active and chronic denervation in upper limbs muscles, whereas motor evoked potentials revealed increased central conduction time. Over the following months, the patient’s symptoms progressed to involve the lower limbs and respiratory muscles. She

died 33 months after disease onset of respiratory failure. No mutation in known ALS-associated genes, including the pathogenic repeat expansion of C9ORF72, segregated with disease in the ITALS#10 kindred.

Description of the UKALS#1 pedigree (Pro154Ser). The proband of the UKALS#1 family (II:1, Fig. 2.1d) was Indian and developed upper limb weakness at 59 years of age. There was no family history of ALS or dementia, though an offspring (III:I) was diagnosed with autism. Over the next 3 years, the patient's symptoms spread to involve the remaining limbs and bulbar musculature. The patient now uses a wheelchair for mobility and requires ventilator support for respiratory failure, a gastrostomy tube for feeding and an eye-tracking system for communication. Neurological examination, at age 62, revealed widespread upper and lower motor neuron signs and bulbar involvement consistent with a diagnosis of ALS.

The affected member of UKALS#1 was negative for mutations in known ALS-associated genes, including the pathogenic repeat expansion of C9ORF72.

2.3.2 Additional Samples

For subsequent mutational screening, we examined exome sequence data that had been generated in our laboratory using DNA obtained from 108 individuals (n = 6 Canadians, n = 14 Germans, n = 9 Israelis, n = 32 Italians, n = 47 from the United States) who had been diagnosed with familial ALS and who were negative for mutations in known ALS-associated genes, including the pathogenic hexanucleotide repeat expansion of C9ORF72. Average age of symptom onset among this cohort was 55.1 (range, 15.0–79.0), and 47.2% were male.

Multiethnic control samples consisted of a series of 1,051 anonymous samples that are part of the Human Gene Diversity Panel (http://www.cephb.fr/en/hgdp/diversity.php/). These samples come from the following geographical regions: Africa (n = 122), Algeria (n = 30), Brazil (n = 45), Cambodia (n = 11), China (n = 182), Colombia (n = 13), France (n = 53), Israel (n = 144), Italy (n = 50), Japan (n = 30), Mexico (n = 50), New Guinea (n = 39), Orkney Islands (n = 16), Pakistan (n = 199) and Russia (n = 67).

Neurologically normal control subjects who were genotyped as part of the genome-wide association study that was ongoing in the Laboratory of Neurogenetics, NIA, consisted of samples from the United States (n = 2,882), the United Kingdom (n = 677), Italy (n = 1,242) and Finland (n = 389).

The appropriate institutional review board (National Institute on Aging Institutional Review Board protocol number 2003-081) approved the study, and informed consent was obtained from all subjects included in this study.

2.3.3 Exome sequencing and bioinformatic analysis pipeline.

DNA from affected individuals II:7, III:1, III:10 and III:11 of the USALS#3 family was enriched using TruSeq technology (version 1.0) and paired-end sequenced on a Hiseq2000 sequencer according to the manufacturer's protocol (Illumina, San Diego, CA). This generated 8.0 gigabases (Gb) of alignable sequence data for individual II:7, 15.4 Gb for III:1, 7.8 Gb for III:10 and 9.7 Gb for III:11 (mean 10× coverage = 95.4%, range 94.3 to 98.0%; mean 30× coverage = 87.9%, range 85.1 to 93.1%). Exome sequence data from the additional 108 familial ALS samples were generated in a similar manner. Sample randomization was not performed and the researchers were not blinded

to genotype. Statistical methods were not used to predetermine sample sizes, but rather our sample sizes were dictated by patient availability and are similar to those generally employed in the field.

Sequence alignment and variant calling were performed against the reference human genome (UCSC hg 19) using the Genome Analysis Toolkit (http://www.broadinstitute.org/gatk/). PCR duplicates were removed before variant calling using Picard software (http://picard.sourceforge.net/index.shtml).

A series of standard filters was applied to the exome sequence data generated for the USALS#3 family to identify the causative mutation. First variants and indels that were not shared by all four affected members were excluded. Next variants and indels that were homozygous or nonautosomal were excluded. Then synonymous and noncoding changes were identified using the SeattleSeq online tool (annotation 137, http://snp.gs.washington.edu/SeattleSeqAnnotation137/index.jsp) and filtered from the variant list. Under the hypothesis that the mutation underlying this rare familial disease was not present in the general population, SNPs identified in the Exome Sequencing Project (n = 6,500, http://evs.gs.washington.edu/, accessed 25 March 2013), the 1000 Genomes project (n = 1,092, 20110521 release, version 3, http://www.1000genomes.org/, accessed 25 March 2013) or dbSNP (build 137, http://www.ncbi.nlm.nih.gov/SNP/, accessed 25 March 2013) were filtered. As an additional step, variants and indels detected in the USALS#3 family were filtered against exome data generated in our laboratory for 200 neurologically normal control subjects. Fig. 2.2 shows the number of variants filtered by each of these steps in the USALS#3 pedigree, Fig 2.3 shows the genomic location of the two novel coding variants identified

by exome sequencing. Sanger sequencing using customized primers was performed to confirm the presence of the two remaining variants. Exome data for the 108 familial ALS cases was processed in an identical manner.

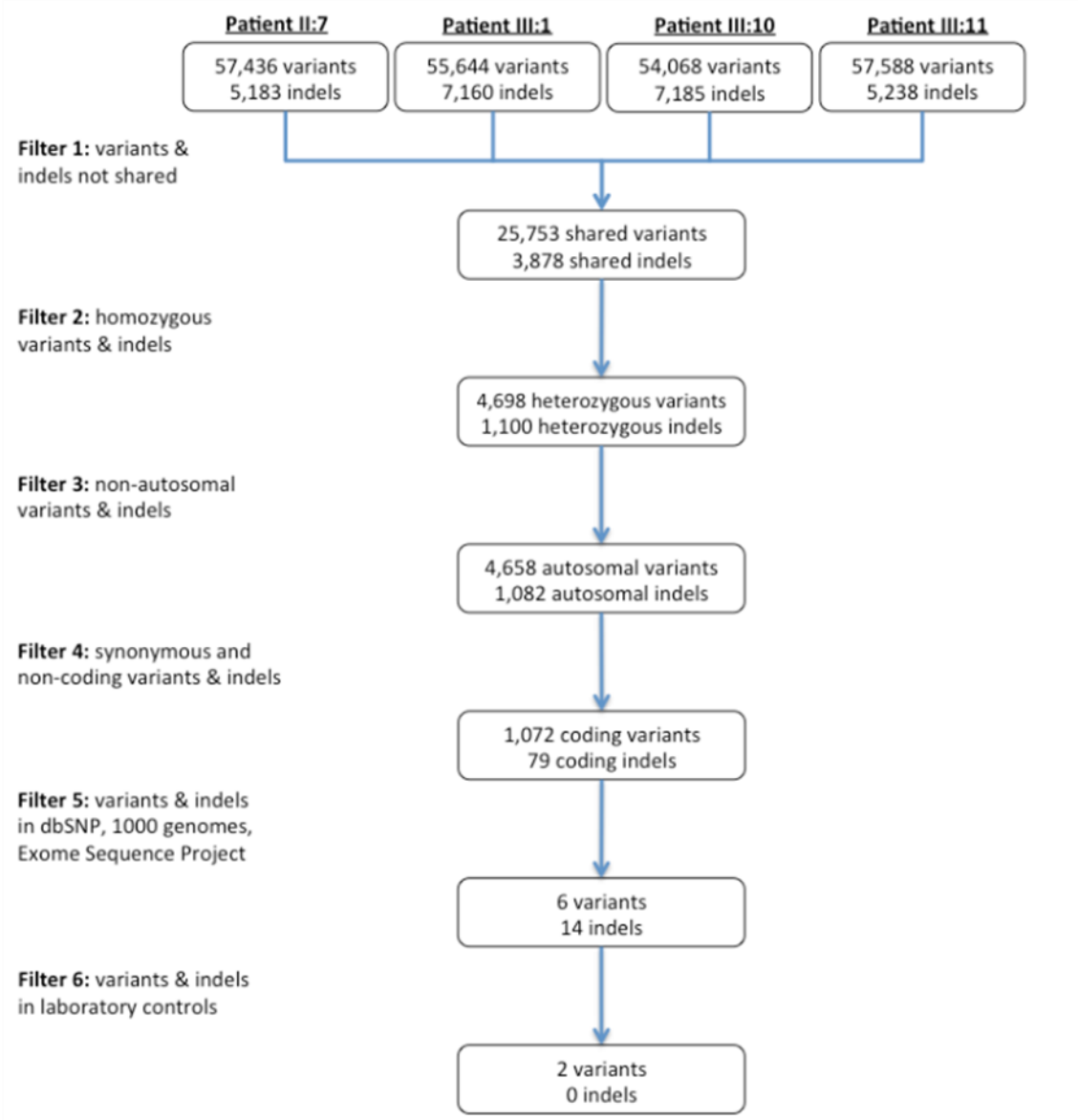

Figure 2.2 Filters applied to variants and indels detected by exome sequencing in affected individuals of the USALS#3 pedigree

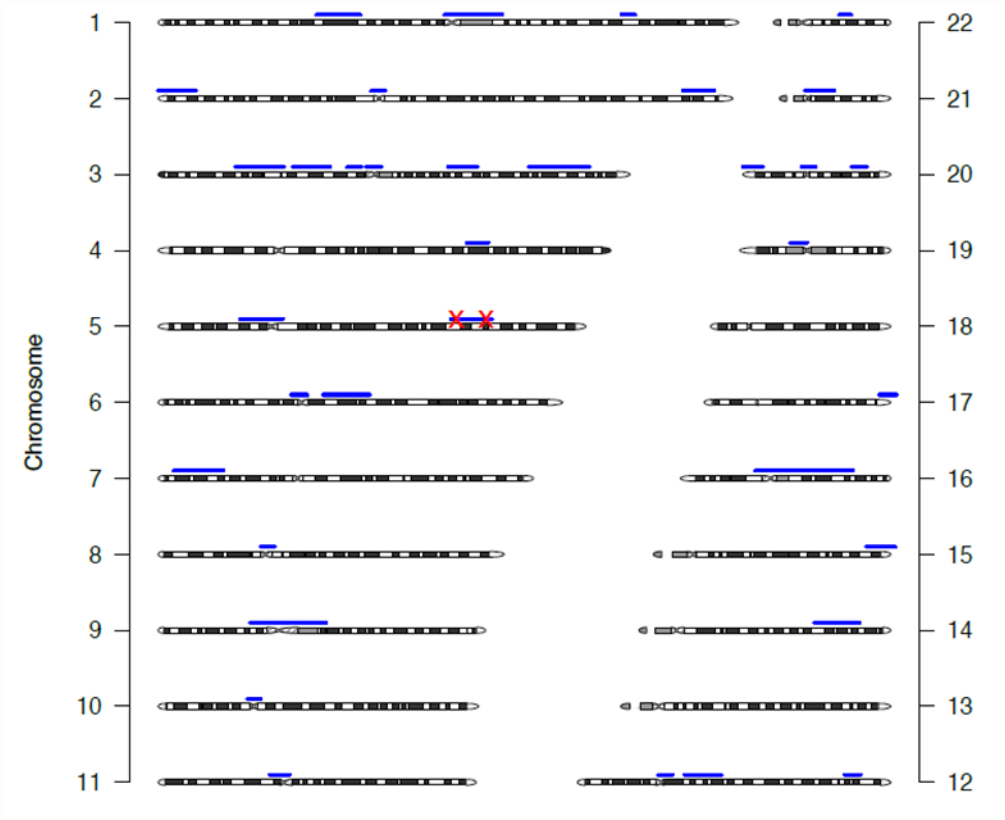

Figure 2.3 Novel Coding Variants Identified in the USALS#3 Kindred by Exome Sequencing.

Graphical representation of autosomes showing genomic regions shared by the four affected individuals of the USALS#3 pedigree (blue lines). Whole genome data was generated using Infinium OmniExpress genotyping arrays (Illumina Inc.). LMNB1 and MATR3 variants are shown as red crosses located within a 17.4 Mb shared segment on chromosome 5q. No other novel, coding variants were shared across affected individuals of the USALS#3 family.

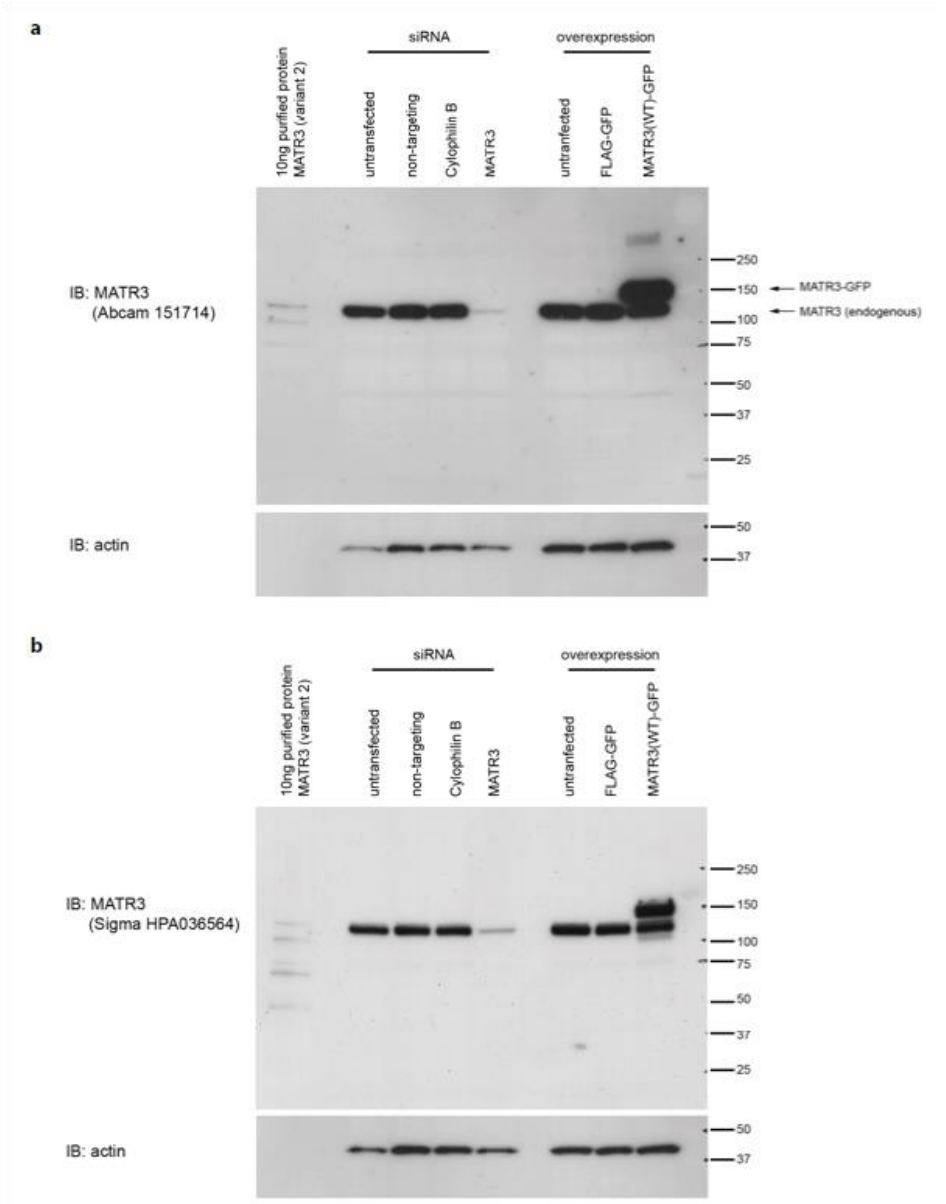

Figure 2.4 Characterization of MATR3 Antibodies.

The specificity of MATR3 antibodies Abcam 151714 (a) and Sigma HPA0036564 (b) were tested against purified MATR3 protein (Origene TP323258), lysates from HEK293FT cells treated with siRNA (untransfected control, non-targeting control, Cyclophilin B and MATR3), and cells overexpressing MATR3(WT)-GFP. Both antibodies were specific to MATR3 as indicated by the MATR3 siRNA sample showing a reduction in MATR3 protein level compared to untransfected, non-targeting and Cyclophilin B controls.

2.3.4 Genotyping

Genotyping of the LMNB1 (chr5:126156748, C>T, Ala436Val, NM_005573.3) and MATR3 (chr5:138643448, T > G, Phe115Cys, NM_199189.2) variants was performed in the Human Gene Diversity Panel samples using Taqman SNP genotyping assays (Life Technologies Corp., Grand Island, NY, USA) on the 7900HT Fast Real Time PCR System according to the manufacturer's instructions (Applied Biosystems Inc., Foster City, CA, USA).

The MATR3 chr5:138643448, T > G (Phe115Cys) and chr5:138643358, C>G (Ser85Cys) variants were assayed in an additional 5,190 neurologically normal control subjects of European ancestry as part of a genome-wide association project that was ongoing in the Laboratory of Neurogenetics, NIA, using the HumanExome+ SNP chip with custom content (Illumina).

2.3.5 Immunohistochemistry of spinal cord and muscle

Immunohistochemistry of spinal cord. Immunohistochemistry was performed on lumbar spinal cord from ALS patients (n = 16), neurologically normal controls (n = 6) and one ALS patient with the Phe115Cys MATR3 mutation as follows: tissues were deparaffinized, rehydrated and subjected to antigen retrieval for 20 min in a steamer in pH 9 buffer (Dako Inc., Carpinteria, CA, USA) for the Sigma antibody, and in pH 6 citrate buffer (BioGenex Inc., Freemont, CA, USA) for the Abcam antibody. This was followed by 20 min incubation in buffer warmed to 100 °C. Next, slides were blocked in Superblock (ScyTek Laboratories Inc., West Logan, UT, USA) with avidin protein (Vector Laboratories Inc., Burlingame, CA, USA) for 1 h, after which primary antibody diluted in Superblock (Pierce Biotechnology, Rockford, IL, USA) with biotin (Vector

Laboratories) was added for a second hour, with PBS washes in between. Slides were then incubated in biotinylated horseradish peroxidase (HRP)-conjugated secondary antibody (catalog number B-2004, 1:200 dilution, Vector Laboratories). The primary anti-MATR3 antibodies were HPA036565 (1:500 dilution, Sigma-Aldrich Corp., St. Louis, MO, USA) and ab151714 (1:500 dilution, Abcam PLC, Cambridge, MA, USA) (see Fig. 2.4 for characterization of these antibodies). Slides were incubated with Vectastain Elite ABC reagent (Vector Laboratories) for 30 min, washed in PBS, and developed for 5 min using Vector NovaRED Substrate Kit (Vector Laboratories). Finally, slides were counterstained with Mayer's hematoxylin (Sigma-Aldrich) for 1 min, dehydrated, and mounted in Permount medium.

All pictures were taken with an Olympus BX40 light microscope, and images were acquired using a Nikon DS L2 digital camera. Image analysis was performed with Photoshop CS5 (Adobe Systems Inc., San Jose, CA, USA). All of the samples shown were processed at the same time.

Immunohistochemistry of skeletal muscle. Cryostat sections of rapidly frozen skeletal muscle were processed in a standard fashion consistent with ref. (Weihl, Temiz et al. 2008). Immunocytochemistry for each antibody was performed on tissue from patients and compared with normal tissue controls processed simultaneously. Primary antibodies used in this study were TDP-43 rabbit polyclonal antibody (catalog number 10782-2-AP, ProteinTech Antibody Group, Chicago, Illinois, USA) and MATR3 mouse monoclonal (catalog number sc-81318, Santa Cruz, Santa Cruz, CA). Dilutions were both 1:1,000. Double-labeling immunofluorescence was performed as previously described using secondary antibodies conjugated to Alexa Fluor 488 and 594 (Invitrogen, catalog

numbers A-21200 and A-21442, 1:200 dilution). Sections were examined using a fluorescence microscope (80i upright; Nikon) and charge-coupled device camera (EZ monochrome; Roper Industries) with deconvolution software analysis (NIS Elements; Nikon). Image processing and analysis were performed with NIS Elements 4.0 software and Photoshop CS3 (Adobe Systems Inc.).

2.3.6 Immunoprecipitation

Mutations (Ser85Cys, Phe115Cys and Thr622Ala) were introduced into Flag-tagged MATR3 cDNA plasmid (Addgene, Cambridge, MA, USA) using a QuikChange II XL Site-Directed Mutagenesis Kit (Agilent Technologies Inc., Santa Clara, CA, USA). All plasmids were sequence-verified. For Flag immunoprecipitation of MATR3, HEK293FT cells (Life Technologies Corp., Grand Island, NY, USA) transiently expressing Flag-MATR3 were lysed with lysis buffer (50 mM Tris-HCl pH 7.5, 150 mM NaCl, 1mM EDTA, 0.5% (v/v) NP-40, phosphatase (Thermo Scientific, number 78427) and protease inhibitor (Roche, catalog number 04693159001) for 30 min at 4 °C. Lysate was precleared with EZview Red Protein G Affinity Gel (Sigma-Aldrich) for 30 min at 4 °C, followed by immunopurification with EZview Red Anti-Flag M2 Affinity Gel (catalog number F2426, Sigma-Aldrich) for 2 h at 4 °C. Protein-gel complexes were washed four times with lysis buffer. MATR3 was eluted using Gentle Ag/Ab Elution Buffer (Thermo Fisher Scientific Inc., Rockford, IL, USA) for 30 min at room temperature.

Protein samples were prepared for SDS-PAGE in SDS sample buffer (Life Technologies) and boiled at 95 °C for 10 min before electrophoresis on 4–20% TGX gels (Bio-Rad Laboratories Inc., Hercules, CA, USA). Proteins were transferred to PVDF

membranes using the semi-dry Trans-Blot Turbo Transfer System (Bio-Rad). Membranes were blocked with 5% non-fat milk OmniBlok (American Bioanalytical Inc., Natick, MA, USA). The following primary antibodies were used at the indicated dilutions: rabbit anti-MATR3 ab151714 (1:200, Abcam), rabbit anti-MATR3 HPA036564 (1:200, Sigma-Aldrich), mouse anti-Flag F1804 (1:5,000, Sigma-Aldrich), rabbit anti-TDP43 10782-2-AP (1:2,000, ProteinTech Group Inc., Chicago, IL, USA) and rabbit anti-DHX9 A300-855A (1:2,000, Bethyl Laboratories Inc., Montgomery, TX, USA). Immunoreactivity was revealed using appropriate HRP-conjugated secondary antibodies (1:5,000, Jackson ImmunoResearch Laboratories Inc., West Grove, PA, USA, catalog numbers 711-035-1521 and 715-035-1501) and the ECL Plus chemiluminescent system (Pierce). Quantitation was performed using ImageJ software (version 1.41, National Institutes of Health, USA). Wilcoxon signed-rank test was used to estimate significance for differences in median values of interaction of MATR3 with TDP-43 and DHX9, comparing the values relative to wild-type protein in each experiment.

2.4 RESULTS

Here, we applied exome sequencing to a Caucasian family in which several individuals had been diagnosed with ALS and dementia (Fig. 2.1a) with the aim of identifying the causative mutation. We found two novel, heterozygous, missense variants that segregated with disease within this kindred, namely p.Ala436Val (chr5:126156748, C>T) in LMNB1 and p.Phe115Cys (chr5:138643448, T>G) in MATR3. Neither variant was present in population polymorphism databases (including the Exome Sequencing Project (n = 13,000 control chromosomes), the 1000 Genomes Project (n = 2,184

chromosomes) and dbSNP), or in the Human Gene Diversity Panel (HGDP, n = 2,102 chromosomes screened in our laboratory). The MATR3 variant was also not present in an additional 5,190 neurologically normal subjects genotyped in our laboratory, bringing the total number of control chromosomes that did not carry this transversion to 27,666.

A p.Ser85Cys (chr5:138643358, C>G) mutation in MATR3 was previously reported as the cause of autosomal dominant, distal, asymmetrical myopathy with vocal cord paralysis in a large multi-generational family (Fig. 2.1b) (Feit, Silbergleit et al. 1998, Senderek, Garvey et al. 2009). Neurophysiological studies and muscle biopsies of affected members were variably reported to be consistent with either a neurogenic or a myopathic pattern. In light of our genetic findings, the senior author (BJT) and the neurologist who initially reported this family (HF) re-evaluated the p.Ser85Cys MATR3 family. Affected individuals developed progressive respiratory failure resulting in death, typically after fifteen years of illness.

Pathologically brisk knee reflexes, indicative of upper motor neuron lesions, were present in four of six examined patients. One patient also had brisk upper limb reflexes, as well as tongue fasciculations and a brisk jaw jerk. All of the examined cases displayed a “split-hand” pattern of weakness suggestive of a lesion in the anterior horn of the cervical spinal cord, a sign commonly observed in ALS patients (Eisen and Kuwabara 2012). These clinical findings supported reclassification of this condition as slowly progressive ALS, and the presence of upper motor neuron signs in the form of brisk reflexes ruled out myopathy as the only cause of disease in this family.

To determine the frequency of MATR3 mutations as a cause of ALS, we examined exome sequence data from 108 additional familial ALS cases. We identified a

p.Thr622Ala (chr5:138658372, A>G) missense change in MATR3 in a 66-year-old Sardinian diagnosed with familial ALS. This variant was present in a first-degree cousin, who had also presented with typical, rapidly progressive ALS at the age of 64 (Fig. 2.1c). In addition, custom resequencing of genes linked to neurodegeneration in 96 British ALS cases identified a p.Pro154Ser (chr5:138643564, C>T) missense variant in MATR3 in an individual diagnosed with sporadic disease (Fig. 2.1d and Fig. 2.5). Again, neither mutation was present in population polymorphism databases or in HGDP (n = 17,286 control chromosomes). Though these data are supportive, additional studies are required to confirm the pathogenicity of these variants, especially p.Pro154Ser, which was found in a single sporadic case and consequently lacks segregation data. We did not find any additional mutations in the LMNB1 gene.

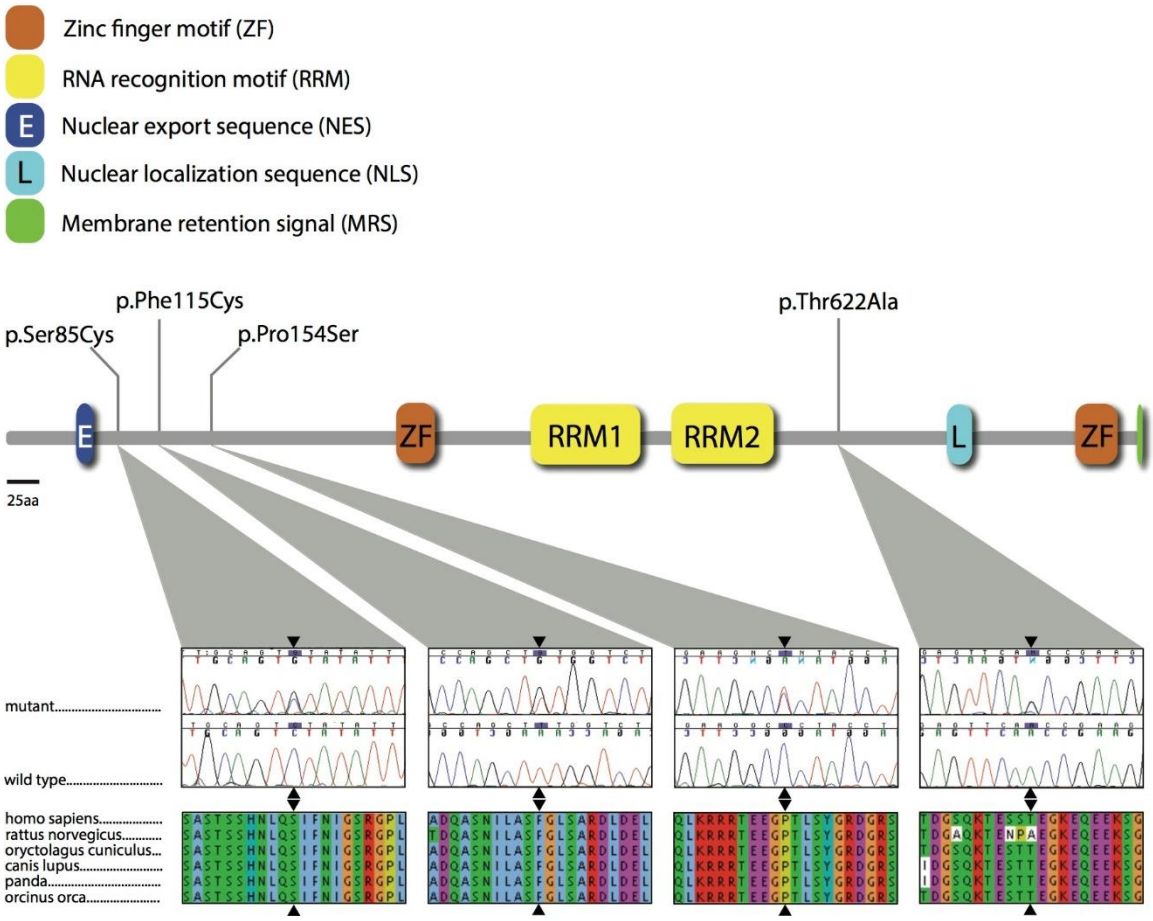

Figure 2.5 Distribution of MATR3 Mutations Detected in Familial ALS Patients.

The upper panel shows the location of detected mutations and of the domains of MATR3 as determined by Hibino, Y., et al. Biochim. Biophys. Acta 1759, 195–207 (2006). Corresponding chromatograms showing mutant and wild-type alleles are as indicated, and conservation of amino acid residue across species is highlighted at the bottom (generated using the Clustal Omega online tool, www.ebi.ac.uk/Tools/msa/clustalo/).

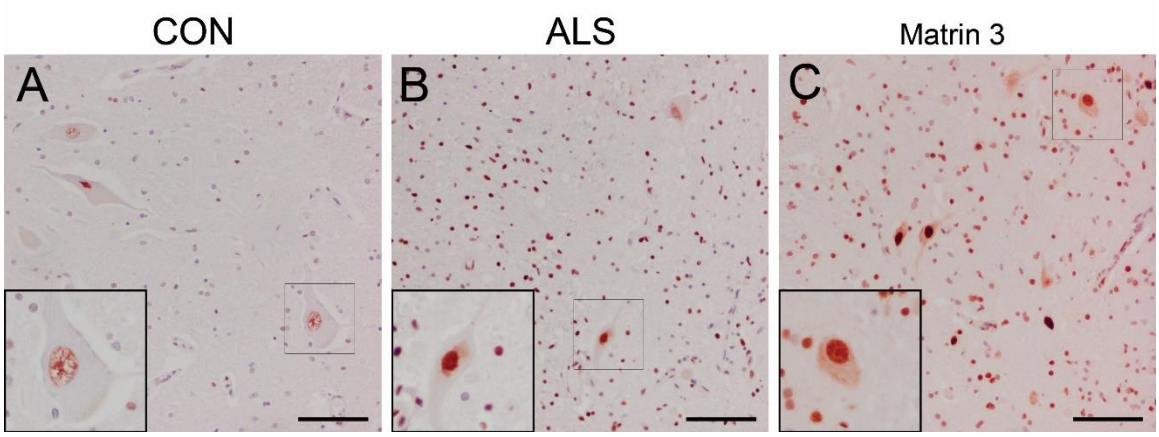

Figure 2.6 Lumbar Spinal Cord Tissue Immunostained for MATR3 and Counterstained with Hematoxylin

(a) Control spinal cord exhibits MATR3 nuclear immunoreactivity in some motor neurons, with weak glial cell immunostaining. (b) Spinal cord from a subject with ALS exhibits strong nuclear immunoreactivity, with cytoplasmic immunoreactivity present in some motor neurons either diffusely or in cytoplasmic puncta. Strong glial immunostaining is also noted in samples from ALS patients. (c) Spinal cord from a patient with the Phe115Cys MATR3 mutation exhibits strong nuclear staining, as well as cytoplasmic staining in many cells. Images were taken at 20x magnification; insets show enlargements of the boxed regions. Scale bars represent 50 µm.

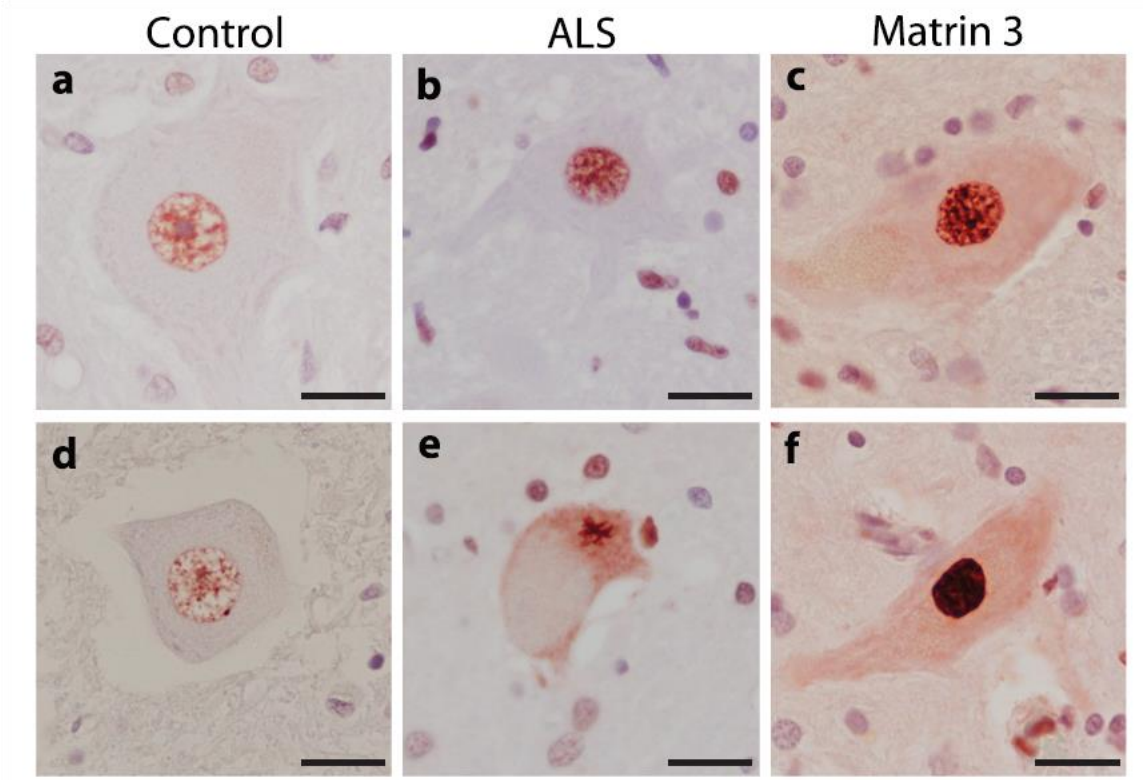

Figure 2.7 MATR3-Immunoreactive Staining in Spinal Cord Neurons of ALS Patients.

(a & d) Control cases exhibit a nuclear staining pattern with staining not filling the entire nucleus. (b & e) ALS cases display stronger nuclear staining pattern with cytoplasmic staining present in some cells. Cytoplasmic staining is either diffuse across the entire cell or found in cytoplasmic puncta. E shows a MATR3-positive cytoplasmic inclusion, which are occasionally observed (this patient was known to carry a pathogenic C9ORF72 repeat expansion). (c & f) Patient carrying the pPhe115Cys MATR3 mutation shows strong nuclear staining and cytoplasmic staining in many cells. Immunohistochemistry was performed using the HPA036565 antibody (Sigma-Aldrich). Similar results were seen with a different anti-MATR3 antibody.All images were taken at 40x magnification, and the scale bars represent 25µm.

We examined subcellular distribution of MATR3 using immunohistochemistry. In control subjects, MATR3 was detected in a granular staining pattern within the nuclei of motor neurons and surrounding glial cells (Fig. 2.6a and Fig.2.7 a and d). In ALS patients, MATR3 was observed in the nuclei of remaining motor neurons and occasionally within the cytoplasm (Fig. 2.6b and Fig. 2.7 b and e). In a patient harboring the p.Phe115Cys MATR3 mutation, MATR3 immunoreactivity was intense within the nucleus of all motor neurons and diffuse cytoplasmic staining was evident in many neurons (Fig. 2.6c and Fig.2.7c and f). Cytoplasmic inclusions were absent in this individual. However, we detected rare MATR3-positive cytoplasmic inclusions in an ALS patient known to carry the C9ORF72 repeat expansion (Fig. 2.7e).

MATR3 is a 125kDa nuclear matrix protein that is known to bind DNA and RNA. Previous unbiased screens found that MATR3 is a protein interactor of TDP-43, an RNA binding protein that is known to cause ALS (Ling, Albuquerque et al. 2010, Salton, Elkon et al. 2011). To confirm this interaction, we performed coimmunoprecipitation of FLAG-tagged MATR3 variants with endogenous TDP-43 in HEK293FT cells. As the genetic data were strongest for the p.Phe115Cys and the p.Ser85Cys, we selected these variants, as well as the p.Thr622Ala variant for which proof of pathogenicity was less clear, for further scrutiny. We found a reliable interaction that, interestingly, was increased by the p.Ser85Cys mutation, but not with the p.Phe115Cys or p.Thr622Ala variants (Fig. 2.8). We also noted that p.Ser85Cys MATR3 was expressed at lower steady state levels than other variants, suggesting a structural effect of the mutation (Fig. 2.8). There was no alteration in interaction between MATR3 and a second protein interactor, DHX9, demonstrating that the effect of p.Ser85Cys is specific for TDP-43 and not generalized to

all interactions of MATR3. Both interactions were abolished by RNase (Fig. 2.9), demonstrating that they are RNA-dependent. Coimmunoprecipitation of endogenous protein confirmed that MATR3 and TDP-43 interact at the endogenous level (Fig. 2.10). Also consistent with an interaction, MATR3 and TDP-43 co-aggregated in skeletal muscle tissue of a patient carrying the p.Ser85Cys mutation (Fig. 2.11). TDP-43 staining patterns were also examined in lumbar spinal cord tissue from the patient with a F115C mutation and Matrin 3 along with tissue from controls and sporadic ALS patients. In control tissue, TDP-43 remained within the nucleus in its normal localization and in sporadic ALS tissue it was found mislocalized to the cytoplasm where it formed inclusions. In Matrin 3 ALS tissue, TDP-43 similarly was found mislocalized to the cytoplasm and in cytoplasmic inclusions (Fig. 2.12).

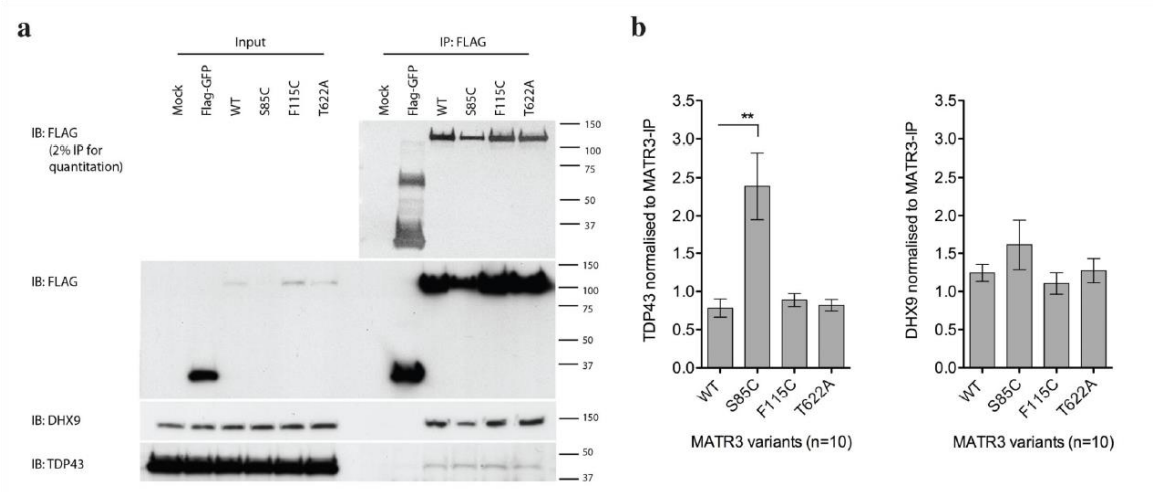

Figure 2.8 Immunoprecipitation of MATR3 with TDP-43

(**a**) FLAG-MATR3 was expressed in HEK293FT cells, immunoprecipitated using anti-FLAG antibody, and probed with TDP-43 and DHX9 antibodies. (**b**) Graphs show mean +/− SEM based on 10 replicate immunoprecipitation experiments. Differences in interaction between MATR3 and TDP-43 were tested with Wilcoxon signed rank test (**$p<0.01$).

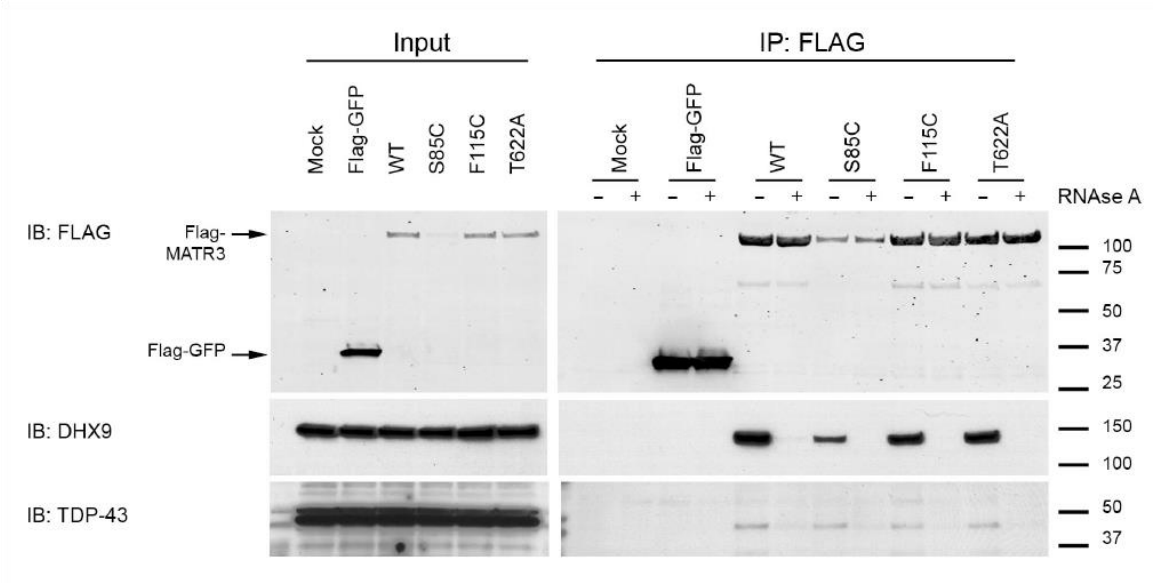

Figure 2.9 MATR3 and TDP-43 Interaction is RNA Dependent.

FLAG-MATR3 was expressed in 293FT cells, immunoprecipitated using anti-FLAG antibody followed by treatment with RNase A and probed with TDP-43 and DHX9 antibodies. Representative blots from two independent experiments are shown. Interaction of MATR3 and DHX9 is consistent with Salton, M. et al., PLoS One 6, e23882 (2011) showing that the interaction is RNA dependent, as is the interaction with TDP-43.

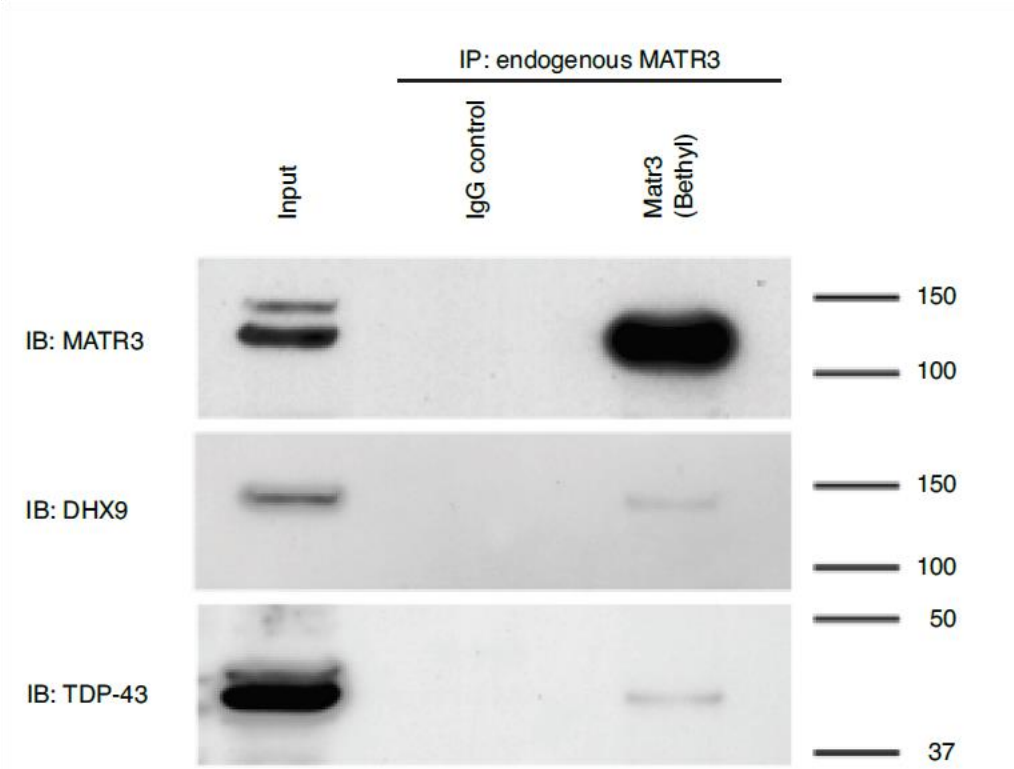

Figure 2.10 Co-immunoprecipitation Experiments using Endogenous MATR3.

Endogenous MATR3 was immunoprecipitated from 293FT cells and probed with DHX9 and TDP-43 antibodies. Representative blots from two independent experiments are shown. These data show that MATR3, TDP-43 and DHX9 interact at the endogenous level.

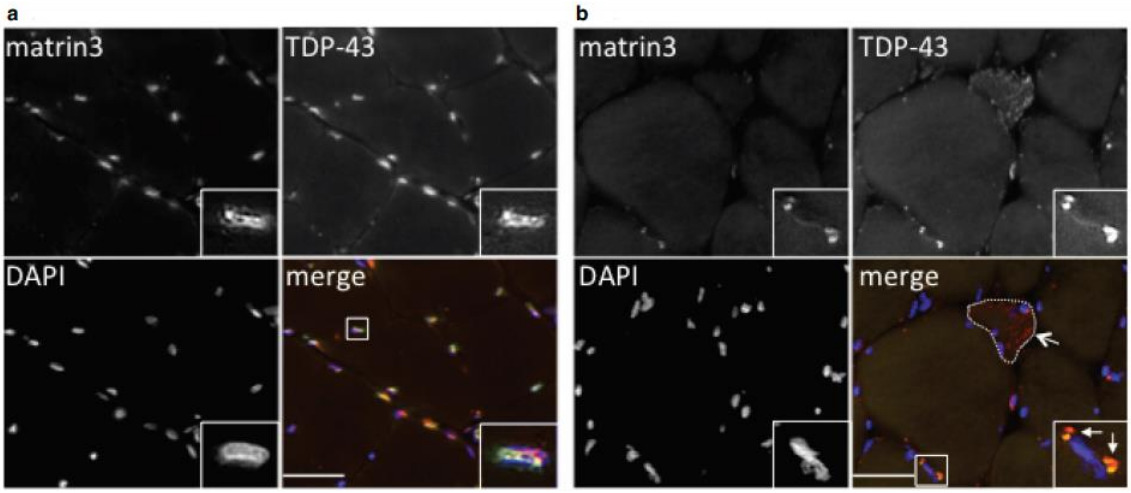

Figure 2.11 Immunofluorescence of Skeletal Muscle Biopsies using anti- TDP-43 and anti-MATR3 Antibodies.

Immunofluorescence of skeletal muscle biopsy from (a) a normal control, and (b) a patient carrying the p.Ser85Cys missense mutation in MATR3 using anti-TDP-43 and anti-MATR3 antibodies. In normal skeletal muscle, MATR3 and TDP-43 localize to nuclei including myonuclei. In the patient with the MATR3 mutation, there is decreased nuclear MATR3 immunoreactivity, whereas TDP-43 accumulates in the sarcoplasm and is restricted from the nucleus. In addition, MATR3 and TDP-43 co-aggregate in the sarcoplasm adjacent to myonuclei. Open arrow highlights a TDP-43 positive fiber (outlined in white). Closed arrows demonstrate MATR3 and TDP-43 co-localized in perinuclear inclusions. Insets are enlarged myonuclei and the scale bar is 50uM.

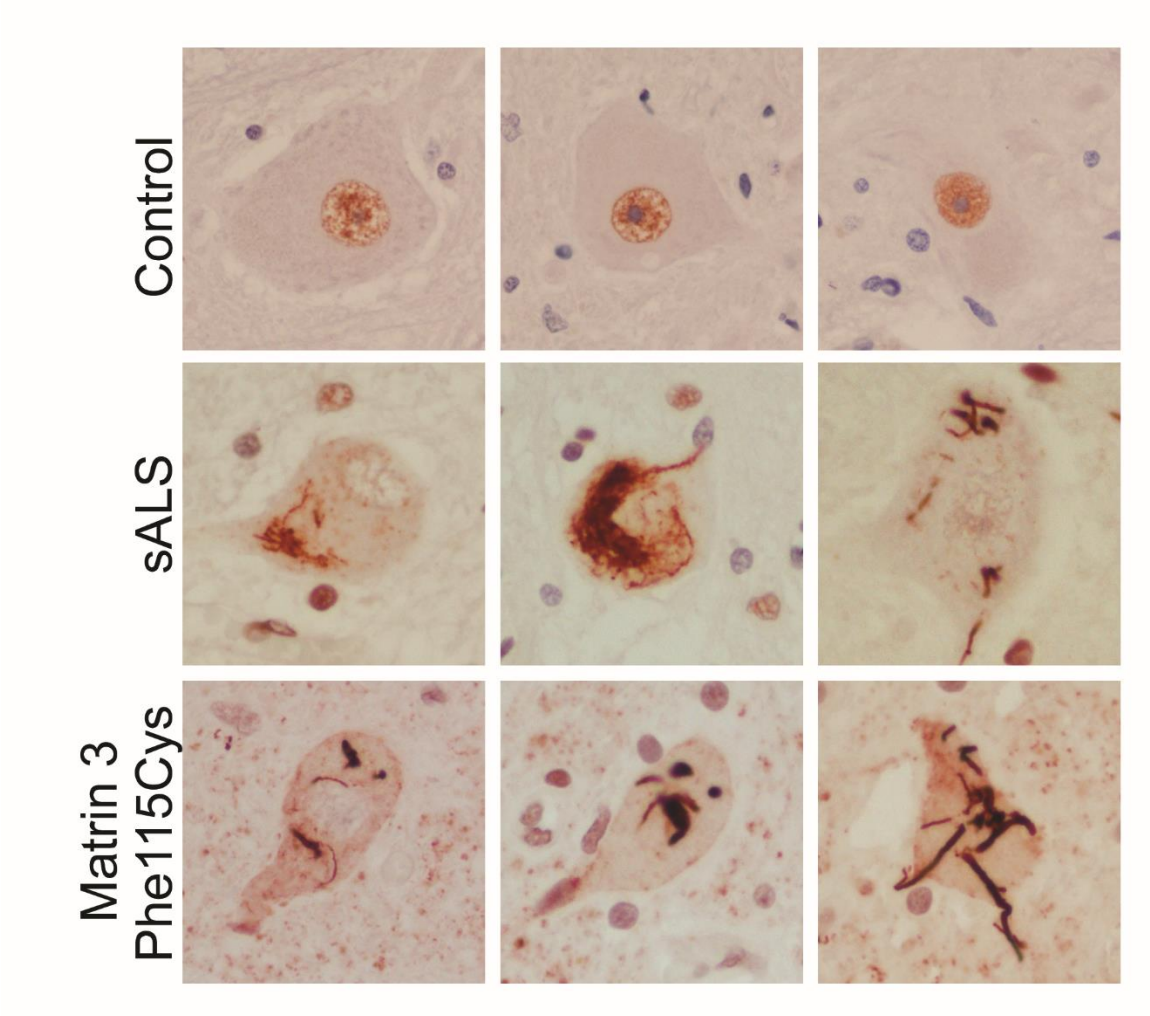

Figure 2.12 Immunohistochemistry of human spinal cord tissue using anti-TDP-43 antibodies.

Immunohistochemsitry of human spinal cord tissue from control individuals, sporadic ALS patients and an ALS patient with a F115C mutation in Matrin 3. TDP-43 staining (red) with hemtoxalyin counterstain (blue) shoes nuclear immunoreactivity in control tissue and cytoplasmic TDP-43 inclusion along with loss of nuclear immunoreactivity in tissue from sporadic ALS patients and the Matrin 3 ALS patient.

2.5 DISCUSSION

Differential effects of different mutations within the same gene have been reported for other neurodegenerative diseases, such as LRRK2 (a cause of familial Parkinson's disease) (Cookson 2012) and FUS (a cause of familial ALS) (van Blitterswijk, Wang et al. 2013). Therefore, the lack of effect of p.Phe115Cys and p.Thr622Ale on MATR3/TDP-43 interaction does not necessarily preclude their pathogenicity, as it is possible that these mutations disrupt other cellular processes in a manner that would not be detected by our assays. The variants found in MATR3 were distributed across the length of protein, perhaps disrupting different nearby domains. Indeed, multiple functions have been associated with MATR3, including RNA processing (Salton, Elkon et al. 2011), retention of hyper-edited RNA (Zhang and Carmichael 2001), gene silencing through interaction with Ago-containing complexes (Hock, Weinmann et al. 2007), chromatin organization (Ma, Siegel et al. 1999), and mediating neuronal cell death in response to NMDA glutamate receptor activation (Giordano, Sanchez-Perez et al. 2005). We also note that the p.Ser85Cys variant only alters interaction with TDP-43 and not another MATR3 partner, DHX9. However, and reminiscent of mutations in VAPB (Aliaga, Lai et al. 2013), p.Ser85Cys is notably less stable than other MATR3 variants. We infer that, of the genetic variants tested, p.Ser85Cys has the strongest effect on protein structure and this is correlated with a change in affinity for TDP-43. The structural basis of this interaction will need to be resolved in future studies. In this regard, it is interesting to note that the p.Ser85Cys mutation in MATR3 was associated with slowly progressive form of ALS, whereas individuals carrying the p.Phe115Cys mutation typically died from respiratory failure within five years of symptom onset. Similar

phenotype variability has been observed for other ALS genes. For example, the A4V mutation of SOD1 is associated with an aggressive form of the disease with an average survival of only nine months after symptom onset (Chio, Logroscino et al. 2009). In contrast, the homozygous D90A mutation in the same gene is associated with an indolent course with patients developing respiratory failure after ten years of illness14. Furthermore, the phenotype observed in some patients carrying MATR3 mutations combined features of ALS and myopathy. This clinical pattern is markedly similar to that observed in patients with mutations in VCP, HNRNPA1 and HNRNPA2B1, and the term "multisystem proteinopathy" has been used to reflect this broad pleiotropy (Johnson, Mandrioli et al. 2010, Kim, Kim et al. 2013). Exome sequencing data from the original USALS#3 family, as well as the 108 familial ALS cases, have been made available on dbGaP (accession number phs000101). The public release of such data allows other ALS researchers around the world to access, reanalyze and combine it with their own sequence data, thereby accelerating the pace of gene discovery. In summary, our genetic data identified mutations of the MATR3 gene as a rare cause of familial ALS and broadens the phenotype associated with this gene beyond the previously reported distal myopathy. This provides further insight into the importance of RNA metabolism in this fatal neurodegenerative disease. Future efforts to unravel the precise mechanism by which defects in RNA processing lead to motor neurodegeneration may provide novel targets for the design of rational therapies

CHAPTER 3

ALS ASSOCIATED MUTATIONS IN MATRIN 3 ALTER PROTEIN-PROTEIN INTERACTIONS AND IMPEDE mRNA NUCLEAR EXPORT

3.1 ABSTRACT

Mutations in Matrin 3 have recently been linked to ALS, though the mechanism that induces disease in these patients is unknown. To define the protein interactome of wild-type and ALS-linked *MATR3* mutations, we performed immunoprecipitation followed by mass spectrometry using NSC-34 cells expressing human wild-type or mutant Matrin 3. Gene ontology analysis identified a novel role for Matrin 3 in mRNA transport centered on proteins in the TRanscription and EXport (TREX) complex, known to function in mRNA biogenesis and nuclear export. ALS-linked mutations in Matrin 3 led to its re-distribution within the nucleus, decreased co-localization with endogenous Matrin 3 and increased co-localization with specific TREX components. Expression of disease-causing Matrin 3 mutations led to nuclear mRNA export defects of both global mRNA and more specifically the mRNA of TDP-43 and FUS. Our findings identify a potential pathogenic mechanism attributable to *MATR3* mutations and further link cellular transport defects to ALS.

3.2 INTRODUCTION

Amyotrophic lateral sclerosis (ALS) is a progressive neurodegenerative disorder that results in the loss of motor neurons in the brain, brain stem, and spinal cord (Kiernan, Vucic et al. 2011) (Pratt, Getzoff et al. 2012). Loss of motor neurons results in muscle atrophy and progressive paralysis, typically leading to death due to respiratory failure

within 2-5 years of diagnosis. Amongst a growing number of genetic mutations linked to ALS, the most common genetic cause of ALS is a repeat expansion of the *C9orf72* locus (DeJesus-Hernandez, Mackenzie et al. 2011) (Renton, Majounie et al. 2011). Of the more than 30 genes associated with ALS (Guerreiro, Bras et al. 2015), the most common mechanistic pathway implicated in ALS is RNA processing and metabolism. Mutations in many proteins that function in RNA processing and regulation such as TDP-43 (Neumann, Sampathu et al. 2006) (Gitcho, Baloh et al. 2008), FUS (Kwiatkowski, Bosco et al. 2009), hnRNPA1, hnRNPA2B1 (Kim, Kim et al. 2013) and Matrin 3 (Johnson, Pioro et al. 2014) have been linked to ALS. However, the manner in which defects in RNA processing lead to neurodegeneration remains poorly understood.

Previously, exome sequencing was used to identify four mutations in the RNA-binding protein Matrin 3 attributed to familial ALS: S85C, F115C, P154S and T622A (Johnson, Pioro et al. 2014). Subsequently, five other groups discovered additional mutations in Matrin 3 linked to ALS (Lin, Tsai et al. 2015, Origone, Verdiani et al. 2015, Leblond, Gan-Or et al. 2016, Xu, Li et al. 2016, Marangi, Lattante et al. 2017). The *MATR3* mutations predominately cluster in two potential hotspots found within amino acids 66-154 (containing six known mutations), and amino acids 610-787 (containing five known mutations) (Fig. 1a). S85C mutations in Matrin 3 have also been linked to vocal cord and pharyngeal weakness with distal myopathy (VCPDM), a progressive autosomal dominant distal myopathy that also results in dysphagia, dysphonia and vocal cord and pharyngeal weakness(Senderek, Garvey et al. 2009, Muller, Kraya et al. 2014, Yamashita, Mori et al. 2015). In human spinal cord tissue, Matrin 3 is predominantly localized within the nucleus of motor neurons; though in sporadic ALS (sALS) patients

as well as a patient harboring the F115C Matrin 3 mutation, nuclear immunostaining was increased compared to non-neurologic disease controls, with occasional cytoplasmic immunostaining(Johnson, Pioro et al. 2014). Rare Matrin 3 positive cytoplasmic inclusions have also been identified in patients harboring the C9orf72 repeat expansion as well as mutations in FUS (Johnson, Pioro et al. 2014, Dreser, Vollrath et al. 2017). Interactions between Matrin 3 and TDP-43 were also reported and this interaction was increased by the S85C mutation (Johnson, Pioro et al. 2014).

Matrin 3 is an RNA-binding protein and a component of the nuclear matrix, and has been shown to be involved in diverse processes including the response to DNA damage (Salton, Lerenthal et al. 2010), mRNA stability (Salton, Elkon et al. 2011), RNA splicing (Coelho, Attig et al. 2015) and is phosphorylated in response to N-methyl-D-aspartate receptor (NMDAR) activation (Giordano, Sanchez-Perez et al. 2005) and murine Matrin 3 protein levels have been shown to be lowest in muscle and the spinal cord (Rayaprolu, D'Alton et al. 2016). Recently, others have shown that expression of ALS linked mutations in Matrin 3 in a cell culture model does not result in gross mislocalization of the protein(Gallego-Iradi, Clare et al. 2015). Due to the diverse roles of Matrin 3, we sought to identify functional alterations caused by ALS-linked mutations. Immunoprecipitation (IP) followed by tandem mass spectrometry (MS) experiments were performed to determine Matrin 3 protein-protein interactions (PPI) and any changes induced by disease-associated mutations. Using NSC-34 cells stably expressing either wild-type or mutant Matrin 3, we performed IP-MS and identified approximately 50 Matrin 3 interacting proteins with either wild-type or each mutant Matrin 3 protein. Multiple proteins within the TRanscription and EXport (TREX) protein complex that

regulates mRNA nuclear export were found to interact with Matrin 3, and mutant Matrin 3 exhibited altered interactions with specific TREX proteins. We further demonstrate altered global mRNA nuclear export in cells expressing mutant Matrin 3 protein. Our results identify proteins that interact with wildtype and each mutant Matrin 3 protein, as well as a novel function of Matrin 3 in regulating mRNA nuclear export. These findings support a critical role for RNA processing and transport in the pathogenesis of ALS.

3.3 METHODS

3.3.1 Immunoprecipitation and Western Blot

Flag immunoprecipitations (IP) were performed using NSC-34 cells stably expressing 3x Flag Matrin 3 wild-type or ALS-associated mutant, endogenous IPs were performed in untransfected NSC-34 cellsImmunoprecipitations were performed on nuclear fractions (400µg of total protein), isolated using a Nuclear Complex Co-IP Kit (Active Motif) with minor modifications, and either Flag M2 affinity gel (Sigma-Aldrich) or antibodies against Ddx39b, Aly or Matrin 3.

Lumbar spinal cord tissue homogenates were prepared from frozen tissue from controls (n= 3) and ALS cases (n= 3) for coimmunoprecipitation studies. Nuclear and postnuclear extracts were prepared as described previously (Kolarcik and Bowser 2012). Briefly, samples were homogenized in a solution containing 10 mM Tris (pH 8.0), 10 mM $MgCl_2$, 15 mM NaCl, and 0.1% Ipegal CA-630 (Sigma) supplemented with protease and phosphatase inhibitors, and nuclei were collected via low-speed centrifugation at 800 × g for 5 min. Nuclei were lysed in buffer containing 0.42M NaCl, 20mM HEPES, 20% glycerol and 0.1% Ipegal CA-630 supplemented with protease and phosphatase inhibitors. Nuclear lysate was collected after a 10 min lysis by centrifugation at 14,000

rpm for 5 min. The resulting supernatant was saved nuclear extract and used for immunoprecipitation (150μg protein per sample). After eluting proteins, the mixture was separated using gel electrophoresis on NuPage 4-12% Bis-Tris gels (Thermo Fisher) and either transferred to Immobilon FL polyvinylidene difluoride (PVDF) membranes (Millipore) or stained with Coomassie blue (BioRad) for mass spectrometry analysis. For IP followed by western blot (IP-WB) membranes were blocked in Odyssey blocking buffer (LiCor) and probed with the indicated primary antibody overnight followed by the appropriate secondary antibody (LiCor). Both WB and Coomassie stained membranes were imaged on an Odyssey CLx imager (LiCor).

3.3.2 In-gel digestion

After IP followed by electrophoresis (see above) lanes were excised into individual bands, excluding heavy and light IgG chains observed at 52kDA and 25kDa respectively. Bands were cut into 1-2mm^3 cubes and processed using published methods (Shevchenko, Tomas et al. 2006). Briefly, resulting fractions were reduced with 10mM DTT (6˚C for 30 min), alkylated with 55mM iodoacetamide (room temperature for 30 min, in the dark) and digested using 20 ng/mL of Trypsin Gold (Promega) (37°C, overnight). Finally, peptides were extracted, vacuum dried and stored at -20°C until LC-MS analysis.

3.3.3 LC-MS analysis

Individual fractions were reconstituted in 0.1% formic acid and analyzed using online liquid chromatography on a Waters nanoAcquity UPLC coupled to a Thermo LTQ Orbitrap Velos mass spectrometer. Chromatography solvents A and B were 0.1% formic acid in water or acetonitrile, respectively. Peptides were first trapped on a 30 mm × 100

μm diameter fused silica column packed with 3 μm 120 Å ReproSil-Pur C18 AQ resin (Dr Maisch GMBH, Ammerbuch-Entringen, Germany) at 7.5 μl/min and 5% solvent B, before separation at 500 nl/min on a 100 mm × 100 μm analytical column (same solid phase as trap column) in a 3–40% solvent B gradient for 17 min, followed by 40-90% in 0.6 min, then 90% B for 2 min and final re-equilibration for 10.5 min. The mass spectrometer was operated in positive ion mode using a spray voltage of 1.8 kV, and a capillary temperature of 200°C. Data were acquired in top-15, data-dependent acquisition mode using a collision voltage of 30 V.

3.3.4 Protein Identification

The raw mass spectra were deconvoluted using Proteome Discoverer v1.4.1.14 (Thermo Fisher Scientific, Waltham, MA). The spectra were searched against *Mus Musculus* (Swissprot, January 2015) supplemented with human Matrin-3 using Mascot v2.4.1 (Matrix Science, London, UK) with the following variable modifications: oxidation (Met) and carbamidomethyl (Cys). Mass tolerances for precursor ions were set at ±10 ppm, for fragment ions at ±0.8 Da. A maximum of 2 missed cleavages was allowed. Data were processed for label-free quantitation using Scaffold v4.5.1 (Proteome Software Inc., Portland, OR) and X!Tandem (The GPM, v2010.12.01.1) to further improve confidence in protein identification. At least 2 peptides were required for protein identification, with 0.1% peptide FDR and 1% protein FDR. Only exclusive spectral counts were used for prediction of protein-protein interactions.

3.3.5 Bioinformatics and Pathway Analysis

Probabilistic scoring of protein-protein interaction (PPI) combined with manual thresholding analysis of interactants to wild-type and mutant forms of Matrin-3 was

performed using SAINTexpress (Teo, Liu et al. 2014). Using SAINTexpress, average probability (AvgP), fold change and a Bayesian False Discovery Rate (BFDR) were computed for each interaction pair. Fold-changes were calculated using average exclusive spectral counts against the empty vector as a background control for non-specific binding. PPIs were filtered by presence in at least 2 out of 3 replicates, fold change ≥2.5 and AvgP ≥0.7. For manual analysis, Matrin-3 interactors were filtered by presence in at least 2 out of 3 replicates and a fold change ≥2.5 based on maximum spectral counts.

3.3.6 Immunofluorescence and RNA FISH

Immunofluorescence staining was performed on NSC-34 cells either transiently or stably expressing Matrin 3 constructs. Cells were grown on glass coverslips, fixed in 4% paraformaldehyde (PFA) in PBS for 5 min, then permeabilized in 0.1% Triton X-100 for 5 min. Cells were then blocked for one hour in SuperBlock (Scytek), and primary antibody was added for either one hour at room temperature or overnight at 4°C followed by the appropriate secondary antibody for one hour at room temperature. Nuclei were labeled with 4', 6-diamidino-2-phenylindole (DAPI) for 5 min (Invitrogen). For co-localization analysis, Pearson's correlation coefficients were calculated using Imaris software (Bitplane) first by masking the DAPI channel to measure only co-localization within the nucleus, and then applying an automatic thresholding algorithm. The number of cells analyzed over the course of three independent experiments are as follows: Matrin 3-WT=41, 85=43, 115=40, 154=41, 622=41, Aly-WT=41, 85=40, 115=42, 154=46, 622=43, Ddx39b-WT=50, 85=43, 115=45, 154=44, 622=43, Sarnp-WT=46, 85=50, 115=44, 154=42, 622=47.

RNA FISH experiments were performed on NSC-34 cells transiently expressing Matrin 3 constructs. Cells were plated on glass coverslips, fixed in 4% PFA for 10 min followed by permeabilization in 0.2% Triton X-100 for 10 min and washes in 70% ethanol and 1M Tris-HCl. Cells were hybridized in buffer containing 2ng/µl Cy3 labeled Oligo dT, 0.5µg/µl tRNA, 2µg/µl BSA fraction V, 10% dextran sulphate, 20% formamide, and 2x saline-sodium citrate (SSC) buffer for 3 hours at 37°C in a humidified chamber. Cells were then washed in SSC and subjected to the same immunocytochemistry protocol as listed above beginning with blocking step. The number of cells analyzed over the course of three independent experiments are as follows: WT transfected=34, WT untransfected=31, 85 transfected=34, 85 untransfected=33, 115 transfected=32, 115 untransfected=33, 154 transfected=32, 154 untransfected=32, 622 transfected=33, 622 untransfected=33.

Images were captured using a Zeiss LSM 710 confocal microscope and image analysis was performed using Imaris software (Bitplane).

3.3.7 Gene Ontology

Gene ontology assessments were performed using ToppGene Suite (ToppFun). Medium confidence lists of proteins were utilized (identified in at least 2 replicates with a fold change of at least 2.5 over controls, and AvgP>0 using the SAINTexpress program) for this analysis. Calculations were made using GO: Biological Processes with a FDR p-value cutoff of 0.01. The top ten results for each group are shown in order along with p-values and the number of proteins identified in each biological process.

To create a visual network of overlapping and unique GO terms across the Matrin-3 mutant samples, ClueGO v2.3.2 was utilized through Cytoscape v3.3.0. The

proteins were aligned to GO:Bbiological Processes using the mouse proteome. GO term fusion was implemented merging parent-child terms with shared proteins. All other default ClueGO parameters were used. Proteins shared between identified GO terms were selected for display on the network map (Bindea, Mlecnik et al. 2009).

3.3.8 Cell Culture and Creation of Matrin 3 stable lines

NSC-34 cells (Cellutions Biosystems) were cultured in DMEM supplemented with 10% FBS and grown in the presence of 1% Pen-Strep at 37°C and 5% CO_2. Matrin 3 cDNA plasmid HsCD00075976 was obtained from the DNASU plasmid repository at Arizona State University. Matrin 3 3x Flag constructs were PCR amplified using Phusion High-Fidelity Polymerase (NEB) then sub-cloned into a pcDNA3 vector (Invitrogen) along with 3 Flag peptides attached to the N-terminus of the protein. Constructs expressing ALS linked mutations were created by performing site directed mutagenesis (Agilent Technologies) on Matrin 3 3x Flag pcDNA3 constructs (Seiler, Park et al. 2014). Cells were transfected using Lipofectamine 3000 (Life Technologies) and stable lines were selected under the using 500µg/ml Genetecin (Life Technologies) applied 24hrs after transfection. For transient transfections cells were used 48hrs after transfection.

3.3.9 Nuclear/Cytoplasmic RNA fractionation

HEK-293 cells were harvested and processed for nuclear and cytoplasmic RNA fractionation as described in (Quaresma, Sievert et al. 2013) adapted from the method developed by (Andersen, Lyon et al. 2002). Briefly, cells were transfected with the various Matr3 constructs, and harvested 48h later. Pellets were rinsed in PBS and resupended in lysis buffer A (10mM HEPES, 1.5mM MgCl2, 10mM KCl, 0.5mM DTT and 2mM vanadylriboside VRC). A fraction was immediately separated for the total

RNA fraction, and the remaining fraction was incubated on ice, and broken down with a chilled Dounce homogenizer to release nuclei. Cells were then spun down at 228xg for 5min to release the cytoplasmic fractions (supernatant) and the nuclei (pellets). Nuclei were washed in buffer A twice, resuspended in Buffer S1 (250mM sucrose, 10mM MgCl2 and 2mM VRC), and layered on top of a cushion of buffer S3 (880mM sucrose, 0.5mMMgCl2, 2mM VRC). Nuclei were spun down at 2800xg and for 10min and pellets were resuspended in buffer A. Trizol was then added to all fractions, and RNA was extracted using the Direct-zol RNA miniprep kit (Zymo Research, Irvine, CA). cDNA was synthesized using Superscript VILO (ThermoFisher Scientific), and cDNA was used for quantitative real-time PCR using PowerUp Sybr Green master mix. All curves were normalized by the comparative ΔΔCt method. Nuclear fraction RNA levels were normalized to tRNA-Lys (For: CGGATAGCTCAGTCGGTAGA and Rev: CCGAACAGGGATCTTGAACC), while cytoplasmic fractions were normalized to mitochondrial cytochrome b (For: CTAGCAGGTGTCTCCTCTATCT and Rev: GGCGTTTGGTATTGGGTTATG). Primers used for TDP43 were (For: GGGAAATCTGGTGTATGTTGTCA and Rev: TTTTCTGGACTGCTCTTTTCACT) and FUS (For:ATGGCCTCAAACGATTATACCCA and Rev:GTAACTCTGCTGTCCGTAGGG).

3.3.10 Antibodies

Antibodies used throughout the paper include Matrin 3 ab151714 and ab70336 (abcam) and HPA036565 (Sigma), Flag F3165 (Sigma) and 2368 (Cell Signaling), actin MAB1501 (Millipore), Aly ab6141 and ab202894 (abcam), ddx39b 14798-1-AP

(Proteintech) and NBP2-52456 (Novus Biologicals), Sarnp HPA030902 (Sigma), and GAPDH 2118S (Cell Signaling).

3.3.11 Tissue Samples

ALS and disease control post-mortem tissue samples were obtained from the Barrow Neurological Institute ALS Tissue Bank, and the Target ALS Human Postmortem Tissue Core. All tissues samples were collected after informed consent from the subjects or by the subjects' next of kin, complying with all relevant ethical regulations. The protocol and consent process were approved by the the Dignity Health Institutional Review Board. Clinical diagnoses were made by board certified neuropathologists according to consensus criteria for ALS. Patient demographics can be found in Supplemental Table 2.

3.4 RESULTS

3.4.1 Matrin 3 Protein-Protein Interactions (PPI) altered by ALS-Linked Mutations

While Matrin 3 performs many functions in the nucleus, few studies have identified proteins that interact with Matrin 3 and regulate its function (Salton, Elkon et al. 2011, Erazo and Goff 2015). To further define the functional role of Matrin 3 and how *MATR3* disease causing mutations alter its function, we examined protein-protein interactions of wild-type and each mutant Matrin 3 protein. Immunoprecipitation followed by tandem mass spectrometry experiments were performed using NSC-34 cells stably expressing either flag-tagged human wild-type or ALS associated mutant Matrin 3 proteins (Fig. 3.1b,c). While additional mutations in *MATR3* have recently been

published, we chose to focus efforts on the original four mutations including a (chr5:138643358, C>G) resulting in a Ser85Cys (S85C) amino acid alteration, (chr5:138643448, T>G) Phe115Cys (F115C), (chr5:138643564, C>T) Pro154Ser (P154S), and (chr5:138658372, A>G) Thr622Ala (T622A) (Fig. 3.1a) (Johnson, Pioro et al. 2014). A recent study demonstrated that mutant Matrin 3 protein remains predominately in the nucleus when transiently overexpressed in multiple cell types (Gallego-Iradi, Clare et al. 2015). In our stable cell lines, these MATR3 mutations do not alter the cellular localization of endogenous or mutant Matrin 3, which remains predominantly nuclear (Fig. 3.1b). Therefore, we examined Matrin 3 PPI specifically in the nucleus of cells expressing wild-type or mutant Matrin 3. All four mutants were expressed at similar levels as wild-type and stable lines were selected to have low overexpression levels (approximately 2.5 fold) to stay close to physiological ranges. It was also noted that overexpression of mutant Matrin 3 did not lead to downregulation of the endogenous protein (Fig. 3.1c). Expression of ALS linked mutations in Matrin 3 did however, lead to increased toxicity which was found in the form of increased cell death when S85C, F115C or P154S Matrin 3 was expressed (Fig. 3.2).

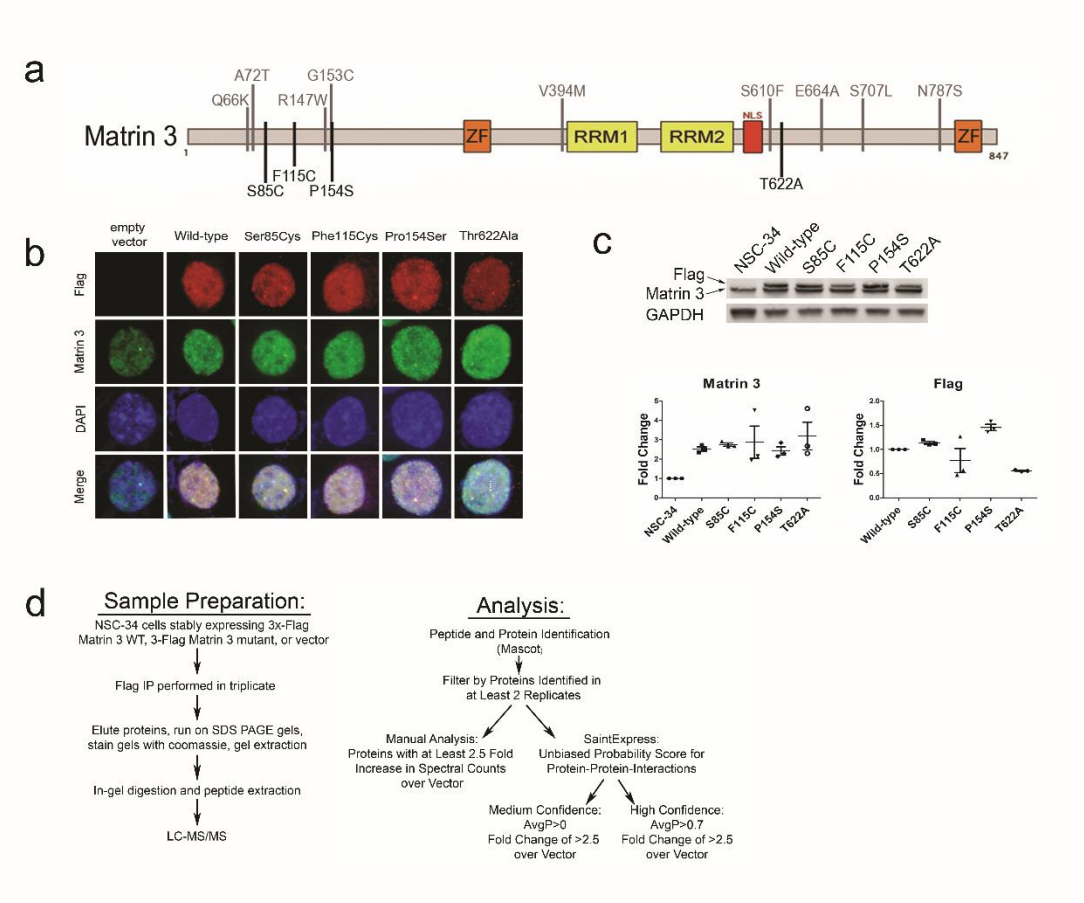

Figure 3.1 Matrin 3 cell culture model and IP-MS workflow.

a) Domain structure of Matrin 3 including location of mutants studied in this work listed below the protein as well as other recently identified mutations shown above. b) Representative immunofluorescence images of NSC-34 cells stably expressing Flag tagged wild-type Matrin 3 or one of S85C, F115C, P154S or T622A Matrin 3 mutants. Cells transfected with empty vector are also shown denoting endogenous levels and localization of Matrin 3. Flag expression is shown in red, Matrin 3 in green, DAPI marking nucleus in blue. c) Western blot of whole cell lysates probed with antibodies against Flag (top) and Matrin 3 (bottom) showing expression levels of endogenous Matrin 3 and Flag tagged Matrin 3 in NSC-34 stable cells lines and quantitation. Full length blots can be found in figure 3.14. Error bars represent standard error of the mean (SEM) of three experiments. One way Analysis of Variance (ANOVA) with Dunnett's post-test showed no significant differences between level of expression of wild-type and any of the four mutations (Flag p-values: WT vs 85: p=0.8163, WT vs 115: p=0.4753, WT vs 154 p=0.0619, WT vs 622 p=0.0715, F-value: 8.671, DF=14, Matrin 3 p-values: WT vs 85: p=0.9957, WT vs 115: p=0.9722, WT vs 154 p=0.9998, WT vs 622 p=0.7550, F-value: 2.716, DF=17). d) Flow chart of IP-MS sample preparation and analysis protocols.

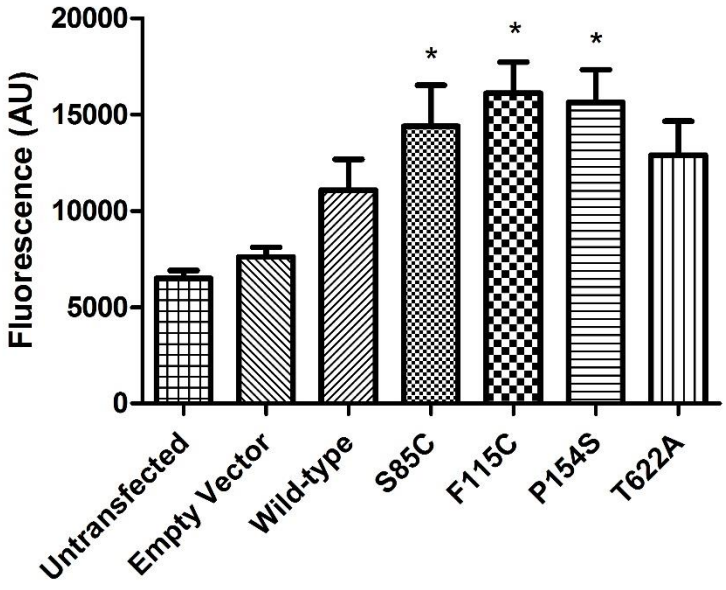

Figure 3.2 Expression of mutant Matrin 3 increases cell death.

NSC-34 cells were transiently transfected with either an empty vector, wild-type Matrin 3 or ALS associated mutations in Matrin 3. After 48 hours cell death was measured using a fluorescent dye that binds to the DNA of cells with impaired membrane integrity. One way ANOVA with Dunnett's post-test showed a significant increase in cell death (* refers to $p<0.05$) for three mutations in Matrin 3; S85C, F115C, P154S, and T622A.

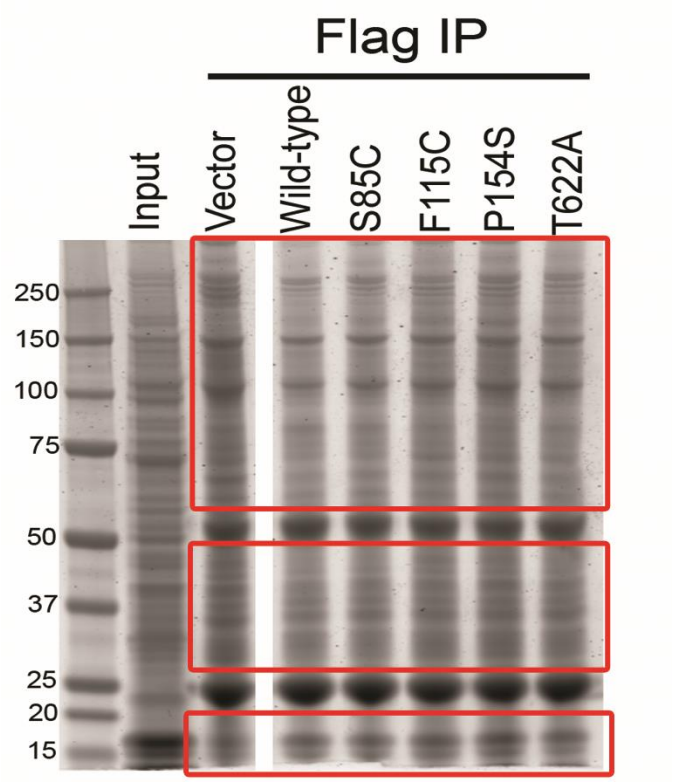

Figure 3.3 Representative image of Coomassie stained gel after IP pull-down.

Input indicates total nuclear lysate before immunoprecipitation experiment (40µg of total protein) followed by immunoprecipitation using Flag agarose gel in NSC-34 cells stably expressing empty vector, wild-type Matrin 3 or one of the four mutations in Matrin 3. Red boxes indicate the area used for mass spectrometry experiments (IgG heavy and light chains were removed).

As outlined in Figure 3.1d, nuclear extracts were prepared from each stable cell line and used for immunoprecipitation of exogenous Flag-tagged Matrin 3, followed by elution of bound proteins and identification by mass spectrometry (Fig. 3.3). After peptide identification, interactions were analyzed by two methods, manual analysis and a probabilistic protein-protein interaction algorithm (SAINTexpress). Manual analysis consisted of filtering proteins to only include those that were identified in two out of three replicates at a fold change of 2.5 or greater over the maximum spectral counts identified in the empty vector control. SAINTexpress analysis was performed on proteins that were identified in two out of three replicates and at a fold change of 2.5 or greater as compared to the average spectral counts of empty vector, and yielded two populations of proteins; a medium confidence list of proteins that either met the manual analysis criteria or the SAINTexpress criteria of (AvgP>0) and a high confidence list (AvgP>0.7) (Figure 3.1e). Overall, we identified approximately 300 proteins for wild-type and each mutant (range of 276-333), approximately 70 proteins that met the thresholding criteria for medium confidence (range of 61-87), and approximately 18 proteins that met the stringent criteria of high confidence interactors (range of 13-31). Across wild-type and all four mutants, a total of 167 unique proteins met the medium confidence threshold (Table 3.1) and 53 proteins met the threshold for high confidence in at least one of the five cell lines (Table 3.2).

Accession	Gene	Wild Type			Ser85Cys Mutant			Phe115Cys Mutant			Pro154Ser Mutant			Thr622Ala Mutant		
		AvgP	SAINT	Manual	AvgP	SAINT	Manual	AvgP	SAINT	Manual	AvgP	SAINT	Manual	AvgP	SAINT	Manual
Q60668	Hnrnpd		+ + +	+ + +	1	+ + +	+ + +	1	+ + +	+ + +	1	+ + +	+ + +	1	+ + +	+ + +
Q61029-3	Tmpo	1	+ +	+ + +	1	+ + +	+ + +			+	0.96	+ +	+ + +			
P62270	Rps18	1	+ + +	+ + +				1	+ + +	+ + +	1	+ +	+ + +	1	+ +	+ + +
P62301	Rps13	1	+ + +	+ + +					+ +	+ + +	0.98	+ +	+ + +	0.99	+ +	+ + +
P84228	Hist1h3b	0.99	+ +	+ + +				0.96	+ +	+ + +						
O08583	Alyref	0.98	+	+												
Q9D1J3	Sarnp	0.97	+ +	+ + +		+	+ + +		+ +	+ + +	1	+ +	+ + +	0.98	+ +	+ + +
Q9QXS1-7	Plec	0.97	+ +	+ + +		+ +	+ + +									+ + +
Q9D554	Sf3a3	0.87	+	+								+				
P57784	Snrpa1	0.85	+	+					+	+		+				
Q8CH18	Ccar1	0.84	+	+	0.74	+	+	0.88	+	+		+			+	
P62281	Rps11	0.73	+	+	0.96	+ +	+	0.9	+ +	+		+	+	0.87	+	+
P08775	Polr2a	0.71	+	+					+	+	0.74	+	+		+	+
Q8BG05	Hnrnpa3			+	1	+	+	1	+	+			+			+
P05213	Tuba1b				1	+ + +	+ + +								+ +	+ + +
P99024	Tubb5				1	+ + +	+ + +									
Q91YR7	Prpf6				0.96	+	+		+		0.87	+	+			
Q9Z1N5	Ddx39b			+	0.95	+	+		+	+		+	+			+
O35691	Pnn				0.9	+	+									
Q9D0E1	Hnrnpm				0.88	+	+						+			
Q99M28	Rnps1		+	+	0.85	+	+		+	+		+	+	0.82	+	+
P14873	Map1b				0.73	+	+		+	+	0.72	+	+	0.98	+	+
Q6NZF1	Zc3h11a		+ +	+ + +				1	+ +	+ + +	1	+ + +	+ + +	1	+ + +	+ + +
P61358	Rpl27		+	+ + +				0.98	+ +	+ + +		+ +	+ + +	0.96	+ +	+ + +
P68134	Acta1							0.98	+ +	+ + +						
A2BDX3	Mocs3					+ +	+ + +	0.98	+ +	+ + +		+ +	+ + +			
P62751	Rpl23a					+ +	+ + +	0.95	+ +	+ + +				0.96	+ +	+ + +
Q9JHJ0	Tmod3		+ +	+ + +				0.95	+ +	+ + +						
Q9DBG3	Ap2b1		+					0.9	+	+	0.86	+ +	+		+	
Q8VHZ7	Imp4		+					0.7	+					0.86	+	+
Q8BG81	Poldip3		+	+		+	+		+	+	1	+	+	0.71	+	+
Q9Z1X4-2	Ilf3										1	+ +	+ + +	1	+ + +	+ + +
Q9DB96	Ngdn								+ +	+ + +	0.98	+ +	+ + +	0.98	+ +	+ + +
P62137	Ppp1ca		+ +	+ + +					+	+ + +	0.98	+ +	+ + +		+	+ + +
Q8K4P0	Wdr33										0.98	+ +	+ + +		+	+ + +
P62911	Rpl32										0.96	+ +	+ + +	1	+ +	+ + +
P62267	Rps23								+ +	+ + +	0.96	+ +	+ + +	0.96	+ +	+ + +
A2AIV2	Kiaa1429										0.96	+ +	+ + +			
Q8BL97-4	Srsf7													1	+ + +	+ + +
P20152	Vim					+ + +	+ + +							1	+ +	+ + +
Q6P5B0	Rrp12		+	+ + +					+ +	+ + +				0.98	+ +	+ + +
Q8CGP2	Hist1h2bp													0.98	+ +	+ + +
P62754	Rps6					+	+ + +							0.98	+ +	+ + +
Q9CZU3	Skiv2l2		+	+ + +					+ +	+ + +		+ +	+ + +	0.96	+ +	+ + +
Q8BMK4	Ckap4								+	+ + +				0.96	+ +	+ + +
Q8K4L0	Ddx54								+ +	+ + +		+	+ + +	0.96	+ +	+ + +
Q07646	Mest													0.96	+ +	+ + +
P62849	Rps24								+ +	+ + +		+	+ + +	0.96	+ +	+ + +
Q8C4J7	Tbl3								+ +	+ + +				0.96	+ +	+ + +
Q501J6	Ddx17								+			+		0.94	+	+
Q8CH25	Sltm								+	+		+	+	0.86	+	+
Q921Y2	Imp3													0.75	+	
P14869	Rplp0		+						+			+	+	0.7	+	+
P02535	Krt10		+						+	+						
P56959	Fus		+													
Q8CFQ3	Aqr		+													
O35326	Srsf5		+	+		+	+		+	+		+	+		+	+
Q9WV55	Vapa		+												+	+
Q91VJ5	Pqbp1		+						+							
O70503	Hsd17b12		+			+	+		+						+	+
Q9DAW6	Prpf4		+			+										
Q8QZY9	Sf3b4		+	+		+										
Q8BTI8	Srrm2		+			+						+				
Q6NV83	U2surp		+	+		+			+	+		+	+ + +			
Q9D287	Bcas2		+	+ + +												
P43276	Hist1h1b		+	+ + +		+	+ + +									
P04104	Krt1		+	+ + +		+ +	+ + +									
Q99PL5	Rrbp1		+	+ + +		+	+ + +								+ +	+ + +
Q9CQI7	Snrpb2		+	+ + +		+	+ + +		+	+ + +						
Q9QX47	Son		+	+ + +												
Q91VR2	Atp5c1		+	+ + +											+	+ + +
Q8BMS1	Hadha		+	+ + +												
Q91YE7	Rbm5		+	+ + +		+	+ + +		+ +	+ + +		+ +	+ + +			

P41105	Rpl28		+	+ + +					+	+ + +		+	+ + +						
P62900	Rpl31		+	+ + +															
P14131	Rps16		+	+ + +					+	+ + +		+	+ + +						
Q0P678	Zc3h18		+	+ + +					+ +	+ + +									
Q9JHS9	Cwc15		+ +	+ + +		+	+ + +												
Q923D5	Wbp11		+ +	+ + +															
P0C0S6	H2afz		+ +	+ + +					+	+ + +									
Q99KG3	Rbm10		+ +	+ + +		+ +	+ + +												
P61222	Abce1																	+	+ + +
Q9JIX8	Acin1					+	+												
Q9QUJ7	Acsl4					+	+		+	+								+	+
O35643	Ap1b1								+	+ + +								+	+ + +
P17427	Ap2a2								+					+					
O35841	Api5								+	+ + +		+ +	+ + +					+ +	+ + +
Q3UL36	Arglu1					+	+ + +												
Q61687	Atrx																	+	+ + +
Q6PDQ2	Chd4								+	+ + +									
Q9CY57	Chtop			+ + +															
Q9EPU4	Cpsf1					+			+			+							
O35218	Cpsf2																	+	
Q9QXK7	Cpsf3											+	+ + +						
P63154	Cmkl1			+															
Q60737	Csnk2a1											+							
Q9CWL8	Ctnnbl1								+	+ + +									
Q3U1J4	Ddb1					+ +	+ + +												
Q8VDW0	Ddx39a								+	+ + +		+ +	+ + +						
Q9D903	Ebna1bp2			+															
Q61701	Elavl4					+	+ + +												
Q9DBE9	Ftsj3											+							
Q922P9	Glyr1								+	+ + +								+ +	+ + +
P10922	H1f0					+	+ + +												
O09106	Hdac1								+	+ + +									
Q8C2B3-2	Hdac7					+	+ + +												
P15864	Hist1h1c					+	+ + +												
P68433	Hist1h3a								+	+ + +									
Q9Z204	Hnrnpc			+			+ +			+				+ +					+ +
O35737	Hnrnph1						+ + +			+									
P61979	Hnrnpk								+			+							
P20029	Hspa5								+	+								+	
P03975	Iap																	+	+
P54071	Idh2																	+	
Q5SF07	Igf2bp2					+ +	+ + +		+	+ + +									
Q60749	Khdrbs1					+ +	+ + +												
Q9Z2K1	Krt16													+ + +					
Q922U2	Krt5									+									
Q8VED5	Krt79								+										
Q61595	Ktn1																	+	+ + +
Q7TNC4	Luc7l2					+ +	+ + +											+	+ + +
Q3V3R1	Mthfd1l								+ +	+ + +		+ +	+ + +					+	+ + +
P46735	Myo1b								+	+ + +									
Q99104	Myo5a								+										
P12979	Myog					+ +	+ + +												
Q9D7Z3	Nol7								+									+	
Q9D6Z1	Nop56			+															
Q8BH74	Nup107																	+	
Q9Z0W3	Nup160																	+	+ + +
Q99JX7	Nxf1					+	+		+	+		+						+	
Q8K010	Oplah								+ +	+ + +									
P01660	P01660								+	+ + +									
Q922V4	Plrg1											+							
Q8CFI7	Polr2b								+	+ + +									
P97760	Polr2c					+	+												
P15331	Prph					+	+												
B2RY56	Rbm25											+						+	
Q8CGC6	Rbm28													+					
Q8VH51	Rbm39					+	+		+			+							
Q9WV02	Rbmx								+	+ + +								+	+ + +
Q91VM5	Rbmxl1			+			+			+				+					+
Q9CZM2	Rpl15					+	+ + +												
P62264	Rps14								+	+ + +									
Q99PL7	Scd3																	+	+ + +
Q62203	Sf3a2					+	+												
Q8VIJ6	Sfpq											+						+	+
Q7TSG5	Sh3d21								+	+ + +									
P50431	Shmt1					+													

P51881	Slc25a5			+			+										
Q3UKJ7	Smu1					+ +	+ + +										
P27048	Snrpb						+ + +										
P62315	Snrpd1								+	+ + +							
P15508	Sptb								+	+ + +							
P47758	Srprb														+ +	+ + +	
Q9D0B0	Srsf9									+							
Q08943	Ssrp1					+ +	+ + +		+ +	+ + +							
Q9WTS6	Tenm3					+	+ + +										
Q9ERA6	Tfip11								+	+							
B1AZI6	Thoc2								+	+ + +					+	+ + +	
Q62318	Trim28			+													
P26369	U2af2					+ +	+ + +		+ +	+ + +		+	+ + +				
Q6EJB6	Utp14b											+	+ + +				
Q5SSI6	Utp18								+						+	+	
Q9JI13	Utp3								+								
Q9DCD2	Xab2											+					
Q8BJ05	Zc3h14					+	+ + +										
O88532	Zfr														+	+ + +	

Table 3.1 High and medium confidence protein interactors of Matrin-3.

Plus signs signify a fold change over empty vector of ≤10 (+), 10-50 (+ +) or ≥50 (+ + +). Medium confidence protein interactors were defined as those identified in two out of three replicates and with a fold change ≥2.5 over empty vector in the manual analysis, or a fold change ≥2.5 over empty vector and an avgP≥0 in the SAINTexpress analysis. High confidence interactors were those with a fold change ≥2.5 over empty vector in both the SAINTexpress analysis and the manual analysis along with a SAINTexpress avgP value ≥0.7.

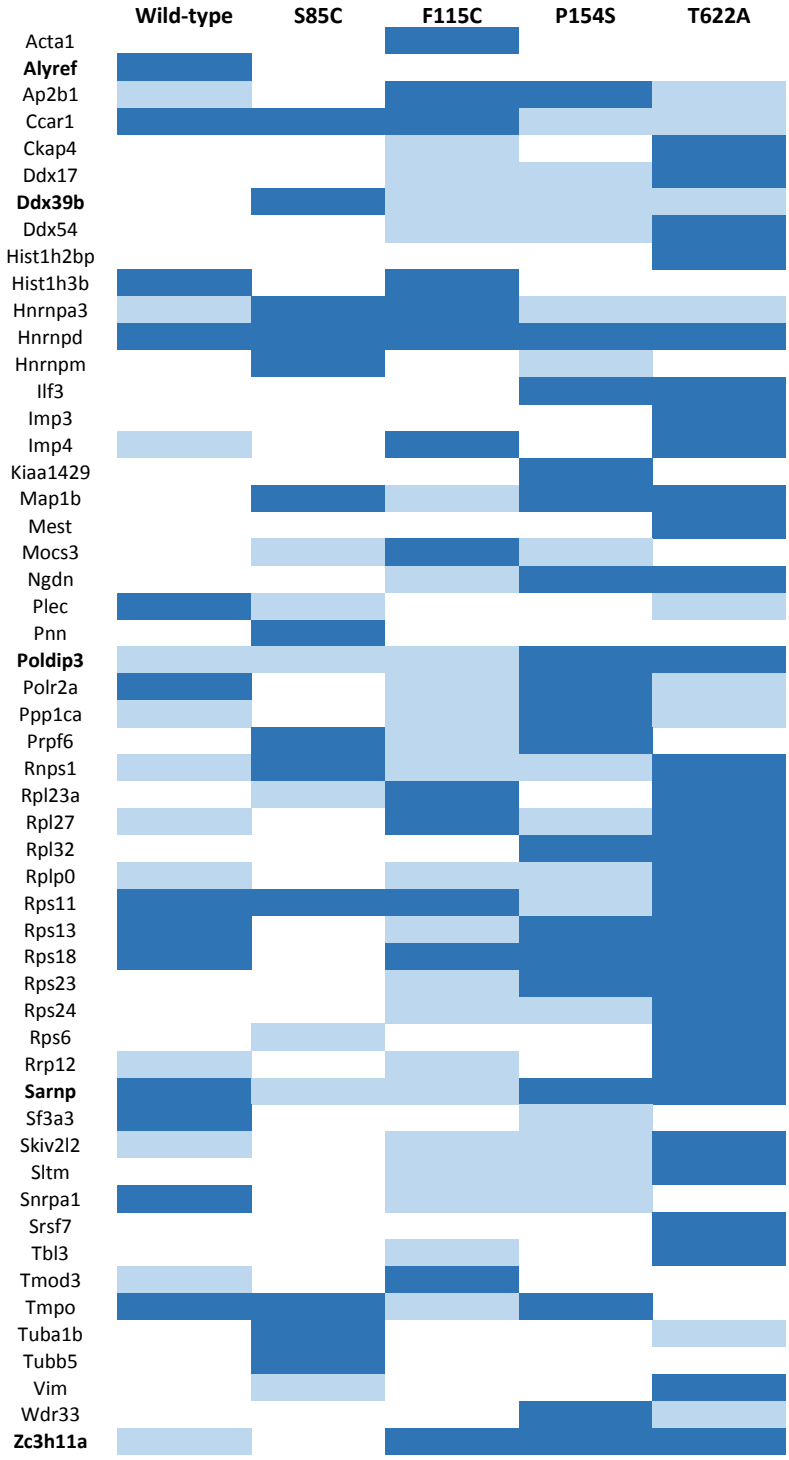

Table 3.2 List of high confidence proteins identified by IP-MS.

List of all proteins that met the threshold criteria for high confidence (identified in at least 2 replicates, fold change of at least 2.5 fold over vector and SaintExpress AvgP>0.7) in wild-type or mutant Matrin 3 IP-MS experiments. Proteins shown in white for a particular cell line were either not identified or did not meet minimum threshold

requirements for medium confidence (identified in at least 2 replicates, fold change of at least 2.5 fold over vector and SaintExpress AvgP>0), proteins shown in light blue met medium confidence thresholds, proteins shown in dark blue met high confidence threshold. Protein names that are bolded denote proteins involved in nuclear export and/or the TREX complex.

3.4.2 Gene Ontology Analysis Highlights mRNA Transport

ToppFun gene enrichment analysis was performed to functionally annotate the Matrin 3 interactome yielding a list of biological processes, many of which were RNA related (Table 3.3). The top biological process shared by wild-type and all four mutants was either "RNA processing" or in the case of Ser85Cys, "mRNA metabolic process". For wild-type Matrin 3 PPIs the top 15 biological processes were all related to RNA, including mRNA and rRNA, processing and biogenesis, transcription and splicing. While the top gene ontology (GO) terms for all four Matrin 3 mutations included these processes, they also included terms involved in mRNA and RNA transport/localization, suggesting a role for Matrin 3 in RNA transport (Table 3.3).

This pathway is particularly interesting due to recent reports describing interactions between the C9orf72 repeat and proteins involved in nuclear transport, as well as the subsequent defect in both protein import and RNA export in cells expressing the *C9orf72* repeat expansion [26-28]. Upon closer examination of Matrin 3 interacting proteins we identified multiple components and interactors of the TREX complex that controls mRNA nuclear export, including Aly (AlyRef), Sarnp (Cip29), Zc3h11a, Poldip3 and DdX39b (UAP56) (Dufu, Livingstone et al. 2010, Katahira 2012) (Table 3.1, 3.2). We further explored and validated interactions of Matrin 3 with TREX proteins and the role of Matrin 3 in mRNA nuclear export.

Wild-type		
GO term	***p*-value**	**# of genes**
RNA processing	2.81E-39	43
mRNA metabolic process	2.81E-38	39
mRNA processing	4.28E-30	31
RNA splicing	1.58E-27	28
RNA splicing, via transesterification reactions with bulged adenosine as nucleophile	1.61E-27	26
mRNA splicing, via spliceosome	1.61E-27	26
RNA splicing, via transesterification reactions	2.27E-27	26
ribonucleoprotein complex biogenesis	2.33E-14	20
rRNA processing	2.70E-09	13

Ser85Cys		
GO term	***p*-value**	**# of genes**
mRNA metabolic process	6.49E-33	36
mRNA processing	2.45E-31	32
RNA processing	6.64E-31	38
RNA splicing, via transesterification reactions with bulged adenosine as nucleophile	3.27E-27	26
mRNA splicing, via spliceosome	3.27E-27	26
RNA splicing, via transesterification reactions	4.61E-27	26
RNA splicing	1.28E-25	27
RNA localization	7.97E-09	12
nucleic acid transport	2.45E-08	11

Phe115Cys		
GO term	***p*-value**	**# of genes**
RNA processing	6.02E-42	51
mRNA metabolic process	4.23E-35	42
mRNA processing	1.12E-24	31
RNA splicing	3.71E-24	29
RNA splicing, via transesterification reactions with bulged adenosine as nucleophile	3.90E-23	26
mRNA splicing, via spliceosome	3.90E-23	26
RNA splicing, via transesterification reactions	5.48E-23	26
ribonucleoprotein complex biogenesis	2.18E-18	26
rRNA processing	3.38E-12	17

Pro154Ser		
GO term	***p*-value**	**# of genes**
RNA processing	1.61E-50	49
mRNA metabolic process	6.07E-44	42
mRNA processing	5.16E-32	32
RNA splicing	2.10E-29	29
RNA splicing, via transesterification reactions with bulged adenosine as nucleophile	4.61E-26	25
mRNA splicing, via spliceosome	4.61E-26	25
RNA splicing, via transesterification reactions	6.41E-26	25
ribonucleoprotein complex biogenesis	7.89E-16	21
termination of RNA polymerase II transcription	6.80E-12	10

Thr622Ala		
GO term	***p*-value**	**# of genes**
RNA processing	1.69E-28	38
mRNA metabolic process	1.44E-23	31
ribonucleoprotein complex biogenesis	2.38E-14	21
mRNA processing	3.97E-14	21
protein localization to endoplasmic reticulum	1.43E-12	13
rRNA processing	2.04E-12	16
rRNA metabolic process	3.10E-12	16
mRNA export from nucleus	6.26E-12	12
mRNA-containing ribonucleoprotein complex export from nucleus	6.26E-12	12

Wild-type			Ser85Cys			Phe115Cys			Pro154Ser			Thr622Ala		
GO term	***p*-value**	**# of genes**	**GO term**	***p*-value**	**# of genes**	**GO term**	***p*-value**	**# of genes**	**GO term**	***p*-value**	**# of genes**	**GO term**	***p*-value**	**# of genes**
rRNA metabolic process	3.78E-09	13	RNA transport	2.45E-08	11	rRNA metabolic process	5.26E-12	17	DNA-templated transcription, termination	2.78E-11	11	RNA splicing	7.46E-12	18
termination of RNA polymerase II transcription	3.04E-08	8	establishment of RNA localization	2.94E-08	11	termination of RNA polymerase II transcription	5.80E-12	11	mRNA export from nucleus	4.30E-11	11	mRNA transport	1.56E-11	13
ribosome biogenesis	3.97E-08	13	termination of RNA polymerase II transcription	4.20E-08	8	mRNA transport	9.80E-12	14	mRNA-containing ribonucleoprotein complex export from nucleus	4.30E-11	11	RNA splicing, via transesterification reactions with bulged adenosine as nucleophile	2.62E-11	16
DNA-templated transcription, termination	5.36E-08	9	mRNA transport	1.05E-07	10	ncRNA processing	2.09E-11	19	mRNA transport	6.96E-11	12	mRNA splicing, via spliceosome	2.62E-11	16
regulation of RNA splicing	1.16E-07	9	nucleobase-containing compound transport	1.77E-07	11	DNA-templated transcription, termination	5.28E-11	12	rRNA processing	1.01E-10	14	RNA export from nucleus	2.88E-11	12
nuclear-transcribed mRNA catabolic process, nonsense-mediated decay	2.52E-07	9	RNA export from nucleus	3.28E-07	9	RNA localization	6.34E-11	15	ncRNA processing	1.29E-10	16	ribonucleoprotein complex export from nucleus	2.88E-11	12

Table 3.3: Gene ontology analysis for biological processes using medium confidence proteins identified by IP-MS.

Top 15 biological processes by Bonferroni corrected *p*-value for wild-type and each mutant are listed. Grey boxes highlight terms involved in RNA transport and localization. Number of genes refers to the total number of Matrin 3 interacting proteins identified for each gene ontology term.

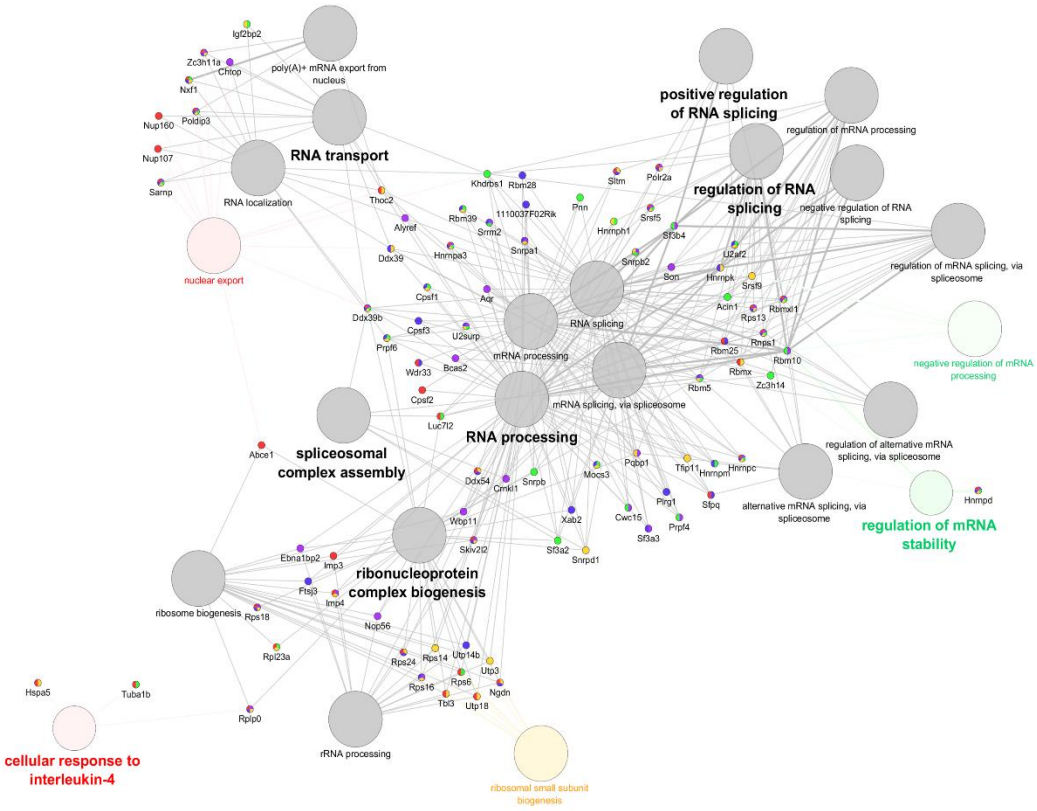

Figure 3.4 Functionally organized GO term network (ClueGO) of binding partners to wild type and mutant Matrin 3 in NSC-34 cells.

Associated gene clusters and functional differences are highlighted. GO terms with a single sample frequency above 50% were color-coded wild type (purple), Ser85Cys(green), Phe115Cys(yellow), Pro154Ser(blue), Thr622Ala(red), and unspecific (grey). Terms were considered unspecific if sample frequency was above 50% across more than one sample. Sample frequency was determined as a percentage based on the number of genes that defined that specific term. Increased size of GO term nodes inversely correlates to p-values computed by a two-sided hypergeometric test, with step-down Bonferroni correction.

ClueGO functional enrichment analysis was performed to aid in the visualization and interpretation of Matrin 3 PPI by grouping interacting proteins by biological processes, highlighting the role of Matrin 3 interacting proteins in RNA processing, RNA splicing, and RNP biogenesis (Figure 3.4). This analysis also emphasizes the role of Matrin 3 in RNA transport with such GO terms as "poly (A)+ mRNA export from the nucleus" and "RNA localization" common across all mutants and wild-type Matrin 3. While most GO terms were not unique to a specific mutation, "negative regulation of mRNA processing," and "regulation of mRNA stability" were linked specifically to Ser85Cys; "cellular response to interleukin-4" and "nuclear export" were linked specifically to Thr622Ala; and "ribosomal small subunit biogenesis" was linked to Phe115Cys (Figure 3.3). Future studies will explore the role of specific Matrin 3 mutations in mRNA stability and ribosomal biogenesis.

3.4.3 Validation of Matrin 3 interactions with TREX proteins

IP-MS results were validated in two manners, co-immunoprecipitation followed by western blot (IP-WB) and double-label immunofluorescence microscopy of cultured cells. Both methods also provided relative quantification of protein interactions with wild-type or mutant Matrin 3. Immunofluorescence microscopy was performed on cells transiently transfected with either wild-type or mutant Matrin 3 and immunostained with antibodies against the Flag tag on Matrin 3 and the protein of interest. Pearson's correlation coefficients were calculated for nuclear immunostaining to quantify levels of co-localization. Co-immunofluorescence against both Flag and Matrin 3 allowed us to explore whether mutant Matrin 3 co-localizes with endogenous Matrin 3 throughout the nucleus. Pearson's correlation coefficients ranged from 0.8 and 0.9 for endogenous Matrin 3 compared to exogenous Flag-Matrin 3 indicating high levels of co-localization

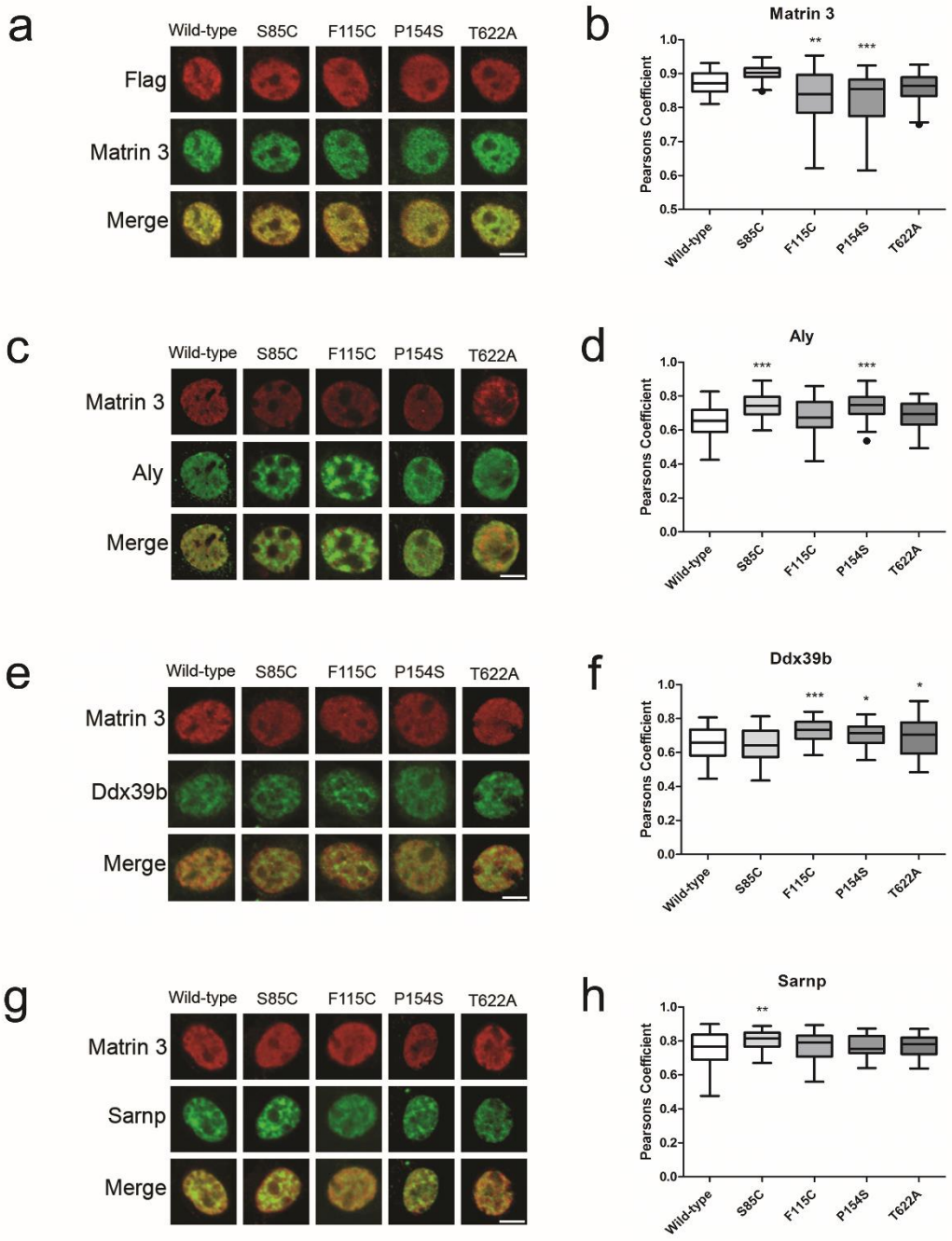

Figure 3.5 Immunofluorescence images of NSC-34 cells transiently transfected with wild-type or mutant Matrin 3 then subjected to co-localization analysis.

a,c,e,g) Representative images from immunofluorescence staining. In each case Flag is shown in red marking exogenous Matrin 3 and the protein of interest (Matrin 3, Aly, Ddx39b and Sarnp, respectively) is shown in green, merged image of two signals below. Scale bar indicates 5μm. b,d,f,h) Average Pearson's correlation coefficient for Flag and the protein of interest, whiskers indicate 1.5 times the interquartile range (IQR) for 40-50 cells per genotype. One way ANOVA followed by Dunnett's post-test, (*) denotes *p*-value <0.05, (**) $p<0.01$ and (***) $p<0.001$ compared to wild-type (Matrin 3 *p*-values: WT vs 85: $p=0.1524$, WT vs 115: $p=0.0035$, WT vs 154 $p=0.0002$, WT vs 622 $p=0.5535$, F-value: 12.61, DF=205; Aly *p*-values: WT vs 85: $p=0.0001$, WT vs 115: $p=0.8307$, WT vs 154 $p=0.0001$, WT vs 622 $p=0.3368$, F-value: 9.284, DF=211; Ddx39b *p*-values: WT vs 85: $p=0.9725$, WT vs 115: $p=0.0002$, WT vs 154 $p=0.0107$, WT vs 622 $p=0.0364$, F-value: 7.701, DF=224; Sarnp *p*-values: WT vs 85: $p=0.0090$, WT vs 115: $p=0.9400$, WT vs 154 $p=0.9791$, WT vs 622 $p=0.8224$, F-value: 2.913, DF=228).

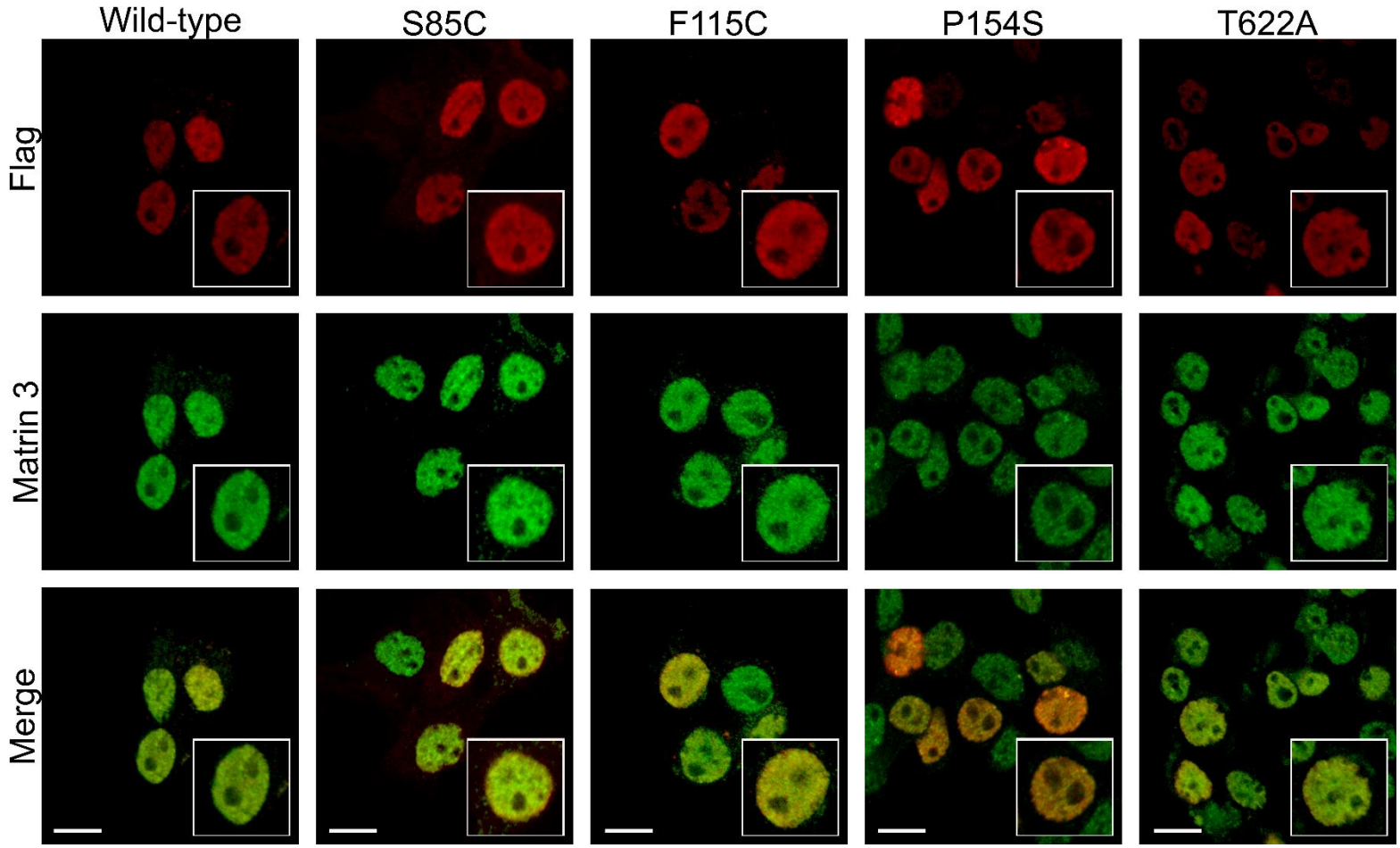

Figure 3.6 Wide Field View of Immunofluorescence Images of Cells Transiently Transfected with Matrin 3 then Subjected to Co-localization Analysis.

Representative images from immunofluorescence staining., flag is shown in red marking exogenous Matrin 3 and endogenous Matrin 3 is shown in green, merged image of two signals below. Insets indicate higher magnification images. Scale bar indicates 10µm

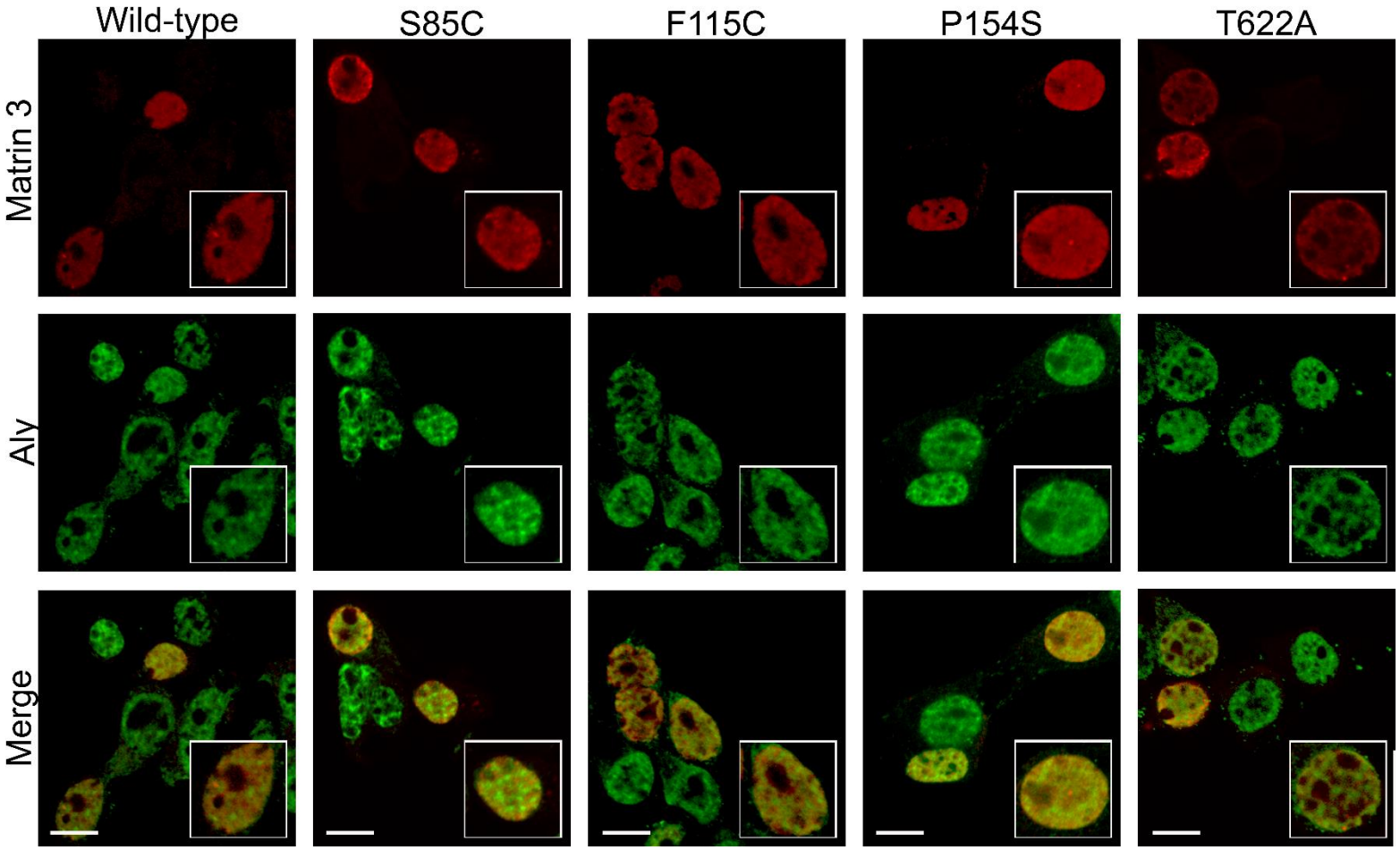

Figure 3.7 Wide Field View of Immunofluorescence Images of Cells Transiently Transfected with Matrin 3 then Subjected to Co-localization Analysis with Aly.

Representative images from immunofluorescence staining., flag is shown in red marking exogenous Matrin 3 and Aly is shown in green, merged image of two signals below. Insets indicate higher magnification images. Scale bar indicates 10µm

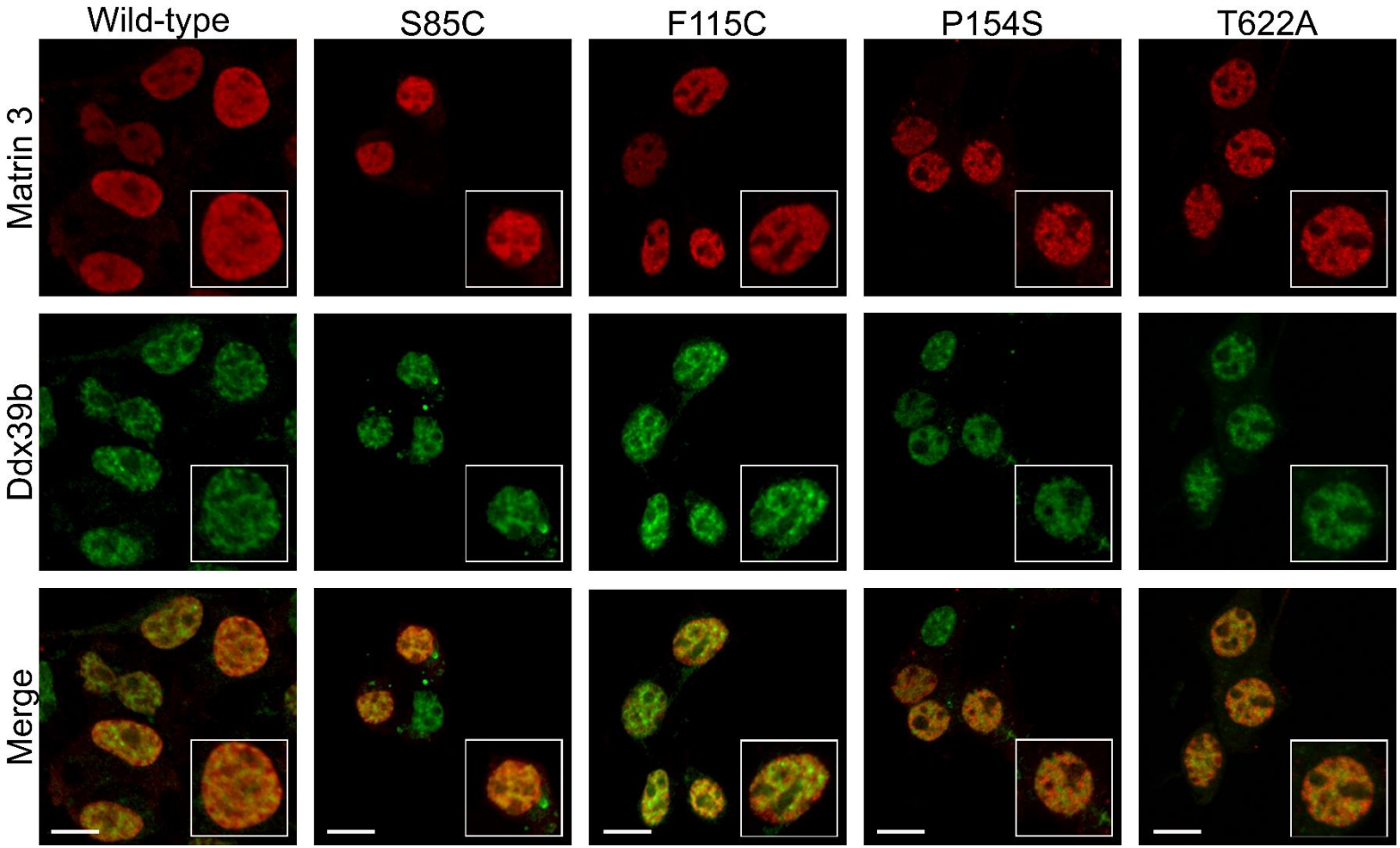

Figure 3.8 Wide Field View of Immunofluorescence Images of Cells Transiently Transfected with Matrin 3 then Subjected to Co-localization Analysis with Ddx39b.

Representative images from immunofluorescence staining., flag is shown in red marking exogenous Matrin 3 and Ddx39b is shown in green, merged image of two signals below. Insets indicate higher magnification images. Scale bar indicates 10μm

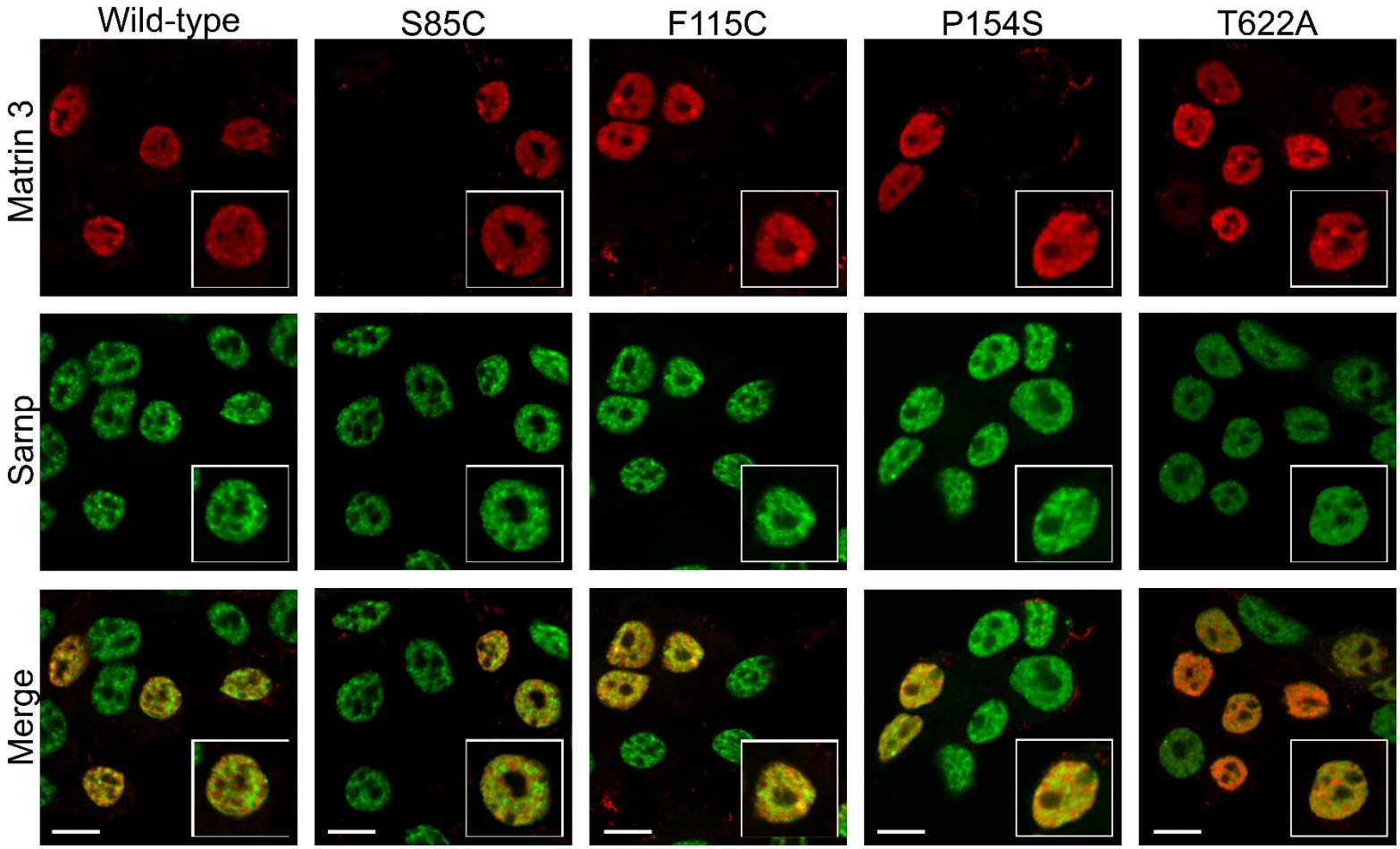

Figure 3.9 Wide Field View of Immunofluorescence Images of Cells Transiently Transfected with Matrin 3 then Subjected to Co-localization Analysis with Sarnp.

Representative images from immunofluorescence staining., flag is shown in red marking exogenous Matrin 3 and Sarnp is shown in green, merged image of two signals below. Insets indicate higher magnification images. Scale bar indicates 10µm

between the two (Figure 3.5). The F115 and P154S mutations of Matrin 3 co-localized significantly less with endogenous Matrin 3, suggesting that ALS-linked mutations alter the localization of mutant protein within the nucleus (Fig. 3.5 a, b, Figure 3.6). This change in mutant Matrin 3 distribution within the nucleus may reflect the altered protein-protein interactions observed by IP-MS and contribute to disease pathogenesis induced by these mutations.

We next explored co-localization between proteins involved in TREX regulated mRNA export (Aly, Sarnp and Ddx39b) with wild-type and mutant Matrin 3. For all three proteins, Pearson's coefficients were found to be 0.6 or higher, implying that the three proteins do co-localize with Matrin 3, further validating our IP-MS results (Figure 3.5c-h). The S85C and P154S mutations in Matrin 3 exhibited increased levels of co-localization with Aly as compared to wild-type Matrin 3 while F115C and T622A levels remained similar to wild-type (Figure 3.5c, d, Figure 3.7). Three of the four Matrin 3 mutations (F115C, P154S, and T622A) exhibited increased co-localization between mutant Matrin 3 and Ddx39b, with S85C showing similar levels to wild-type (Figure 3.5 e, f, Figure 3.8). S85C did, however, show increased levels of co-localization with Sarnp while the other mutants showed no difference (Figure 3.5 g, h Figure 3.9). Taken together, ALS-linked mutations in Matrin 3 co-localized less with endogenous Matrin 3 and exhibited increased co-localization with components of the TREX complex. A shift in protein interactions may induce alterations in TREX function within cells expressing ALS associated mutations in Matrin 3.

Using co-IP coupled with western blot, Matrin 3 interactions were confirmed for each of the TREX proteins (Figure 3.10a). We also confirmed protein-protein interactions between endogenous Matrin 3 and Aly and Ddx39b (Figure 3.10b, c). To rule out potential non-specific pull-down by the Flag antibody, reverse IP experiments were performed using antibodies against Aly or Ddx39b. Our results confirm the predicted interaction of Matrin 3 with Aly and Ddx39b (Figure 3.10d). Quantitation of these blots showed a trend towards increased binding of both Aly and Ddx39b to the S85C and P154S mutations in Matrin 3, while increased binding of S85C Matrin 3 to Ddx39b reached statistical significance (Figure 3.10e, f).Co-immunopreciptiation between Matrin 3 and Ddx39b was also performed in human post-mortem lumbar spinal cord tissue, confirming that these proteins interact *in vivo* and in the context of sporadic ALS (Figure 3.10g). Patient demographics for samples used in Figure 3.10g are listed in Table 3.4.

In addition to proteins within the TREX complex, the interaction between Matrin 3 and hnRNPL as well as other proteins involved in ALS were examined. hnRNPL was chosen as a positive control as it has been identified previously as a Matrin 3 interacting protein. TDP-43, FUS, hnRNPA1 and hnRNPA2/B1 were all examined due to their links to other genetic forms of ALS. In all cases the proteins identified by IP-MS were also identified by IP-WB. In the case of TDP-43 which had previously been shown to bind to Matrin 3 and the interaction increased by the S85C mutation the same results were found with the addition of increased binding between TDP-43 and P154S Matrin 3 (Figure 3.11).

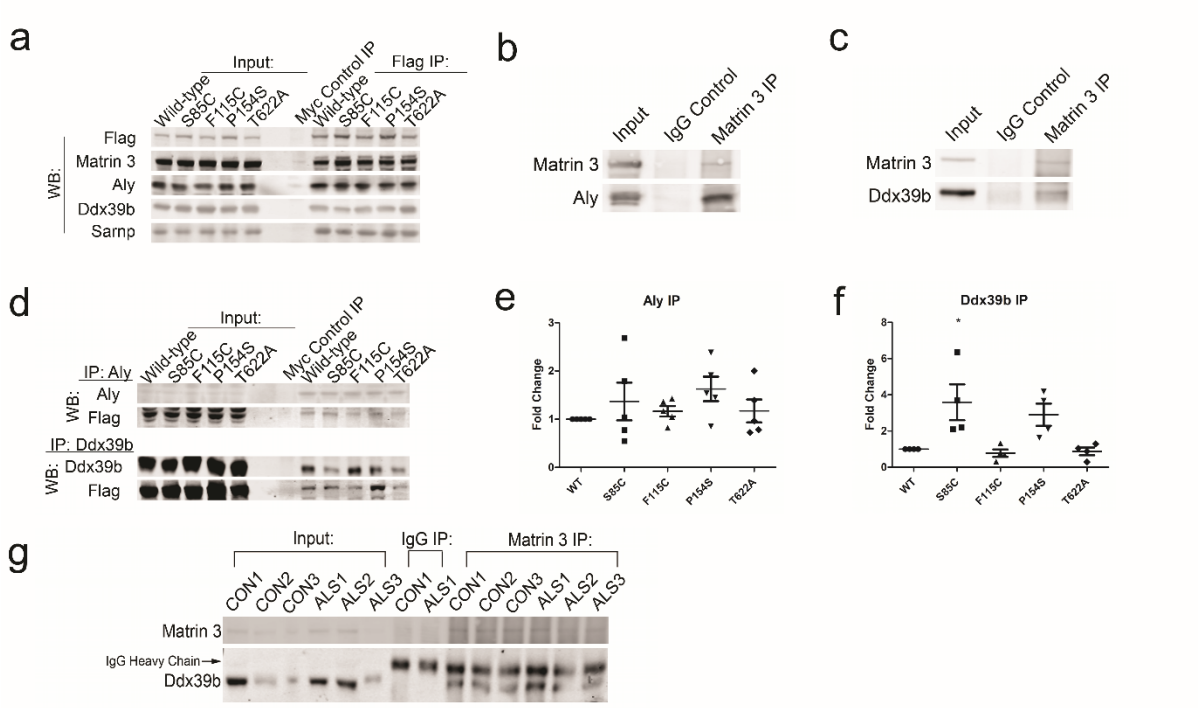

Figure 3.10 Immunoprecipitation followed by western blot from NSC-34 cell lines and human lumbar spinal cord tissue.

a) Immunoprecipitation using Flag antibody followed by western blot which was probed with Flag and Matrin 3 to confirm efficient pull down of Matrin 3, or TREX components Aly, Ddx39b and Sarnp; representative blots are shown, and all experiments were performed a minimum of three times with similar results. Full length blots in figure 3.15. b,c)Matrin 3 IP performed on endogenous Matrin 3 in untransfected NSC-34 cells. Immunoblots are probed with Aly (b) or Ddx39b (c). Full length blots can be found in figure 3.16. d) Reverse immunoprecipitation experiments using antibodies against Aly and Ddx39b followed by western blot probed with either Aly or Ddx39b confirming pull-down of the target and Flag to measure the amount of mutant Matrin 3 bound, representative blots shown. Full length blots can be found in figure 3.17. e,f) Quantification of Aly and Ddx39b IP-WB experiments; values are expressed as Flag signal over signal of the bait protein (Aly or Ddx39b respectively) to control for IP efficiency, Aly IP values from five replicates, Ddx39b IP values from four replicates. Values are expressed as fold change over wild-type and error bars represent SEM. One way ANOVA followed by Dunnett's post-test,(*) denotes *p*-value <0.05 (Aly *p*-values: WT vs 85: $p=0.6561$, WT vs 115: $p=0.9670$, WT vs 154 $p=0.2250$, WT vs 622 $p=0.9611$, F-value: 1.011, DF=24; Ddx39b *p*-values: WT vs 85: $p=0.0133$, WT vs 115: $p=0.9944$, WT vs 154 $p=0.0760$, WT vs 622 $p=0.9993$, F-value: 6.025, DF=19).g) Matrin 3 IP performed in human lumbar spinal cord nuclear lysates of controls n=3 and

ALS patients n=3. Immunoblot is probed with Ddx39b and Matrin 3. Arrow indicates IgG heavy chain band. Full length blots can be found in figure 3.18.

Case ID	Gender	Age	PMI (hrs)
CON1	F	74	3
CON2	M	81	17
CON3	F	57	32
ALS1	M	72	3
ALS2	M	39	5.5
ALS3	M	83	21

Table 3.4 Patient Demographics of lumbar spinal cord tissues used in the study...

PMI = post-mortem interval. All diagnoses were performed by licensed neuropathologists.

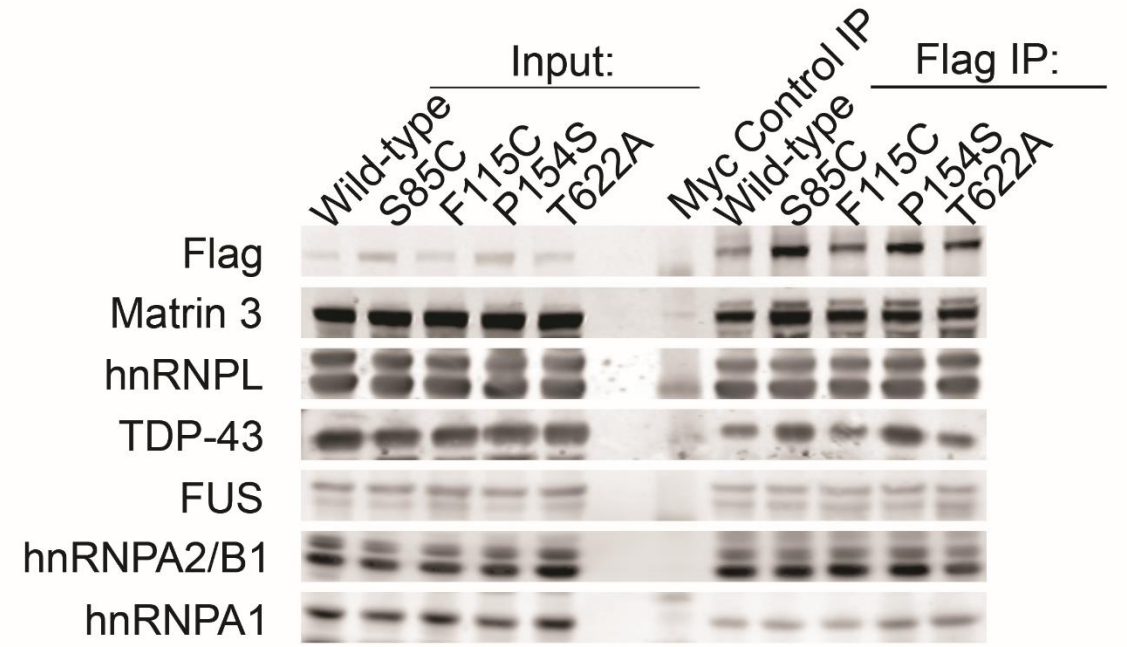

Figure 3.11 Flag IP followed by western blot showing binding between Matrin 3 and proteins additional proteins identified by mass spectrometry

Immunoprecipitation using Flag antibody followed by western blot which was probed with Flag and Matrin 3 to confirm efficient pull down of Matrin 3. Western blots were also probed with hnRNPL, a known binding partner of Matrin 3 as a positive control and ALS linked proteins TDP-43, FUS, hnRNPA2/B1 and hnRNPA1; representative blots are shown, and all experiments were performed a minimum of three times with similar results

3.4.4 Matrin 3 mutations reduce mRNA nuclear export

Unlike other nuclear export machinery, the TREX complex is restricted to the export of mRNA (Strasser, Masuda et al. 2002). To confirm the role of Matrin 3 in nuclear mRNA export we performed fluorescence in situ hybridization (mRNA-FISH) using an oligo dT probe against poly(A) containing mRNA in cells transiently expressing either wild-type or mutant Matrin 3, and measured the amount of mRNA in the nucleus and cytoplasm of each cell. Nuclear to cytoplasmic ratios of mRNA were calculated for cells expressing mutant Matrin 3 (Transfected), and neighboring non-transfected cells (Untransfected) (Fig. 3.12a-f). There was a trend towards an increased nuclear to cytoplasmic ratio of mRNA for transfected vs. non-transfected for wild-type and all mutant expressing cells. There was a statistically significant increase in polyA-mRNA nuclear to cytoplasmic ratio in cells expressing S85C and P154S Matrin 3 (Fig. 3.12f). Expression of S85C resulted in a 34% increase in the nuclear to cytoplasmic ratio of mRNA and P154S expression resulted in a 29% increase in the ratio (Fig. 3.12f). The increased nuclear to cytoplasmic ratio implies that mRNA is sequestered within the nucleus in cells expressing mutant Matrin 3 protein and S85C and P154S Matrin 3 mutations induce significant defects in mRNA nuclear export.

3.4.5 Mutations in Matrin 3 lead to export defects of TDP-43 and FUS mRNA

After demonstrating a global defect in mRNA export from the nucleus, we explored whether this defect affected specific mRNAs for proteins relevant to ALS. We focused on the mRNA of TDP-43 (Johnson, Pioro et al. 2014) and FUS (Yamaguchi and Takanashi 2016) ,two RNA-binding proteins previously linked to ALS, both of which

have been shown to bind to Matrin 3. To demonstrate the role of Matrin 3 in the nuclear export of TDP-43 and FUS mRNA, cellular fractionation followed by RT-PCR for TDP-43 and FUS mRNA in each compartment was performed using HEK-293 cells expressing either wild-type or ALS associated mutant Matrin 3. HEK-293 cells were utilized in this experiment to demonstrate the role of Matrin 3 in nuclear export in a human cell line, though similar results were obtained using the NSC-34 cell lines (data not shown). Expression of wild-type Matrin 3 generated no change when compared to control cells but expression of S85C, and T622A Matrin 3 mutations led to an increase in the nuclear to cytoplasmic ratio of TDP-43 mRNA compared to an empty vector control (Fig. 3.12g). The nuclear to cytoplasmic ratio of FUS mRNA was increased by expression of S85C, P154S and T622A mutant Matrin 3 (Fig. 3.12h). In both cases RT-PCR with primers specific for TDP-43 and FUS was also performed on whole cells to confirm that the difference in mRNA levels was not due to differential mRNA expression or degradation (Fig. 3.13).

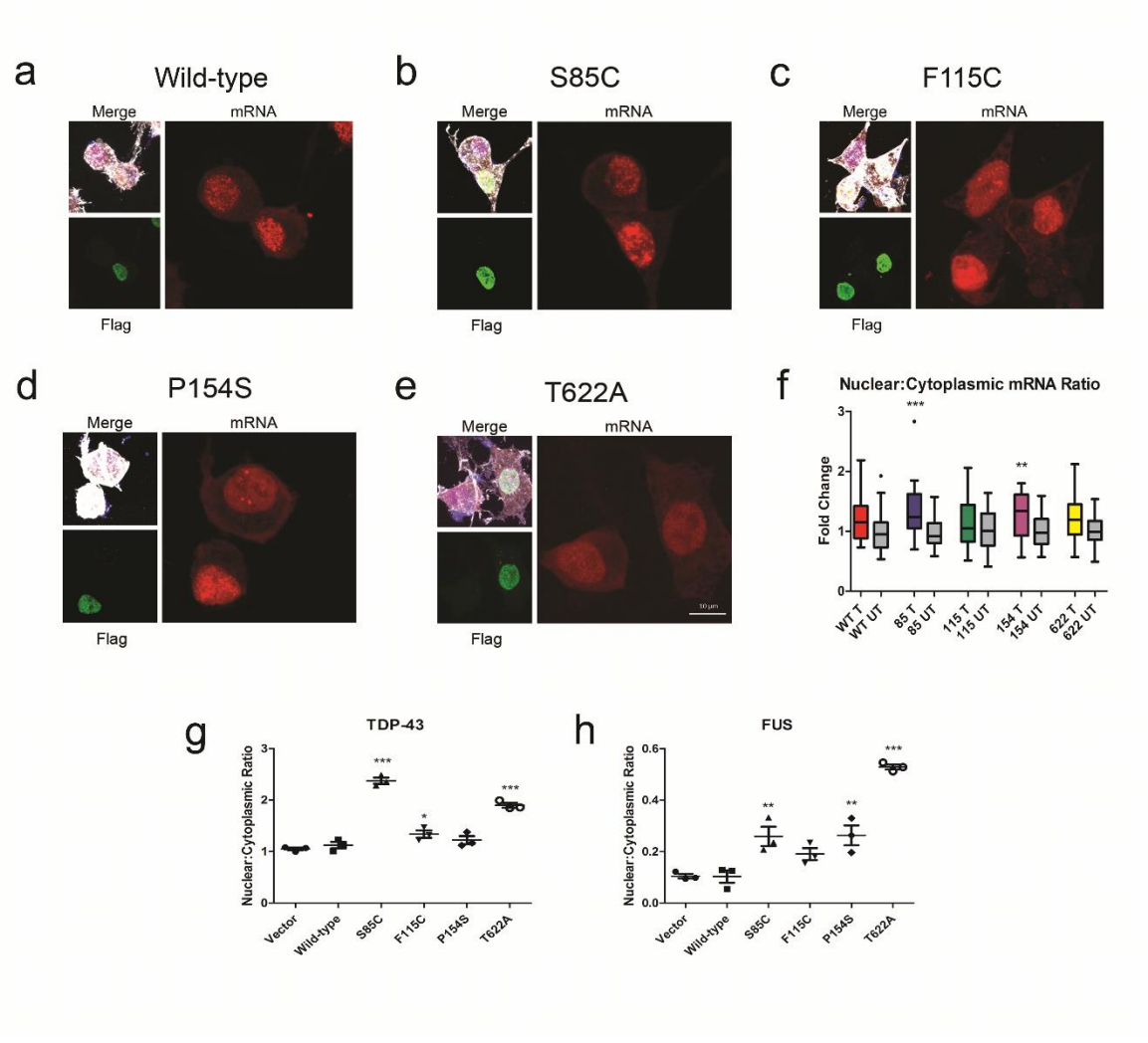

Figure 3.12 RNA-FISH and cellular fractionation followed by RT-PCR show defects in RNA export.

Experiments performed in NSC-34 cells transiently transfected with either wild-type or mutant Matrin 3. a-e) mRNA signal of RNA-FISH experiment shown in red, immunofluorescence staining of cells using actin to mark the cell body (white), Flag to mark transfected cells (green) and DAPI to mark the nucleus (blue) (representative images). f) Nuclear to cytoplasmic mRNA ratio of transfected (T) vs. untransfected (UT) cells for wild-type Matrin 3 and each mutant expressed as fold change over untransfected cells on the same slide, 31-34 cells were measured per genotype collected from three independent experiments. Whiskers indicate 1.5(IQR). One way ANOVA followed by Bonferroni post-test, WT *p*-value: 0.0697, 85 *p*-value: 0.0005, 115 *p*-value: 0.4100, 154 *p*-value: 0.0073, 622 *p*-value: 0.0596). g,h). Cell fractionation followed by RT-PCR on nuclear and cytoplasmic fractions of HEK-293 cells. Values are expressed as average nuclear to cytoplasmic ratio of either TDP-43 or FUS mRNA, normalized to tRNA-Lys

for the nuclear fraction and cytochrome b for the cytoplasmic fraction. Error bars represent mean and SEM of three replicates. Experiments were each performed three times, graphs show representative experiment. One way ANOVA followed by Dunnett's post-test (TDP-43 *p*-values: WT vs Vector: $p=0.8529$, WT vs 85: $p=0.0001$, WT vs 115: $p=0.1003$, WT vs 154 $p=0.6840$, WT vs 622 $p=0.0001$, F-value: 74.31, DF=17; FUS *p*-values: WT vs Vector $p=0.9999$, WT vs 85: $p=0.0054$, WT vs 115: $p=0.1336$, WT vs 154 $p=0.0045$, WT vs 622 $p=0.0001$, F-value: 35.21, DF=17, (*) denotes p-value <0.05, (**) p<0.01 and (***) p<0.001 for both RNA FISH and RT-PCR data.

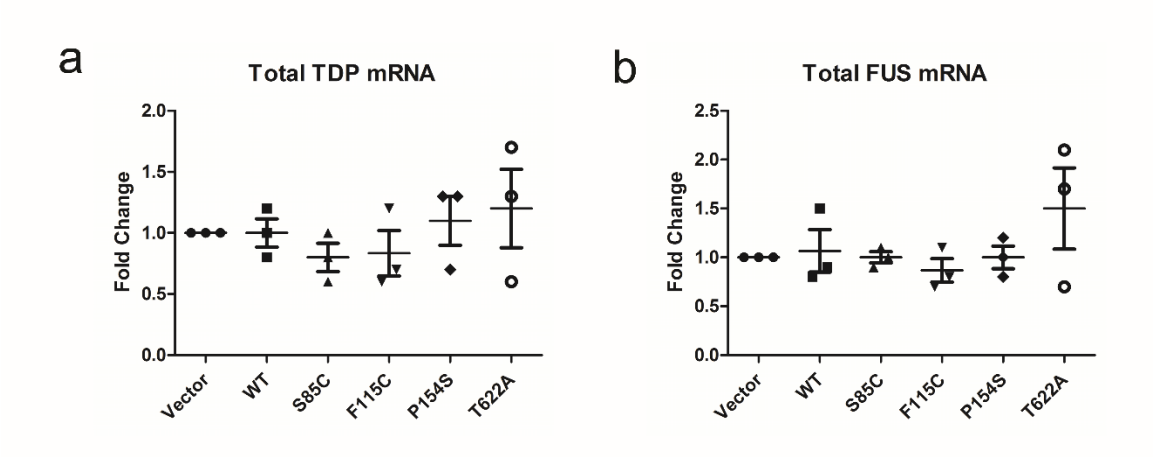

Figure 3.13 Total TDP-43 and FUS mRNA levels by RT-PCR.

Prior to fractionation experiments an aliquot of cells was separated and total RNA was extracted, followed by RTPCR to determine the total levels of a) TDP-43 and b) FUS. mRNA levels were not altered by expression of wild-type or mutant Matrin 3. Error bars represent the mean +/- SEM of three independent experiments

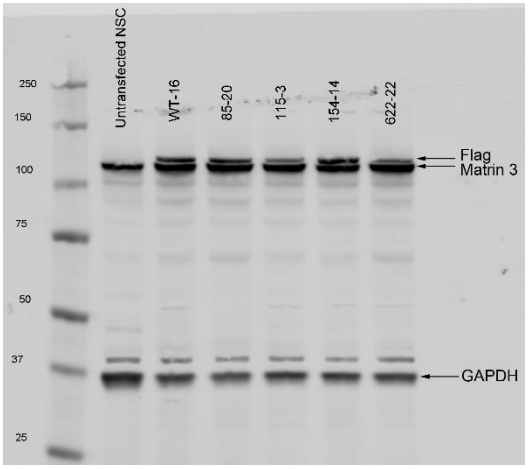

Figure 3.14 Full length western blot of RIPA lysates.

Full length western blot of representative image shown in figure 3.1c. Blot was probed three times with antibodies for Flag, Matrin 3 and GAPDH. Each band is identified with an arrow and label.

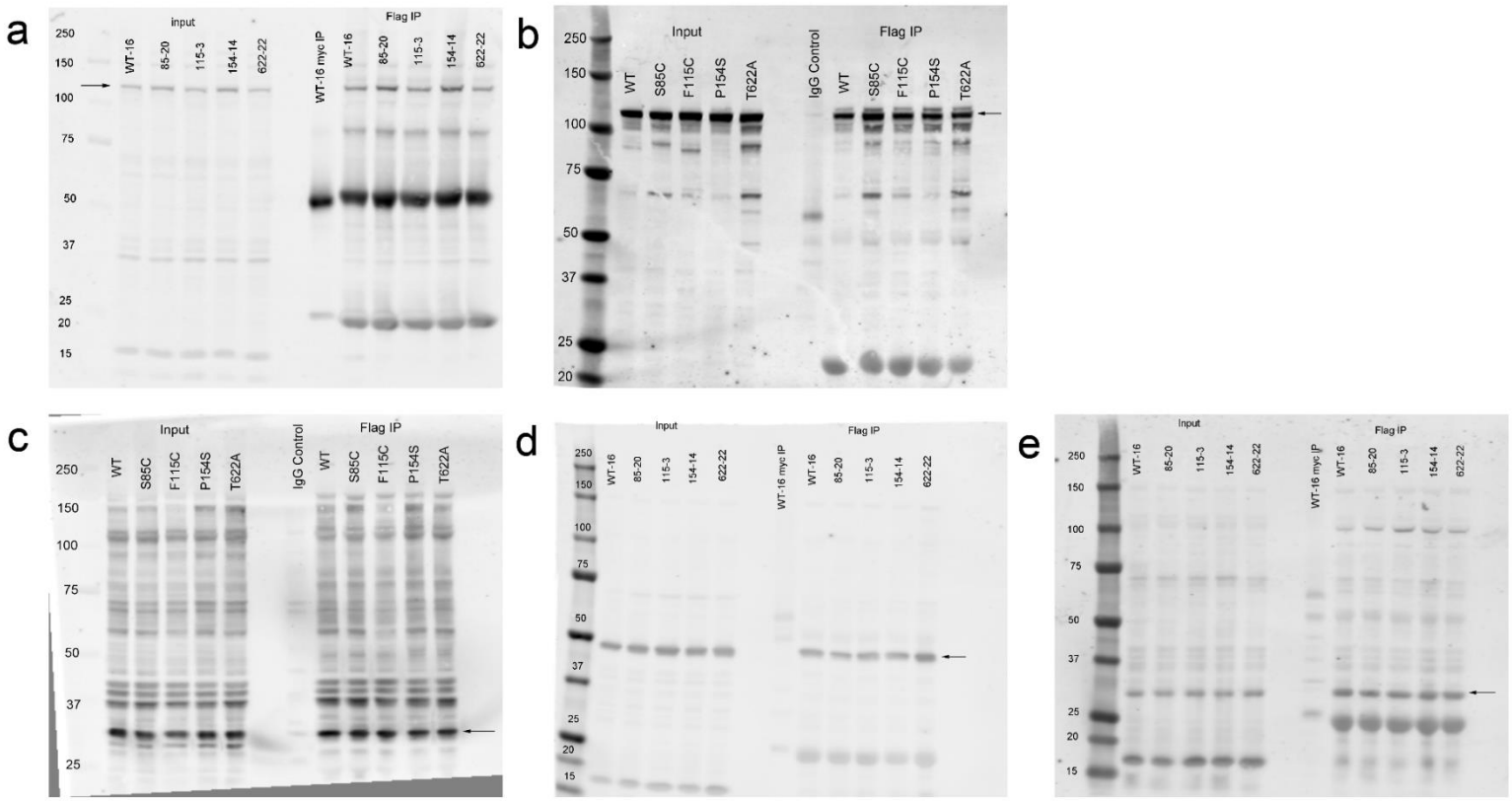

Figure 3.15 Full length western blots of Flag IPs

Full length western blots of Flag IPs from figure 3.9a probed with a) Flag, b) Matrin 3, c) Aly ,d) Ddx39b, e) Sarnp . Arrows mark band for each protein in question.

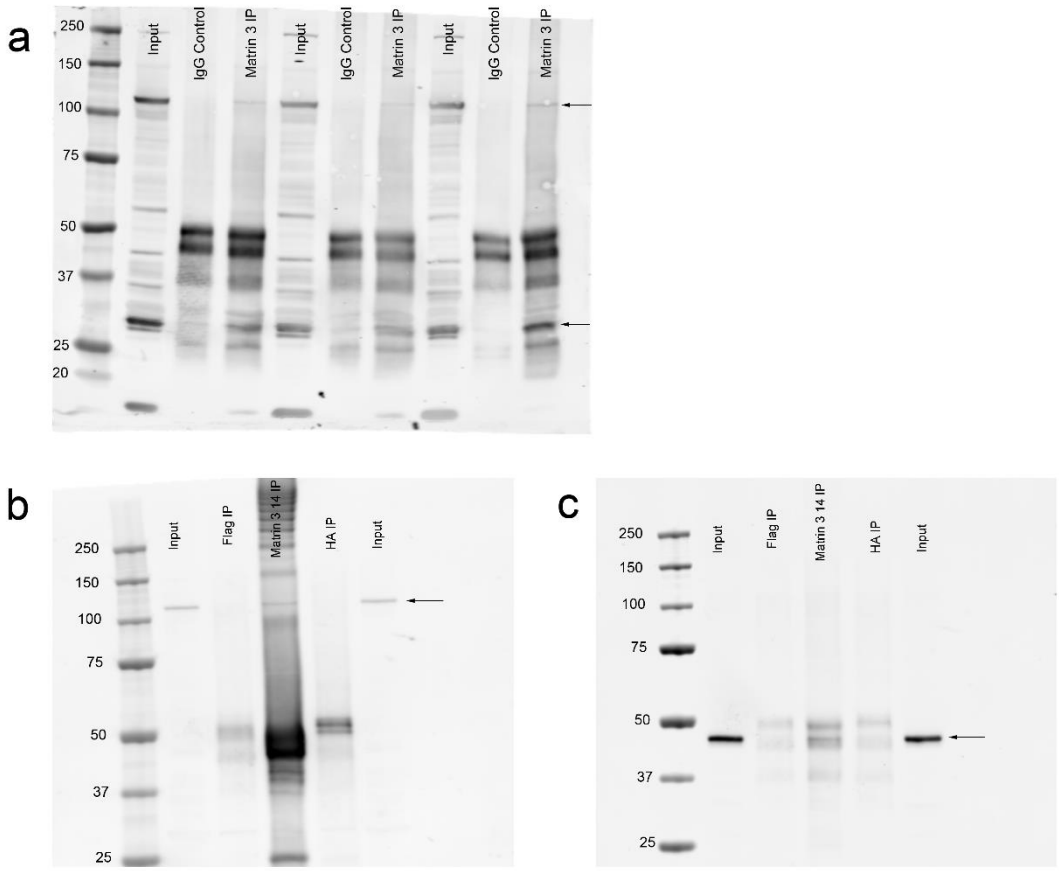

Figure 3.16 Full length western blots of Matrin 3 endogenous IPs.

Full length western blots of Matrin 3 endogenous IPs from figure 3.9 b and c. a) Matrin 3 IP probed with Matrin 3 (top arrow) and Aly (bottom arrow). b,c) Matrin 3 IP probed with Matrin 3 (b) band denoted by arrow, and Ddx39b (c) band denoted by arrow.

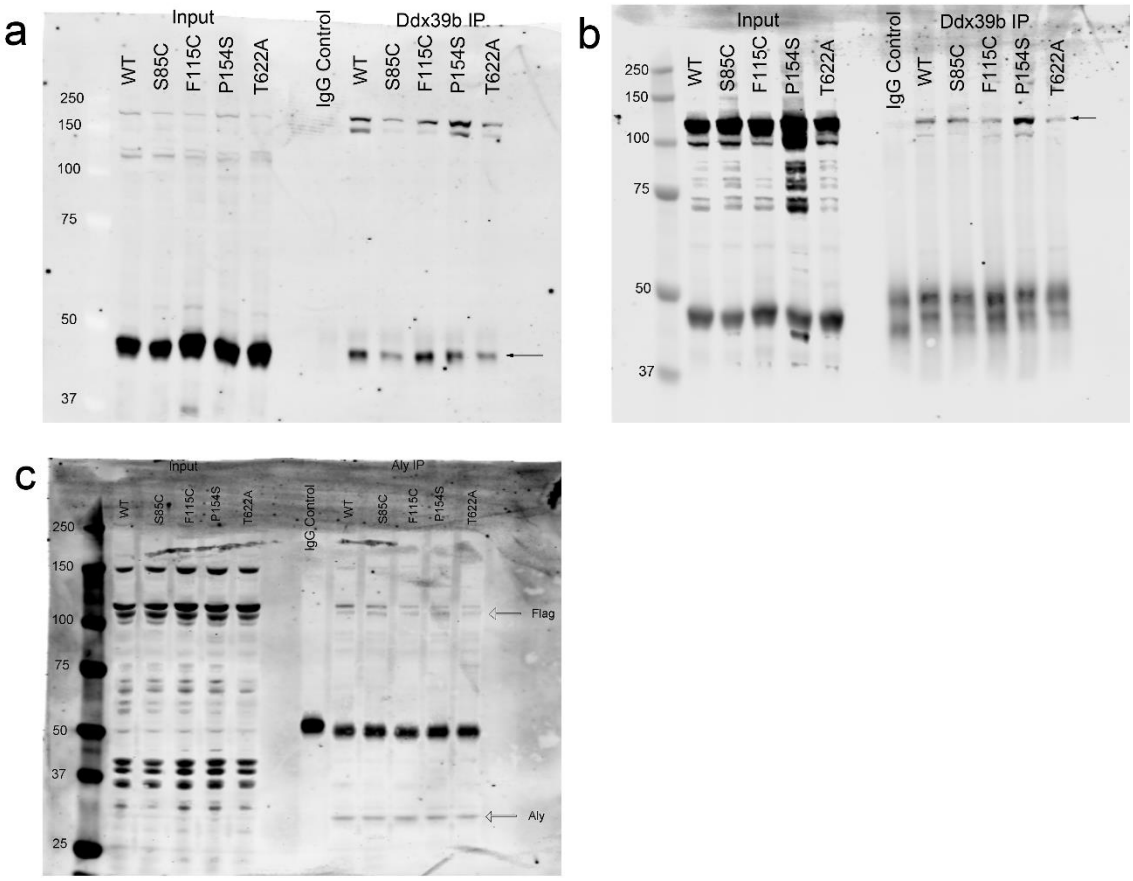

Figure 3.17 Full length western blots for Ddx39b and Aly IPs.

Full length western blots from figure 3.9d showing Ddx39b IPs (a and b) probed with Ddx39b (a) and Flag (b) and Aly IPs (c) probed with Aly and Flag. Arrows denote bands of interest.

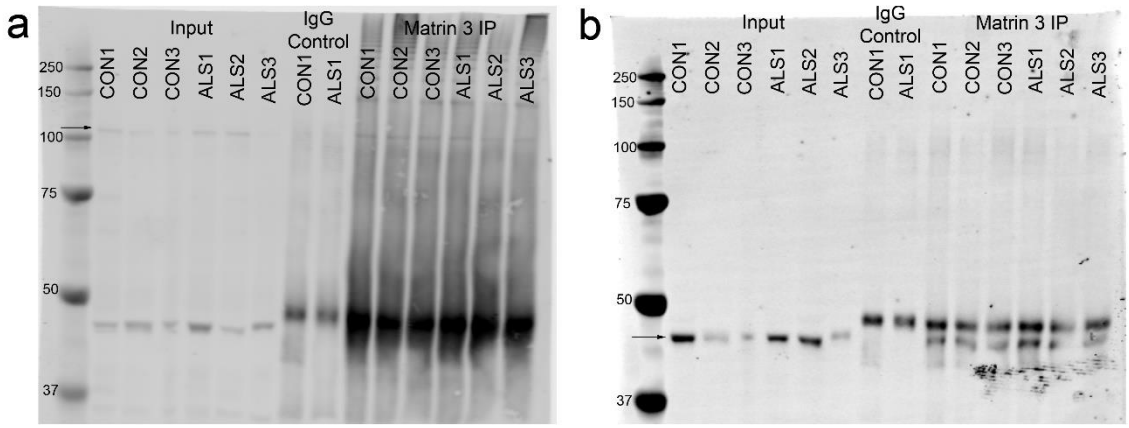

Figure 3.18 Full length western blots for Matrin 3 IPs performed in spinal cord tissue lysates.

Full length western blots from figure 3.9g showing Matrin 3 IPs performed in spinal cord tissue lysates probed with Matrin 3 (a) and Ddx39b (b). Arrows denote bands of interest.

3.5 DISCUSSION

We performed IP-MS to identify Matrin 3 interacting proteins, and determine alterations in PPIs caused by ALS-linked mutations. This yielded 167 total proteins that met our confidence threshold for interacting with either wild-type or one of the four mutant Matrin 3 proteins (Table 3.1). This contrasts with previously published IP-MS experiments which each identified only eight wild-type Matrin 3 interacting proteins (Salton, Elkon et al. 2011, Erazo and Goff 2015). Our results identified 6 of the 8 proteins identified in Salton et al., and 7 out of the 8 proteins identified in Erazo et al., though these proteins did not meet our stringent confidence thresholds for protein interaction. In comparison to other studies, the discrepancies in the number of Matrin 3 interactors identified in our work is likely due to the different cell types and methodologies used for the proteomic analysis. We also identified differences in PPIs induced by disease causing mutations in *MATR3*. On average, each mutant Matrin 3 protein exhibited approximately 60% different interactors than the wild-type interactome (ranging between 54-63%), suggesting that these mutations allow for novel Matrin 3 protein interactions that may impact its function and contribute to disease.

Gene ontology analysis highlighted terms including “RNA localization,” “RNA transport,” and “mRNA transport” within the top 15 most enriched biological processes for mutant but not wild-type Matrin 3. Examination of Matrin 3 PPIs involved in RNA localization, transport and export yielded several members of the TREX complex. The role of the TREX complex is to link transcription, mRNA processing and mRNA nuclear export. After transcription, pre-mRNA molecules associate with several proteins to form

a dynamic messenger ribonucleoprotein (mRNP). TREX proteins are components of this mRNP from the initial stages of transcription, throughout splicing and processing, and ultimately to delivery of the mRNP for transfer to the nuclear pore and export (Heath, Viphakone et al. 2016). Interestingly, we identified Matrin 3 interactions not only with proteins that are core components of TREX such as Aly, Sarnp, Ddx39b, Zc3h11a, Chtop, Poldip3, and Thoc2, but also interactions between Matrin 3 and proteins involved in all stages of mRNA biogenesis and export (Supplemental Table 1). Matrin 3 also interacted with three RNA polymerase II subunits, Polr2a, Polr2b, and Polr2c that function at early steps of transcription. Proteins involved in RNA splicing that interact with Matrin 3 include Pnn (Wang, Lou et al. 2002), Prpf6 (Tanackovic, Ransijn et al. 2011), Sf3a3 (Tanackovic and Kramer 2005), Skiv2l2 (Nag and Steitz 2012), Snrpa1 (Makarov, Owen et al. 2012), and Srsf7 (Muller-McNicoll, Botti et al. 2016). Interestingly Pnn, Prpf6 and Srsf7 bind to various mutations in Matrin 3 but were not found on the wild-type list. While we have not explored the role of Matrin 3 in mRNA splicing, others have shown a role for wild-type Matrin 3 as a splicing regulator which tends to repress exon inclusion (Coelho, Attig et al. 2015). One of the transcripts shown to be regulated by Matrin 3 was ADAR1B which is altered in ALS (Hideyama, Yamashita et al. 2012). Future work will explore the role of wild-type and mutant Matrin 3 in RNA splicing.

We also identified Matrin 3 interactions with proteins involved in the delivery of mRNPs from TREX to the nuclear pore complex, including interactions with the nuclear export receptor NXF1, and nuclear pore proteins Nup107 and Nup160. While we have

not validated these mass spectrometry based results, our data suggests that Matrin 3 participates in processes throughout mRNA processing, transport and export from the nucleus. It is unclear whether Matrin 3 performs these functions as a resident nuclear matrix protein or if there is a soluble pool of Matrin 3 that functions within and travels with TREX. We determined that mutant Matrin 3 proteins are less co-localized with endogenous Matrin 3 (when compared to exogenously expressed wild-type Matrin 3) and instead more co-localized with TREX proteins Aly, Ddx39b and Sarnp. This suggests that while there are no gross overall changes in the localization of mutant Matrin 3 within the cell, there is a re-distribution in the localization of mutant Matrin 3 within the nucleus. Altered protein-protein interactions with TREX proteins may explain the observed defects in mRNA nuclear export induced by Matrin 3 mutant proteins in our study. The two Matrin 3 mutations with the strongest global export defects, S85C and P154S, were also the two mutations that showed increases in co-localization with Aly and increased binding to both Aly and Ddx39b. This suggests that alterations in the associations of Aly and Ddx39b with Matrin 3 caused by ALS-linked mutations may be key to the downstream phenotype of nuclear mRNA retention. Future studies will define the role of Matrin 3 interactions with Aly and Ddx39b in regulating mRNA nuclear export. In addition, prior studies have shown a role for Matrin 3 in the nuclear export of HIV transcripts via CRM1 mediated nuclear export (Kula, Gharu et al. 2013). Since CRM1 mediated nuclear export can also export some mRNAs, future studies will also explore the potential roles of Matrin 3 mutations in modulating RNA nuclear export of retroviral infected cells. We previously reported increased binding between the S85C

Matrin 3 mutant protein and TDP-43, suggesting this mutation could have increased affinity to many different nuclear proteins (Johnson, Pioro et al. 2014). Interestingly, the S85C Matrin 3 also showed the largest change in the nuclear to cytoplasmic ratio of TDP-43 mRNA (Fig. 5g), and patients with this genotype have been shown to exhibit ALS and distal myopathy phenotypes (Johnson, Pioro et al. 2014, Muller, Kraya et al. 2014, Yamashita, Mori et al. 2015, Palmio, Evila et al. 2016). While various Matrin 3 mutations impact TDP-43 or FUS mRNA nuclear export to various degrees, we did not detect global changes in TDP-43 or FUS protein levels or subcellular distribution in these same cells (data not shown).

The cell culture model utilized in these experiments (NSC-34) is a mouse motor neuron like hybrid cell line. Matrin 3 is highly conserved between human and mouse with 98.5% sequence homology at the amino acid level and 94.8% at the DNA level (HomoloGene, NCBI). Three of the four mutations that were studied in this work are in highly conserved regions of Matrin 3 (S85C, P115C, P154S), however the sequence differs at amino acid 622, which is threonine in humans and alanine in mice. While this is a limitation of the model system used in this study, IP-MS experiments were also performed in a human cell line (HEK-293) and identical interactions between Matrin 3 and TREX proteins including Chtop, Aly, and Zc3h11a were observed in this human cell line (data not shown). We also demonstrate interactions of endogenous Matrin 3 with TREX proteins and interactions of wildtype Matrin 3 with the TREX protein Ddx39b in human post-mortem tissue samples. Future studies will further explore interactions of

mutant Matrin 3 and TREX proteins in human post-mortem tissue samples or patient derived stem cells.

While a role for Matrin 3 in TREX and nuclear export is novel, a functional role for Matrin 3 in splicing has been recently demonstrated (Coelho, Attig et al. 2015), and splicing is an integral functional role of TREX. Matrin 3 was linked to the export of viral RNA via the CRM1 mediated nuclear export pathway (Kula, Gharu et al. 2013), as discussed above. Finally, Matrin 3 was identified by mass spectrometry using isolated nuclear pore fractions (Cronshaw, Krutchinsky et al. 2002), suggesting that this protein can be located at the nuclear pore. The role of nuclear transport in ALS was initially implicated due to the discovery of mutations in the export protein GLE1 in familial ALS (Kaneb, Folkmann et al. 2015). More recently, nucleocytoplasmic transport has moved to the forefront of ALS pathobiology due to nuclear transport defects in numerous model systems expressing either the *C9orf72* repeat expansion or dipeptide repeat proteins (DPRs) (Freibaum, Lu et al. 2015, Jovicic, Mertens et al. 2015, Zhang, Donnelly et al. 2015) as well as in cells expressing c-terminal fragments of TDP-43 (Woerner, Frottin et al. 2016). Proteins that modified the C9orf72 phenotype were found to be interactors of Matrin 3 in our study including Aly, Nup 107, and Nup 160 (Freibaum, Lu et al. 2015). Though most studies have suggested a deficiency in the import of proteins, a similar nuclear accumulation of mRNA was seen in cells expressing the G_4C_2 repeat(Freibaum, Lu et al. 2015), as well as cells expressing TDP-43 c-terminal fragments (Woerner, Frottin et al. 2016), suggesting a defect in nuclear export of RNA. While the mechanism by which either the C9orf72 repeat expansion, TDP-43 c-terminal fragments and *MATR3*

mutations result in mRNA export defects is unknown, the fact that Matrin 3 interacts with both suggests that either all three mutations impact the same functional pathway, or this defect is mediated by interactions with one another (Haeusler, Donnelly et al. 2014, Johnson, Pioro et al. 2014, Lee, Zhang et al. 2016). This link between Matrin 3 and C9orf72 is further supported by the finding of rare Matrin 3 positive inclusions in a patient with a C9orf72 repeat expansion but not in other sALS cases (Johnson, Pioro et al. 2014, Dreser, Vollrath et al. 2017).

In this study, we demonstrated binding of Matrin 3 to 167 total proteins with 53 that met high confidence thresholds for protein interactions, greatly increasing the known Matrin 3 PPIs. This is the first study describing the PPI of the ALS-associated Matrin 3 mutations S85C, F115C, P154S and T622A. Importantly, our results demonstrate a novel role for Matrin 3 in mRNA nuclear export, possibly mediated via direct interactions with proteins of the TREX complex. Disease causing mutations in *MATR3* alter interactions with TREX proteins and nuclear export of mRNA, further highlighting the role for mRNA processing and nuclear export in the pathogenesis of ALS.

CHAPTER 4

DISCUSSION

While mutations in over 30 genes have been identified in ALS patients, it has been suggested that only a portion of the heritability of ALS (estimated at 21%) has been accounted for (Keller, Ferrucci et al. 2014). This suggests that a better understanding of the genetics of ALS is required to search for pathogenic mechanisms, build novel models of the disease, and ultimately create new therapeutics. My body of work spans from the discovery of a novel gene mutated in ALS to the creation of a cell culture model of Matrin 3 linked disease which was used to discover a possible disease mechanism. Mutations in Matrin 3 were discovered in a family with ALS that lacked mutations in other known ALS genes. After the initial discovery of four mutations in Matrin 3, other scientists searched and discovered a total of 9 additional missense mutations as well as two splicing alterations in ALS patients. Altogether, estimates of the incidence of Matrin 3 mutations in ALS patients are approximately 2% of patients, making it a rare cause of ALS. Interestingly, with the additional mutations discovered there seem to be two mutational hot spots between amino acids 66 and 154 which contains 7 mutations and between 610 and 787 which contains 5 mutations. The function of these two hotspots is currently unknown and both regions lack any of the known domains making the understanding of these regions an area for future study.

While many proteins linked to ALS form cytoplasmic inclusions and aggregates, immunohistochemistry performed on tissue from patients with sporadic ALS as well as a patient with a F115C mutation in Matrin 3 did not exhibit Matrin 3 positive inclusions.

We did however note rare Matrin 3 positive cytoplasmic inclusions in a patient carrying the C9orf72 repeat expansion, a phenotype that was recapitulated by others in both C9orf72 patient tissue as well as tissue from patients with mutations in FUS (Dreser, Vollrath et al. 2017). It was recently reported that Matrin 3 positive inclusions are present in 60% of the cases examined (Tada, Doi et al. 2017). This discrepancy is likely due to the use of different antibodies by the different groups, either due to non-specific binding of the antibody or due to the use of antibodies with different epitopes. We used two different antibodies with epitopes at the n-terminal and c-terminal of Matrin 3 (amino acids 145-233 and 773-787) and found a similar staining pattern with both and Dreser et al. used an antibody with a similar c-terminal epitope (amino acids 800-847). The antibody used by Tada et al. however, has a more central epitope in the middle of the Matrin 3 protein (475-500) suggesting that Matrin 3 found in inclusions might have a different conformation such that the two termini of the protein are hidden and the central region is exposed. As there is currently no crystal structure published for full length Matrin 3, the confirmation of both normal wild-type Matrin 3 as well as Matrin 3 found in inclusions would be of interest. It will also be important to test whether Matrin 3 positive inclusions are found within patient tissue from patients carrying Matrin 3 mutations as they have currently only been discovered in sporadic ALS patients and familial patients with mutations in C9orf72 and FUS. It will also be of interest to determine whether Matrin 3 inclusions are present in any of the cell culture models we have created when stained with the antibody used by Tada and colleagues.

Our initial study of Matrin 3 provided evidence that ALS linked mutations alter the interactions between Matrin 3 and other proteins. TDP-43 a protein linked to ALS due to its propensity to be found in aggregates in most ALS cases as well as being mutated in rare forms of the disease, had been previously suggested to bind to Matrin 3. This interaction was further confirmed by immunoprecipitating flag tagged Matrin 3 and probing the resulting western blot with TDP-43. This experiment suggested that the S85C mutation was able to pull down more TDP-43 than wild-type Matrin 3 and was the first indication that ALS linked mutations in Matrin 3 might alter its protein-protein interactions.

To test the hypothesis that Matrin 3 mutations alter its protein-protein interactions and that these alterations are involved in mechanisms of disease pathogenesis were tested in a cell culture model of Matrin 3. Multiple cell culture models were utilized in which wild-type or mutant Matrin 3 was expressed either stably or transiently in either HEK293 cells or NSC-34 cells. These models allowed for us to examine the protein-protein interactions of wild-type and mutant Matrin 3 and search for alterations that are a result of disease causing mutations. IP-MS experiments were chosen as a way to perform large scale unbiased analysis of protein-protein interactions and allowed for both the identification of novel Matrin 3 binding partners and a more systems level analysis of the functions of Matrin 3 interacting proteins. To the first point our work greatly increased the number of proteins identified as interacting with Matrin 3 compared to previous IP-MS experiments published by others. Unlike prior experiments where particular bands were cut from gels and identified by mass spectrometry, the entire lane with the

exception of the IgG heavy and light chain were used for downstream protein identification. This work was also the first to explore protein-protein interactions of any form of mutant Matrin 3.

Numerous publications have identified hnRNPL as a strong Matrin 3 interacting protein, and we used this protein as a positive control in our IP-WB experiments. Next, a number of proteins linked to ALS were identified by this technique including TDP-43 which had previously been examined. We were able to confirm the interaction between both wild-type and mutant Matrin 3 and TDP-43 as well as an apparent increased affinity between S85C Matrin 3 and TDP-43. This increased interaction between Matrin 3 and TDP-43 was also present with the P154S mutation which had not previously been examined. We also identified the proteins FUS, hnRNPA2/B1 and hnRNPA1 as Matrin 3 interacting proteins and confirmed the interaction by performing IPs followed by western blots.

Gene ontology analysis and functional enrichment analysis allowed us to cluster Matrin 3 interacting proteins by their biological processes and function. All of the top 15 categories of biological processes for both wild-type and mutant Matrin 3 were involved in RNA biogenesis and processing. This revelation is unsurprising due to the initial characterization of Matrin 3 as an RNA binding protein but also adds additional evidence that defects and alterations in RNA processing play a role in ALS pathogenesis. One group of processes that was of particular interest due to recent work performed in models of C9orf72 ALS, were terms involved in mRNA transport and localization. The proteins within these lists were of particular interest first because they were found at the top of the

gene ontology lists for mutant Matrin 3 but lower on the gene ontology lists for wild-type Matrin 3, and due to the fact that many of the proteins within these terms were part of a single complex called TREX.

While a role for defects in nucleocytoplasmic trafficking has been established in ALS a role for TREX is fairly novel to the field. TREX has a very specific role in the export of mRNA from the nucleus where it is transcribed, to the cytoplasm where it is translated. Others have demonstrated the accumulation of poly (A+) mRNA within the nucleus of cells expressing the C9orf72 repeat expansion. The TREX component Aly has also been identified as a top hit in a number of genetic screens aimed at identifying modifiers of the C9orf72 phenotype (Freibaum, Lu et al. 2015). The TREX complex member Thoc2 has been shown to mislocalize and form inclusion in both mouse models of Huntington's disease as well as in tissue from Huntington's patients. This aggregation was accompanied by nuclear mRNA retention suggestive of defects in TREX function (Woerner, Frottin et al. 2016) (Gasset-Rosa, Chillon-Marinas et al. 2017). This evidence led us to focus on examining the interaction between Matrin 3 and the TREX components Aly, Ddx39b and Sarnp. The interactions were first confirmed through multiple IP-WB experiments. First by pulling down with Flag antibody and probing blots with antibodies against Aly, Ddx39b and Sarnp and then by pulling down with Aly and Ddx39b and probing with Matrin 3 and Flag. These complementary approaches helped to validate the interaction and ensure that the binding was not dependent on the antibody used for the immunoprecipitation. Reverse IP experiments were also utilized to quantify and compare the level of interaction between wild-type and mutant Matrin 3. Reverse IPs were used as

in each case they appeared to pull down the equal amounts of Aly and Ddx39b respectively, in each of the different cell lines. This quantitation suggested an increase in binding between mutant Matrin 3 and Aly and Ddx39b similar to what was seen with the interaction between Matrin 3 and TDP-43. To ensure that these interactions occur under endogenous expression levels of Matrin 3, we also performed Matrin 3 IPs in untransfected cells, and again observed the interactions between Matrin 3 and Aly and Ddx39b. Finally, the interaction between Matrin 3 and Ddx39b was tested in tissue lysates prepared from lumbar spinal cord tissue from control and ALS patients. Again this confirmed the interaction between Matrin 3 and Ddx39b. Unfortunately we did not have access to spinal cord tissue lysates from any patients with mutations in Matrin 3 so we were unable to test the hypothesis suggested from our work performed in cell culture that in patients with mutations in Matrin 3 there is an increased and aberrant interaction between Matrin 3 and TREX components.

We next performed immunofluorescence on cells expressing wild-type or mutant Matrin 3 to ensure that Matrin 3 is found in the same areas of the nucleus as TREX components. While Matrin 3 immunostaining appears to fill the nucleus with the exception of the nucleolus, it is found in a granular, punctate staining pattern that is very similar to the staining pattern observed for Aly, Ddx39b and Sarnp. As Matrin 3 was flag tagged we were able to compare the level of co-localization between an antibody against Matrin 3 and an antibody against Flag. This analysis was vital as it allowed us to identify both endogenous and flag tagged Matrin 3 in the same cell and quantify the level of co-localization, allowing us to identify changes in staining patterns that are not obvious

qualitatively. The analysis performed was also unique in that it was performed only within the nucleus which was segregated by DAPI staining and that it was performed using an unbiased automated thresholding algorithm. While the Matrin 3 antibody used was able to detect both endogenous Matrin 3 and the exogenous flag tagged Matrin 3, the statistically significant decrease in the level of co-localization of the two would suggest that there were areas in the nucleus where endogenous Matrin 3 was found but exogenous flag tagged mutant Matrin 3 was not present. As all comparisons were performed between cells overexpressing wild-type Matrin 3 and those overexpressing mutant Matrin 3, it is likely that the small but significant change that we identified is due primarily to the mutation in Matrin 3 and not merely the overexpression of the protein.

Interestingly, when the same analysis was performed between Matrin 3 and Aly, Ddx39b and Sarnp there were also small but significant changes between the levels of co-localization of wild-type and mutant Matrin 3 with these TREX proteins. In all three cases there was an increase in the level of co-localization of mutant Matrin 3 with TREX proteins compared to the level of co-localization with wild-type. This data is in agreement with our IP-WB experiments and indicates increased affinity between mutant Matrin 3 and TREX proteins. This suggests that either mutations in Matrin 3 cause a small change in its localization within the nucleus which puts it in closer proximity to TREX proteins thus increasing their interaction or that the mutations in Matrin 3 increase the affinity for TREX components and this increased interaction results in the change in localization. Our IP experiments were performed using nuclear extracts without any crosslinking agents, suggesting strong interactions between Matrin 3 and TREX proteins.

It would be of interest to determine where exactly in the nucleus these interactions occur and to determine if the interaction between mutant Matrin 3 affects the interactions between various TREX proteins with one another. TREX proteins are located both diffusely throughout the nucleus at splicing sites such as nuclear speckles and components have even been found at sites of active transcription.

While the mechanism by which mutations in Matrin 3 increases the affinity and co-localization with TREX is unknown, we have shown that these ALS linked mutations in Matrin 3 result in accumulation of poly (A+) mRNA within the nucleus. We observed an approximately 30% increase in the nuclear to cytoplasmic ratio of mRNA. This modest increase however fits with the levels of nuclear retention observed in cells expressing C9orf72 repeat expansions. A modest level of mRNA retention also makes biological sense as cells could not survive without any export of mRNA and alternative mRNA export pathways do exist. What we have observed does not appear to be a complete shutdown of mRNA export but rather a slowing of the process. While it is unclear how exactly the slowing of mRNA export would cause this disease it is a model that would fit with a neurodegenerative disease with an onset late in life. While export by the TREX complex is thought to be the main export pathway for all mRNA there does seem to be some specificity to the export defects we uncovered as the mRNA for both TDP-43 and FUS are affected whereas the mRNA for GAPDH is not. It is possible that the difference could be due to the fact that different adapter proteins are available to function within TREX and there appear to be different forms of the TREX complex within cells. Unfortunately, the exact composition of which adapter proteins export

specific mRNAs is not currently known and it is likely that multiple proteins are involved under different conditions.

The identification of defects in mRNA export in cells expressing mutant Matrin 3 adds additional evidence that trafficking between the nucleus and the cytoplasm is affected in ALS. We have added Matrin 3 to the list of ALS causing proteins that have been shown to impact mRNA transport including SOD1, TDP-43, and C9orf72. Additionally, a similar phenotype of mRNA nuclear retention and alteration of a TREX protein were identified in Huntington's disease mouse models and tissue suggesting that defects in mRNA export could be found broadly not just in ALS but in other neurodegenerative diseases as well suggesting a possible vulnerability of more than just motor neurons to this phenotype.

While we have identified defects in the export of mRNA within NSC-34 motor neuron like cells it will be important to perform future studies in other cell types. iPS cells have been created from a patient carrying a F115C mutation in Matrin 3 which can be utilized in the future to examine this pathology in human iPS derived motor neurons. These cells can also be differentiated into other cell types including other types of neurons, glial cells or even muscle. In the future it will be important to confirm the results we have presented here in both the iPS derived motor neurons and in patient tissue. In our initial publication we identified regions within the sarcoplasm of muscle from a patient with a S85C mutation in Matrin 3 in which Matrin 3 and TDP-43 appear to be found in perinuclear inclusions. It would be interesting to determine whether these inclusions are present in muscle from ALS patients with either other mutations in Matrin 3 which are

not linked to myopathy as S85C is, as well as if these inclusions are present in ALS patients without mutations in Matrin 3. The link between Matrin 3 and both myopathy and ALS, as well as the primarily muscle phenotype identified in a mouse model of Matrin 3, makes muscle a particularly interesting area of future study

Overall, my thesis spanned from the discovery of a novel genetic form of ALS to the characterization of Matrin 3 within patient tissue and the creation of an *in vitro* model of Matrin 3 mutations. This cell culture model allowed us to test the hypothesis that mutations in Matrin 3 change its protein-protein interactions and the functional impact of disease causing mutations. We identified a novel role for Matrin 3 in modulating TREX mediated nuclear export of mRNA and found that expression of ALS linked mutations in Matrin 3 leads to the nuclear retention of global mRNA.

REFERENCES

Aliaga, L., C. Lai, J. Yu, N. Chub, H. Shim, L. Sun, C. Xie, W. J. Yang, X. Lin, M. J. O'Donovan and H. Cai (2013). "Amyotrophic lateral sclerosis-related VAPB P56S mutation differentially affects the function and survival of corticospinal and spinal motor neurons." Hum Mol Genet **22**(21): 4293-4305.

Andersen, J. S., C. E. Lyon, A. H. Fox, A. K. Leung, Y. W. Lam, H. Steen, M. Mann and A. I. Lamond (2002). "Directed proteomic analysis of the human nucleolus." Curr Biol **12**(1): 1-11.

Arts, G. J., M. Fornerod and I. W. Mattaj (1998). "Identification of a nuclear export receptor for tRNA." Curr Biol **8**(6): 305-314.

Banerjee, A., K. E. Vest, G. K. Pavlath and A. H. Corbett (2017). "Nuclear poly(A) binding protein 1 (PABPN1) and Matrin3 interact in muscle cells and regulate RNA processing." Nucleic Acids Res **45**(18): 10706-10725.

Belgrader, P., R. Dey and R. Berezney (1991). "Molecular cloning of matrin 3. A 125-kilodalton protein of the nuclear matrix contains an extensive acidic domain." J Biol Chem **266**: 9893-9899.

Bensimon, G., L. Lacomblez, V. Meininger and A. R. S. Group (1994). "A controlled trial of riluzole in amyotrophic lateral sclerosis." N. Engl. J. Med. **330**: 585-591.

Bernert, G., M. Fountoulakis and G. Lubec (2002). "Manifold decreased protein levels of matrin 3, reduced motor protein HMP and hlark in fetal Down's syndrome brain." Proteomics **2**(12): 1752-1757.

Bindea, G., B. Mlecnik, H. Hackl, P. Charoentong, M. Tosolini, A. Kirilovsky, W. H. Fridman, F. Pages, Z. Trajanoski and J. Galon (2009). "ClueGO: a Cytoscape plug-in to decipher functionally grouped gene ontology and pathway annotation networks." Bioinformatics **25**(8): 1091-1093.

Bischoff, F. R. and H. Ponstingl (1991). "Catalysis of guanine nucleotide exchange on Ran by the mitotic regulator RCC1." Nature **354**(6348): 80-82.

Boehringer, A., K. Garcia-Mansfield, G. Singh, N. Bakkar, P. Pirrotte and R. Bowser (2017). "ALS Associated Mutations in Matrin 3 Alter Protein-Protein Interactions and Impede mRNA Nuclear Export." Sci Rep **7**(1): 14529.

Bohnsack, M. T., K. Czaplinski and D. Gorlich (2004). "Exportin 5 is a RanGTP-dependent dsRNA-binding protein that mediates nuclear export of pre-miRNAs." RNA **10**(2): 185-191.

Boylan, K. (2015). "Familial Amyotrophic Lateral Sclerosis." Neurol Clin **33**(4): 807-830.

Brennan, C. M., I. E. Gallouzi and J. A. Steitz (2000). "Protein ligands to HuR modulate its interaction with target mRNAs in vivo." J Cell Biol **151**(1): 1-14.

Brown, R. H. and A. Al-Chalabi (2017). "Amyotrophic Lateral Sclerosis." The New England Journal of Medicine **377**(2): 162-172.

Bruijn, L. I., M. K. Houseweart, S. Kato, K. L. Anderson, S. D. Anderson, E. Ohama, A. G. Reaume, R. W. Scott and D. W. Cleveland (1997). "Aggregation and motor neuron toxicity of an ALS-linked SOD1 mutant independent from wild-type SOD1." Science **281**: 1851-1854.

Burns, C. M., H. Chu, S. M. Rueter, L. K. Hutchinson, H. Canton, E. Sanders-Bush and R. B. Emeson (1997). "Regulation of serotonin-2C receptor G-protein coupling by RNA editing." Nature **387**(6630): 303-308.

Charcot, J.-M. (1874). "De la sclerose laterale amytrophique." Prog Med **2**: 325-327, 341-342, 453-455.

Chaudhary, R., B. Gryder, W. S. Woods, M. Subramanian, M. F. Jones, X. Li, L. M. Jenkins, S. A. Shabalina, M. Mo, M. Dasso, Y. Yang, L. M. Wakefield, Y. Zhu, S. M. Frier, B. S. Moriarity, K. V. Prasanth, P. Perez-Pinera and A. Lal (2017). "Prosurvival long noncoding RNA PINCR regulates a subset of p53 targets in human colorectal cancer cells by binding to Matrin 3." eLife **6**.

Chen-Plotkin, A. S., F. Geser, J. B. Plotkin, C. M. Clark, L. K. Kwong, W. Yuan, M. Grossman, V. M. Van Deerlin, J. Q. Trojanowski and V. M. Lee (2008). "Variations in the progranulin gene affect global gene expression in frontotemporal lobar degeneration." Hum Mol Genet **17**(10): 1349-1362.

Cheng, H., K. Dufu, C. S. Lee, J. L. Hsu, A. Dias and R. Reed (2006). "Human mRNA export machinery recruited to the 5' end of mRNA." Cell **127**(7): 1389-1400.

Chio, A., G. Logroscino, O. Hardiman, R. Swingler, D. Mitchell, E. Beghi, B. G. Traynor and C. Eurals (2009). "Prognostic factors in ALS: A critical review." Amyotroph Lateral Scler **10**(5-6): 310-323.

Chio, A., G. Logroscino, B. J. Traynor, J. Collins, J. C. Simeone, L. A. Goldstein and L. A. White (2013). "Global epidemiology of amyotrophic lateral sclerosis: a systematic review of the published literature." Neuroepidemiology **41**(2): 118-130.

Cho, K. I., K. Searle, M. Webb, H. Yi and P. A. Ferreira (2012). "Ranbp2 haploinsufficiency mediates distinct cellular and biochemical phenotypes in brain and retinal dopaminergic and glia cells elicited by the Parkinsonian neurotoxin, 1-methyl-4-phenyl-1,2,3,6-tetrahydropyridine (MPTP)." Cell Mol Life Sci **69**(20): 3511-3527.

Cho, K. I., D. Yoon, S. Qiu, Z. Danziger, W. M. Grill, W. C. Wetsel and P. A. Ferreira (2017). "Loss of Ranbp2 in motoneurons causes disruption of nucleocytoplasmic and chemokine signaling, proteostasis of hnRNPH3 and Mmp28, and development of amyotrophic lateral sclerosis-like syndromes." Dis Model Mech **10**(5): 559-579.

Coelho, M. B., J. Attig, N. Bellora, J. Konig, M. Hallegger, M. Kayikci, E. Eyras, J. Ule and C. W. Smith (2015). "Nuclear matrix protein Matrin3 regulates alternative splicing and forms overlapping regulatory networks with PTB." EMBO J **34**(5): 653-668.

Cookson, M. R. (2012). "Cellular effects of LRRK2 mutations." Biochem Soc Trans **40**(5): 1070-1073.

Cronshaw, J. M., A. N. Krutchinsky, W. Zhang, B. T. Chait and M. J. Matunis (2002). "Proteomic analysis of the mammalian nuclear pore complex." J Cell Biol **158**(5): 915-927.

D'Angelo, M. A., M. Raices, S. H. Panowski and M. W. Hetzer (2009). "Age-dependent deterioration of nuclear pore complexes causes a loss of nuclear integrity in postmitotic cells." Cell **136**(2): 284-295.

De Robertis, E. M., R. F. Longthorne and J. B. Gurdon (1978). "Intracellular migration of nuclear proteins in Xenopus oocytes." Nature **272**(5650): 254-256.

DeJesus-Hernandez, M., I. R. Mackenzie, B. F. Boeve, A. L. Boxer, M. Baker, N. J. Rutherford, A. M. Nicholson, N. A. Finch, H. Flynn, J. Adamson, N. Kouri, A. Wojtas, P. Sengdy, G.-Y. R. Hsiung, A. Karydas, W. W. Seeley, K. A. Josephs, G. Coppola, D. H. Geschwind, Z. K. Wszolek, H. Feldman, D. S. Knopman, R. C. Petersen, B. L. Miller, D. W. Dickson, K. B. Boylan, N. R. Graff-Radford and R. Rademakers (2011). "Expanded GGGGCC hexanucleotide repeat in noncoding region of C9ORF72 causes chromosome 9p-linked FTD and ALS." Neuron **72**(2): 245-256.

Depreux, F. F., M. J. Puckelwartz, A. Augustynowicz, D. Wolfgeher, C. M. Labno, D. Pierre-Louis, D. Cicka, S. J. Kron, J. Holaska and E. M. McNally (2015). "Disruption of the lamin A and matrin-3 interaction by myopathic LMNA mutations." Hum Mol Genet **24**(15): 4284-4295.

Dingwall, C., S. V. Sharnick and R. A. Laskey (1982). "A polypeptide domain that specifies migration of nucleoplasmin into the nucleus." Cell **30**(2): 449-458.

Dreser, A., J. T. Vollrath, A. Sechi, S. Johann, A. Roos, A. Yamoah, I. Katona, S. Bohlega, D. Wiemuth, Y. Tian, A. Schmidt, J. Vervoorts, M. Dohmen, C. Beyer, J. Anink, E. Aronica, D. Troost, J. Weis and A. Goswami (2017). "The ALS-linked E102Q mutation in Sigma receptor-1 leads to ER stress-mediated defects in protein homeostasis and dysregulation of RNA-binding proteins." Cell Death Differ.

Dufu, K., M. J. Livingstone, J. Seebacher, S. P. Gygi, S. A. Wilson and R. Reed (2010). "ATP is required for interactions between UAP56 and two conserved mRNA export proteins, Aly and CIP29, to assemble the TREX complex." Genes Dev **24**(18): 2043-2053.

Eisen, A. and S. Kuwabara (2012). "The split hand syndrome in amyotrophic lateral sclerosis." J Neurol Neurosurg Psychiatry **83**(4): 399-403.

Erazo, A. and S. P. Goff (2015). "Nuclear matrix protein Matrin 3 is a regulator of ZAP-mediated retroviral restriction." Retrovirology **12**: 57.

Erazo, A., M. B. Yee, B. W. Banfield and P. R. Kinchington (2011). "The alphaherpesvirus US3/ORF66 protein kinases direct phosphorylation of the nuclear matrix protein matrin 3." J Virol **85**(1): 568-581.

Feit, H., A. Silbergleit, L. B. Schneider, J. A. Gutierrez, R. P. Fitoussi, C. Reyes, G. A. Rouleau, B. Brais, C. E. Jackson, J. S. Beckmann and E. Seboun (1998). "Vocal cord and pharyngeal weakness with autosomal dominant distal myopathy: clinical description and gene localization to 5q31." Am J Hum Genet **63**(6): 1732-1742.

Fifita, J. A., K. L. Williams, E. P. McCann, A. O'Brien, D. C. Bauer, G. A. Nicholson and I. P. Blair (2015). "Mutation analysis of MATR3 in Australian familial amyotrophic lateral sclerosis." Neurobiology of Aging **36**(3): 16020-160200.

Fornerod, M., M. Ohno, M. Yoshida and I. W. Mattaj (1997). "CRM1 is an export receptor for leucine-rich nuclear export signals." Cell **90**(6): 1051-1060.

Freibaum, B. D., Y. Lu, R. Lopez-Gonzalez, N. C. Kim, S. Almeida, K.-H. Lee, N. Badders, M. Valentine, B. L. Miller, P. C. Wong, L. Petrucelli, H. J. Kim, F.-B. Gao and J. P. Taylor (2015). "GGGGCC repeat expansion in C9orf72 compromises nucleocytoplasmic transport." Nature **525**(7567): 129-133.

Frey, S. and D. Gorlich (2007). "A saturated FG-repeat hydrogel can reproduce the permeability properties of nuclear pore complexes." Cell **130**(3): 512-523.

Fujita, T. and H. Fujii (2011). "Direct Identification of Insulator Components by Insertional Chromatin Immunoprecipitation." PLoS ONE **6**(10).

Fukuda, M., S. Asano, T. Nakamura, M. Adachi, M. Yoshida, M. Yanagida and E. Nishida (1997). "CRM1 is responsible for intracellular transport mediated by the nuclear export signal." Nature **390**(6657): 308-311.

Gallego-Iradi, M. C., A. M. Clare, H. H. Brown, C. Janus, J. Lewis and D. R. Borchelt (2015). "Subcellular Localization of Matrin 3 Containing Mutations Associated with ALS and Distal Myopathy." PLoS One **10**(11): e0142144.

Gasset-Rosa, F., C. Chillon-Marinas, A. Goginashvili, R. S. Atwal, J. W. Artates, R. Tabet, V. C. Wheeler, A. G. Bang, D. W. Cleveland and C. Lagier-Tourenne (2017). "Polyglutamine-Expanded Huntingtin Exacerbates Age-Related Disruption of Nuclear Integrity and Nucleocytoplasmic Transport." Neuron **94**(1): 48-57 e44.

Giordano, G., A. M. Sanchez-Perez, C. Montoliu, R. Berezney, K. Malyavantham, L. G. Costa, J. J. Calvete and V. Felipo (2005). "Activation of NMDA receptors induces protein kinase A-mediated phosphorylation and degradation of matrin 3. Blocking these effects prevents NMDA-induced neuronal death." J Neurochem **94**: 808-818.

Gitcho, M. A., R. H. Baloh, S. Chakraverty, K. Mayo, J. B. Norton, D. Levitch, K. J. Hatanpaa, C. L. White, 3rd, E. H. Bigio, R. Caselli, M. Baker, M. T. Al-Lozi, J. C. Morris, A. Pestronk, R. Rademakers, A. M. Goate and N. J. Cairns (2008). "TDP-43 A315T mutation in familial motor neuron disease." Ann Neurol **63**(4): 535-538.

Grima, J. C., J. G. Daigle, N. Arbez, K. C. Cunningham, K. Zhang, J. Ochaba, C. Geater, E. Morozko, J. Stocksdale, J. C. Glatzer, J. T. Pham, I. Ahmed, Q. Peng, H. Wadhwa, O. Pletnikova, J. C. Troncoso, W. Duan, S. H. Snyder, L. P. Ranum, L. M. Thompson, T. E. Lloyd, C. A. Ross and J. D. Rothstein (2017). "Mutant Huntingtin Disrupts the Nuclear Pore Complex." Neuron **94**(1): 93-107 e106.

Guerreiro, R., J. Bras and J. Hardy (2015). "SnapShot: Genetics of ALS and FTD." Cell **160**(4): 798 e791.

Haeusler, A. R., C. J. Donnelly, G. Periz, E. A. Simko, P. G. Shaw, M. S. Kim, N. J. Maragakis, J. C. Troncoso, A. Pandey, R. Sattler, J. D. Rothstein and J. Wang (2014). "C9orf72 nucleotide repeat structures initiate molecular cascades of disease." Nature **507**(7491): 195-200.

Heath, C. G., N. Viphakone and S. A. Wilson (2016). "The role of TREX in gene expression and disease." Biochem J **473**(19): 2911-2935.

Henderson, B. R. and A. Eleftheriou (2000). "A comparison of the activity, sequence specificity, and CRM1-dependence of different nuclear export signals." Exp Cell Res **256**(1): 213-224.

Herold, A., T. Klymenko and E. Izaurralde (2001). "NXF1/p15 heterodimers are essential for mRNA nuclear export in Drosophila." RNA **7**(12): 1768-1780.

Hewitt, C., J. Kirby, J. R. Highley, J. A. Hartley, R. Hibberd, H. C. Hollinger, T. L. Williams, P. G. Ince, C. J. McDermott and P. J. Shaw (2010). "Novel FUS/TLS mutations and pathology in familial and sporadic amyotrophic lateral sclerosis." Arch Neurol **67**(4): 455-461.

Hibino, Y. (2000). "[Functional arrangement of genomic DNA and structure of nuclear matrix]." Yakugaku Zasshi **120**(6): 520-533.

Hibino, Y., T. Usui, Y. Morita, N. Hirose, M. Okazaki, N. Sugano and K. Hiraga (2006). "Molecular properties and intracellular localization of rat liver nuclear scaffold protein P130." Biochimica et Biophysica Acta (BBA) - Gene Structure and Expression **1759**(5): 195-207.

Hideyama, T., T. Yamashita, H. Aizawa, S. Tsuji, A. Kakita, H. Takahashi and S. Kwak (2012). "Profound downregulation of the RNA editing enzyme ADAR2 in ALS spinal motor neurons." Neurobiol Dis **45**(3): 1121-1128.

Higuchi, M., F. N. Single, M. Kohler, B. Sommer, R. Sprengel and P. H. Seeburg (1993). "RNA editing of AMPA receptor subunit GluR-B: a base-paired intron-exon structure determines position and efficiency." Cell **75**(7): 1361-1370.

Hock, J., L. Weinmann, C. Ender, S. Rudel, E. Kremmer, M. Raabe, H. Urlaub and G. Meister (2007). "Proteomic and functional analysis of Argonaute-containing mRNA-protein complexes in human cells." EMBO Rep **8**(11): 1052-1060.

Johnson, J. O., J. Mandrioli, M. Benatar, Y. Abramzon, V. M. Van Deerlin, J. Q. Trojanowski, J. R. Gibbs, M. Brunetti, S. Gronka, J. Wuu, J. Ding, L. McCluskey, M. Martinez-Lage, D. Falcone, D. G. Hernandez, S. Arepalli, S. Chong, J. C. Schymick, J. Rothstein, F. Landi, Y. D. Wang, A. Calvo, G. Mora, M. Sabatelli, M. R. Monsurro, S. Battistini, F. Salvi, R. Spataro, P. Sola, G. Borghero, I. Consortium, G. Galassi, S. W. Scholz, J. P. Taylor, G. Restagno, A. Chio and B. J. Traynor (2010). "Exome sequencing reveals VCP mutations as a cause of familial ALS." Neuron **68**(5): 857-864.

Johnson, J. O., E. P. Pioro, A. Boehringer, R. Chia, H. Feit, A. E. Renton, H. A. Pliner, Y. Abramzon, G. Marangi, B. J. Winborn, J. R. Gibbs, M. A. Nalls, S. Morgan, M. Shoai, J. Hardy, A. Pittman, R. W. Orrell, A. Malaspina, K. C. Sidle, P. Fratta, M. B. Harms, R. H. Baloh, A. Pestronk, C. C. Weihl, E. Rogaeva, L. Zinman, V. E. Drory, G. Borghero, G. Mora, A. Calvo, J. D. Rothstein, ITALSGEN, C. Drepper, M. Sendtner, A. B. Singleton, J. P. Taylor, M. R. Cookson, G. Restagno, M. Sabatelli, R. Bowser, A. Chio and B. J. Traynor (2014). "Mutations in the *Matrin 3* gene cause familial amyotrophic lateral sclerosis." Nat Neurosci **17**(5): 664-666.

Jovicic, A., J. Mertens, S. Boeynaems, E. Bogaert, N. Chai, S. B. Yamada, J. W. Paul Iii, S. Sun, J. R. Herdy, G. Bieri, N. J. Kramer, F. H. Gage, L. Van Den Bosch, W. Robberecht and A. D. Gitler (2015). "Modifiers of C9orf72 dipeptide repeat toxicity connect nucleocytoplasmic transport defects to FTD/ALS." Nat Neurosci **18**(9): 1226-1229.

Kabashi, E., P. N. Valdmanis, P. Dion, D. Spiegelman, B. J. McConkey, C. Vande Velde, J. P. Bouchard, L. Lacomblez, K. Pochigaeva, F. Salachas, P. F. Pradat, W. Camu, V. Meininger, N. Dupre and G. A. Rouleau (2008). "TARDBP mutations in individuals with sporadic and familial amyotrophic lateral sclerosis." Nat Genet **40**(5): 572-574.

Kalderon, D., B. L. Roberts, W. D. Richardson and A. E. Smith (1984). "A short amino acid sequence able to specify nuclear location." Cell **39**(3 Pt 2): 499-509.

Kaneb, H. M., A. W. Folkmann, V. V. Belzil, L. E. Jao, C. S. Leblond, S. L. Girard, H. Daoud, A. Noreau, D. Rochefort, P. Hince, A. Szuto, A. Levert, S. Vidal, C. Andre-Guimont, W. Camu, J. P. Bouchard, N. Dupre, G. A. Rouleau, S. R. Wente and P. A. Dion (2015). "Deleterious mutations in the essential mRNA metabolism factor, hGle1, in amyotrophic lateral sclerosis." Hum Mol Genet **24**(5): 1363-1373.

Katahira, J. (2012). "mRNA export and the TREX complex." Biochim Biophys Acta **1819**(6): 507-513.

Keller, M. F., L. Ferrucci, A. B. Singleton, P. J. Tienari, H. Laaksovirta, G. Restagno, A. Chio, B. J. Traynor and M. A. Nalls (2014). "Genome-Wide Analysis of the Heritability of Amyotrophic Lateral Sclerosis." JAMA Neurol.

Kiernan, M. C., S. Vucic, B. C. Cheah, M. R. Turner, A. Eisen, O. Hardiman, J. R. Burrell and M. C. Zoing (2011). "Amyotrophic lateral sclerosis." Lancet **377**(9769): 942-955.

Kim, H. J., N. C. Kim, Y. D. Wang, E. A. Scarborough, J. Moore, Z. Diaz, K. S. MacLea, B. Freibaum, S. Li, A. Molliex, A. P. Kanagaraj, R. Carter, K. B. Boylan, A. M. Wojtas, R. Rademakers, J. L. Pinkus, S. A. Greenberg, J. Q. Trojanowski, B. J. Traynor, B. N. Smith, S. Topp, A. S. Gkazi, J. Miller, C. E. Shaw, M. Kottlors, J. Kirschner, A. Pestronk, Y. R. Li, A. F. Ford, A. D. Gitler, M. Benatar, O. D. King, V. E. Kimonis, E. D. Ross, C. C. Weihl, J. Shorter and J. P. Taylor (2013). "Mutations in prion-like domains in hnRNPA2B1 and hnRNPA1 cause multisystem proteinopathy and ALS." Nature **495**(7442): 467-473.

Kim, J. E., Y. H. Hong, J. Y. Kim, G. S. Jeon, J. H. Jung, B. N. Yoon, S. Y. Son, K. W. Lee, J. I. Kim and J. J. Sung (2017). "Altered nucleocytoplasmic proteome and transcriptome distributions in an in vitro model of amyotrophic lateral sclerosis." PLoS One **12**(4): e0176462.

Kinoshita, Y., H. Ito, A. Hirano, K. Fujita, R. Wate, M. Nakamura, S. Kaneko, S. Nakano and H. Kusaka (2009). "Nuclear contour irregularity and abnormal transporter protein distribution in anterior horn cells in amyotrophic lateral sclerosis." J Neuropathol Exp Neurol **68**(11): 1184-1192.

Kohler, A., M. Schneider, G. G. Cabal, U. Nehrbass and E. Hurt (2008). "Yeast Ataxin-7 links histone deubiquitination with gene gating and mRNA export." Nat Cell Biol **10**(6): 707-715.

Kolarcik, C. and R. Bowser (2012). "Retinoid signaling alterations in amyotrophic lateral sclerosis." Am J Neurodegener Dis **1**(2): 130-145.

Kraya, T., B. Schmidt, T. Muller and F. Hanisch (2015). "Impairment of respiratory function in late-onset distal myopathy due to MATR3 Mutation." Muscle Nerve **51**(6): 916-918.

Kula, A., L. Gharu and A. Marcello (2013). "HIV-1 pre-mRNA commitment to Rev mediated export through PSF and Matrin 3." Virology **435**(2): 329-340.

Kula, A., J. Guerra, A. Knezevich, D. Kleva, M. P. Myers and A. Marcello (2011). "Characterization of the HIV-1 RNA associated proteome identifies Matrin 3 as a nuclear cofactor of Rev function." Retrovirology **8**: 60.

Kumar, M. and G. G. Carmichael (1997). "Nuclear antisense RNA induces extensive adenosine modifications and nuclear retention of target transcripts." Proc Natl Acad Sci U S A **94**(8): 3542-3547.

Kutay, U., G. Lipowsky, E. Izaurralde, F. R. Bischoff, P. Schwarzmaier, E. Hartmann and D. Gorlich (1998). "Identification of a tRNA-specific nuclear export receptor." Mol Cell **1**(3): 359-369.

Kwiatkowski, T. J., Jr., D. A. Bosco, A. L. Leclerc, E. Tamrazian, C. R. Vanderburg, C. Russ, A. Davis, J. Gilchrist, E. J. Kasarskis, T. Munsat, P. Valdmanis, G. A. Rouleau, B. A. Hosler, P. Cortelli, P. J. de Jong, Y. Yoshinaga, J. L. Haines, M. A. Pericak-Vance, J. Yan, N. Ticozzi, T. Siddique, D. McKenna-Yasek, P. C. Sapp, H. R. Horvitz, J. E. Landers and R. H. Brown, Jr. (2009). "Mutations in the FUS/TLS gene on chromosome 16 cause familial amyotrophic lateral sclerosis." Science **323**(5918): 1205-1208.

Leblond, C. S., Z. Gan-Or, D. Spiegelman, S. B. Laurent, A. Szuto, A. Hodgkinson, A. Dionne-Laporte, P. Provencher, M. de Carvalho, S. Orru, D. Brunet, J. P. Bouchard, P. Awadalla, N. Dupre, P. A. Dion and G. A. Rouleau (2016). "Replication study of MATR3 in familial and sporadic amyotrophic lateral sclerosis." Neurobiol Aging **37**: 209 e217-221.

Lee, K. H., P. Zhang, H. J. Kim, D. M. Mitrea, M. Sarkar, B. D. Freibaum, J. Cika, M. Coughlin, J. Messing, A. Molliex, B. A. Maxwell, N. C. Kim, J. Temirov, J. Moore, R. M. Kolaitis, T. I. Shaw, B. Bai, J. Peng, R. W. Kriwacki and J. P. Taylor (2016). "C9orf72 Dipeptide Repeats Impair the Assembly, Dynamics, and Function of Membrane-Less Organelles." Cell **167**(3): 774-788 e717.

Lenglet, T. and J. P. Camdessanché (2017). "Amyotrophic lateral sclerosis or not: Keys for the diagnosis." Revue Neurologique **173**(5): 280-287.

Lin, K. P., P. C. Tsai, Y. C. Liao, W. T. Chen, C. P. Tsai, B. W. Soong and Y. C. Lee (2015). "Mutational analysis of MATR3 in Taiwanese patients with amyotrophic lateral sclerosis." Neurobiol Aging.

Ling, S. C., C. P. Albuquerque, J. S. Han, C. Lagier-Tourenne, S. Tokunaga, H. Zhou and D. W. Cleveland (2010). "ALS-associated mutations in TDP-43 increase its stability and promote TDP-43 complexes with FUS/TLS." Proc Natl Acad Sci U S A **107**(30): 13318-13323.

Ling, S. C., M. Polymenidou and D. W. Cleveland (2013). "Converging mechanisms in ALS and FTD: disrupted RNA and protein homeostasis." Neuron **79**(3): 416-438.
Lomen-Hoerth, C., J. Murphy, S. Langmore, J. H. Kramer, R. K. Olney and B. Miller (2003). "Are amyotrophic lateral sclerosis patients cognitively normal?" Neurology **60**(7): 1094-1097.

Lund, E., S. Guttinger, A. Calado, J. E. Dahlberg and U. Kutay (2004). "Nuclear export of microRNA precursors." Science **303**(5654): 95-98.

Ma, H., A. J. Siegel and R. Berezney (1999). "Association of chromosome territories with the nuclear matrix. Disruption of human chromosome territories correlates with the release of a subset of nuclear matrix proteins." J Cell Biol **146**(3): 531-542.

Mackenzie, I. R., P. Frick and M. Neumann (2014). "The neuropathology associated with repeat expansions in the C9ORF72 gene." Acta Neuropathol **127**(3): 347-357.

Makarov, E. M., N. Owen, A. Bottrill and O. V. Makarova (2012). "Functional mammalian spliceosomal complex E contains SMN complex proteins in addition to U1 and U2 snRNPs." Nucleic Acids Res **40**(6): 2639-2652.

Malyavantham, K. S., S. Bhattacharya, M. Barbeitos, L. Mukherjee, J. Xu, F. O. Fackelmayer and R. Berezney (2008). "Identifying functional neighborhoods within the cell nucleus: proximity analysis of early S-phase replicating chromatin domains to sites of transcription, RNA polymerase II, HP1gamma, matrin 3 and SAF-A." J Cell Biochem **105**(2): 391-403.

Marangi, G., S. Lattante, P. N. Doronzio, A. Conte, G. Tasca, M. Monforte, A. K. Patanella, G. Bisogni, E. Meleo, S. La Spada, M. Zollino and M. Sabatelli (2017). "Matrin 3 variants are frequent in Italian ALS patients." Neurobiol Aging **49**: 218 e211-218 e217.

McCloskey, A., I. Taniguchi, K. Shinmyozu and M. Ohno (2012). "hnRNP C tetramer measures RNA length to classify RNA polymerase II transcripts for export." Science **335**(6076): 1643-1646.

Millecamps, S., A. Septenville, E. Teyssou, M. Daniau, A. Camuzat, M. Albert, E. LeGuern, D. Galimberti, o. research network, T. Ftd-Als, A. Brice, Y. Marie and I. Ber (2014). "Genetic analysis of matrin 3 gene in French amyotrophic lateral sclerosis patients and frontotemporal lobar degeneration with amyotrophic lateral sclerosis patients." Neurobiology of Aging **35**(12): 644694016-644892160.

Miller, R. G., J. D. Mitchell and D. H. Moore (2012). "Riluzole for amyotrophic lateral sclerosis (ALS)/motor neuron disease (MND)." Cochrane Database Syst Rev(3): CD001447.

Moloney, C., S. Rayaprolu, J. Howard, S. Fromholt, H. Brown, M. Collins, M. Cabrera, C. Duffy, Z. Siemienski, D. Miller, M. S. Swanson, L. Notterpek, D. R. Borchelt and J. Lewis (2016). "Transgenic mice overexpressing the ALS-linked protein Matrin 3 develop a profound muscle phenotype." Acta Neuropathol Commun **4**(1): 122.

Muller-McNicoll, M., V. Botti, A. M. de Jesus Domingues, H. Brandl, O. D. Schwich, M. C. Steiner, T. Curk, I. Poser, K. Zarnack and K. M. Neugebauer (2016). "SR proteins are NXF1 adaptors that link alternative RNA processing to mRNA export." Genes Dev **30**(5): 553-566.

Muller, T. J., T. Kraya, G. Stoltenburg-Didinger, F. Hanisch, M. Kornhuber, D. Stoevesandt, J. Senderek, J. Weis, P. Baum, M. Deschauer and S. Zierz (2014). "Phenotype of matrin-3-related distal myopathy in 16 German patients." Ann Neurol **76**(5): 669-680.

Nag, A. and J. A. Steitz (2012). "Tri-snRNP-associated proteins interact with subunits of the TRAMP and nuclear exosome complexes, linking RNA decay and pre-mRNA splicing." RNA Biol **9**(3): 334-342.

Neumann, M., D. M. Sampathu, L. K. Kwong, A. C. Truax, M. C. Micsenyi, T. T. Chou, J. Bruce, T. Schuck, M. Grossman, C. M. Clark, L. F. McCluskey, B. L. Miller, E. Masliah, I. R. Mackenzie, H. Feldman, W. Feiden, H. A. Kretzschmar, J. Q. Trojanowski and V. M. Lee (2006). "Ubiquitinated TDP-43 in frontotemporal lobar degeneration and amyotrophic lateral sclerosis." Science **314**(5796): 130-133.

Nishikura, K. (1992). "Modulation of double-stranded RNAs in vivo by RNA duplex unwindase." Ann N Y Acad Sci **660**: 240-250.

Okada, C., E. Yamashita, S. J. Lee, S. Shibata, J. Katahira, A. Nakagawa, Y. Yoneda and T. Tsukihara (2009). "A high-resolution structure of the pre-microRNA nuclear export machinery." Science **326**(5957): 1275-1279.

Origone, P., S. Verdiani, M. Bandettini Di Poggio, R. Zuccarino, M. Vignolo, C. Caponnetto and P. Mandich (2015). "A novel Arg147Trp MATR3 missense mutation in a slowly progressive ALS Italian patient." Amyotroph Lateral Scler Frontotemporal Degener **16**(7-8): 530-531.

Osman, A. M. and H. van Loveren (2014). "Matrin 3 co-immunoprecipitates with the heat shock proteins glucose-regulated protein 78 (GRP78), GRP75 and glutathione S-transferase π isoform 2 (GST π 2) in thymoma cells." Biochimie **101**: 208-214.

Paine, P. L. (1975). "Nucleocytoplasmic movement of fluorescent tracers microinjected into living salivary gland cells." J Cell Biol **66**(3): 652-657.

Palmio, J., A. Evila, A. Bashir, F. Norwood, K. Viitaniemi, A. Vihola, S. Huovinen, V. Straub, P. Hackman, M. Hirano, K. Bushby and B. Udd (2016). "Re-evaluation of the phenotype caused by the common MATR3 p.Ser85Cys mutation in a new family." J Neurol Neurosurg Psychiatry **87**(4): 448-450.

Park, S. and J. Lee (2011). "Proteome profile changes in SH-SY5y neuronal cells after treatment with neurotrophic factors." Journal of Cellular Biochemistry **112**(12): 3845-3855.

Petosa, C., G. Schoehn, P. Askjaer, U. Bauer, M. Moulin, U. Steuerwald, M. Soler-Lopez, F. Baudin, I. W. Mattaj and C. W. Muller (2004). "Architecture of CRM1/Exportin1 suggests how cooperativity is achieved during formation of a nuclear export complex." Mol Cell **16**(5): 761-775.

Pratt, A. J., E. D. Getzoff and J. J. Perry (2012). "Amyotrophic lateral sclerosis: update and new developments." Degener Neurol Neuromuscul Dis **2012**(2): 1-14.

Przygodzka, P., J. Boncela and C. S. Cierniewski (2011). "Matrin 3 as a key regulator of endothelial cell survival." Experimental Cell Research **317**(6): 802-811.

Quaresma, A. J., R. Sievert and J. A. Nickerson (2013). "Regulation of mRNA export by the PI3 kinase/AKT signal transduction pathway." Mol Biol Cell **24**(8): 1208-1221.

Quintero-Rivera, F., Q. J. Xi, K. M. Keppler-Noreuil, J. H. Lee, A. W. Higgins, R. M. Anchan, A. E. Roberts, I. S. Seong, X. Fan, K. Lage, L. Y. Lu, J. Tao, X. Hu, R.

Berezney, B. D. Gelb, A. Kamp, I. P. Moskowitz, R. V. Lacro, W. Lu, C. C. Morton, J. F. Gusella and R. L. Maas (2015). "MATR3 disruption in human and mouse associated with bicuspid aortic valve, aortic coarctation and patent ductus arteriosus." Hum Mol Genet **24**(8): 2375-2389.

Rabut, G., P. Lenart and J. Ellenberg (2004). "Dynamics of nuclear pore complex organization through the cell cycle." Curr Opin Cell Biol **16**(3): 314-321.

Rajgor, D., J. G. Hanley and C. M. Shanahan (2016). "Identification of novel nesprin-1 binding partners and cytoplasmic matrin-3 in processing bodies." Molecular Biology of the Cell **27**(24): 3894-3902.

Rayaprolu, S., S. D'Alton, K. Crosby, C. Moloney, J. Howard, C. Duffy, M. Cabrera, Z. Siemienski, A. R. Hernandez, C. Gallego-Iradi, D. R. Borchelt and J. Lewis (2016). "Heterogeneity of Matrin 3 in the developing and aging murine central nervous system." J Comp Neurol **524**(14): 2740-2752.

Reed, R. and H. Cheng (2005). "TREX, SR proteins and export of mRNA." Current Opinion in Cell Biology **17**(3): 269-273.

Reichelt, R., A. Holzenburg, E. L. Buhle, Jr., M. Jarnik, A. Engel and U. Aebi (1990). "Correlation between structure and mass distribution of the nuclear pore complex and of distinct pore complex components." J Cell Biol **110**(4): 883-894.

Renton, A. E., A. Chio and B. J. Traynor (2014). "State of play in amyotrophic lateral sclerosis genetics." Nat Neurosci **17**(1): 17-23.

Renton, A. E., E. Majounie, A. Waite, J. Simon-Sanchez, S. Rollinson, J. R. Gibbs, J. C. Schymick, H. Laaksovirta, J. C. van Swieten, L. Myllykangas, H. Kalimo, A. Paetau, Y. Abramzon, A. M. Remes, A. Kaganovich, S. W. Scholz, J. Duckworth, J. Ding, D. W. Harmer, D. G. Hernandez, J. O. Johnson, K. Mok, M. Ryten, D. Trabzuni, R. J. Guerreiro, R. W. Orrell, J. Neal, A. Murray, J. Pearson, I. E. Jansen, D. Sondervan, H. Seelaar, D. Blake, K. Young, N. Halliwell, J. B. Callister, G. Toulson, A. Richardson, A. Gerhard, J. Snowden, D. Mann, D. Neary, M. A. Nalls, T. Peuralinna, L. Jansson, V.-M. Isoviita, A.-L. Kaivorinee, M. Holtta-Vuori, E. Ikonen, R. Sulkava, M. Benatar, J. Wuu, A. Chio, G. Restagno, G. Borghero, M. Sabatelli, T. I. Consortium, D. Heckerman, E. Rogaeva, L. Zinman, J. D. Rothstein, M. Sendtner, C. Drepper, E. E. Eichler, C. Alkan, Z. Abdullaey, S. D. Pack, A. Dutra, E. Pak, J. Hardy, A. Singleton, N. M. Williams, P. Heutink, S. Pickering-Brown, H. R. Morris, P. J. Tienari and B. J. Traynor (2011). "A hexanucleotide repeat expansion in C9ORF72 is the cause of chromosome 9p21-linked ALS-FTD." Neuron **72**(2): 257-268.

Rosen, D. R., T. Siddique, D. Patterson, D. A. Figlewicz, P. Sapp, A. Hentati, D. Donaldson, J. Goto, O. R. J.P., H.-X. Deng, Z. Rahmani, A. Krizus, D. McKenna-Yasek,

A. Cayabyab, S. M. Gaston, R. Berger, R. E. Tanzi, J. J. Halperin, B. Herzfeldt, R. Van den Bergh, W.-Y. Hung, T. Bird, G. Deng, D. W. Mulder, C. Smyth, N. G. Laing, E. Soriano, M. A. Pericak-Vance, J. Haines, G. A. Rouleau, J. S. Gusella, H. R. Horvitz and R. H. Brown (1993). "Mutations in Cu/Zn superoxide dismutase gene are associated with familial amyotrophic lateral sclerosis." Nature **362**(March 4): 59-62.

Rossi, S., A. Serrano, V. Gerbino, A. Giorgi, L. Di Francesco, M. Nencini, F. Bozzo, M. E. Schinina, C. Bagni, G. Cestra, M. T. Carri, T. Achsel and M. Cozzolino (2015). "Nuclear accumulation of mRNAs underlies G4C2-repeat-induced translational repression in a cellular model of C9orf72 ALS." J Cell Sci **128**(9): 1787-1799.

Rouquette, J., V. Choesmel and P. E. Gleizes (2005). "Nuclear export and cytoplasmic processing of precursors to the 40S ribosomal subunits in mammalian cells." EMBO J **24**(16): 2862-2872.

Salton, M., R. Elkon, T. Borodina, A. Davydov, M.-L. Yaspo, E. Halperin and Y. Shiloh (2011). "Matrin 3 binds and stabilizes mRNA." PLoS One **6**(8): e23882. doi:23810.21371/journal.pone.0023882.

Salton, M., Y. Lerenthal, S. Y. Wang, D. J. Chen and Y. Shiloh (2010). "Involvement of Matrin 3 and SFPQ/NONO in the DNA damage response." Cell Cycle **9**: 1568-1576.

Savas, J. N., B. H. Toyama, T. Xu, J. R. Yates, 3rd and M. W. Hetzer (2012). "Extremely long-lived nuclear pore proteins in the rat brain." Science **335**(6071): 942.

Segref, A., K. Sharma, V. Doye, A. Hellwig, J. Huber, R. Luhrmann and E. Hurt (1997). "Mex67p, a novel factor for nuclear mRNA export, binds to both poly(A)+ RNA and nuclear pores." EMBO J **16**(11): 3256-3271.

Seiler, C. Y., J. G. Park, A. Sharma, P. Hunter, P. Surapaneni, C. Sedillo, J. Field, R. Algar, A. Price, J. Steel, A. Throop, M. Fiacco and J. LaBaer (2014). "DNASU plasmid and PSI:Biology-Materials repositories: resources to accelerate biological research." Nucleic Acids Res **42**(Database issue): D1253-1260.

Senderek, J., S. M. Garvey, M. Krieger, V. Guergueltcheva, A. Urtizberea, A. Roos, M. Elbracht, C. Stendel, I. Tournev, V. Mihailova, H. Feit, J. Tramonte, P. Hedera, K. Crooks, C. Bergmann, S. Rudnik-Schoneborn, K. Zerres, H. Lochmuller, E. Seboun, J. Weis, J. S. Beckmann, M. A. Hauser and C. E. Jackson (2009). "Autosomal-dominant distal myopathy associated with a recurrent missense mutation in the gene encoding the nuclear matrix protein, matrin 3." Am J Hum Genet **84**(4): 511-518.

Shang, J., T. Yamashita, Y. Nakano, R. Morihara, X. Li, T. Feng, X. Liu, Y. Huang, Y. Fukui, N. Hishikawa, Y. Ohta and K. Abe (2017). "Aberrant distributions of nuclear pore complex proteins in ALS mice and ALS patients." Neuroscience **350**: 158-168.

Sheffield, L. G., H. B. Miskiewicz, L. B. Tannenbaum and S. S. Mirra (2006). "Nuclear pore complex proteins in Alzheimer disease." J Neuropathol Exp Neurol **65**(1): 45-54.
Shevchenko, A., H. Tomas, J. Havlis, J. V. Olsen and M. Mann (2006). "In-gel digestion for mass spectrometric characterization of proteins and proteomes." Nat Protoc **1**(6): 2856-2860.

Shi, K. Y., E. Mori, Z. F. Nizami, Y. Lin, M. Kato, S. Xiang, L. C. Wu, M. Ding, Y. Yu, J. G. Gall and S. L. McKnight (2017). "Toxic PRn poly-dipeptides encoded by the C9orf72 repeat expansion block nuclear import and export." Proc Natl Acad Sci U S A **114**(7): E1111-E1117.

Skowronska-Krawczyk, D., Q. Ma, M. Schwartz, K. Scully, W. Li, Z. Liu, H. Taylor, J. Tollkuhn, K. A. Ohgi, D. Notani, Y. Kohwi, T. Kohwi-Shigematsu and M. G. Rosenfeld (2014). "Required enhancer-matrin-3 network interactions for a homeodomain transcription program." Nature **514**(7521): 257-261.

Sreedharan, J., I. P. Blair, V. Tripathi, X. Hu, C. Vance, B. Rogeli, S. Ackerley, J. C. Durnall, K. L. Williams, E. Buratti, F. Baralle, J. de Belleroche, J. D. Mitchell, P. N. Leigh, A. Al-Chalabi, C. C. Miller, G. Nicholson and C. E. Shaw (2008). "TDP-43 mutations in familial and sporadic amyotrophic lateral sclerosis." Science **319**: 1668-1672.

Stalekar, M., X. Yin, K. Rebolj, S. Darovic, C. Troakes, M. Mayr, C. E. Shaw and B. Rogelj (2015). "Proteomic analyses reveal that loss of TDP-43 affects RNA processing and intracellular transport." Neuroscience **293**: 157-170.

Strasser, K., S. Masuda, P. Mason, J. Pfannstiel, M. Oppizzi, S. Rodriguez-Navarro, A. G. Rondon, A. Aguilera, K. Struhl, R. Reed and E. Hurt (2002). "TREX is a conserved complex coupling transcription with messenger RNA export." Nature **417**(6886): 304-308.

Suhr, S. T., M. C. Senut, J. P. Whitelegge, K. F. Faull, D. B. Cuizon and F. H. Gage (2001). "Identities of sequestered proteins in aggregates from cells with induced polyglutamine expression." J Cell Biol **153**(2): 283-294.

Tada, M., H. Doi, S. Koyano, S. Kubota, R. Fukai, S. Hashiguchi, N. Hayashi, Y. Kawamoto, M. Kunii, K. Tanaka, K. Takahashi, Y. Ogawa, R. Iwata, S. Yamanaka, H. Takeuchi and F. Tanaka (2017). "Matrin 3 is a component of neuronal cytoplasmic inclusions of motor neurons in sporadic amyotrophic lateral sclerosis." The American Journal of Pathology.

Tanackovic, G. and A. Kramer (2005). "Human splicing factor SF3a, but not SF1, is essential for pre-mRNA splicing in vivo." Mol Biol Cell **16**(3): 1366-1377.

Tanackovic, G., A. Ransijn, P. Thibault, S. Abou Elela, R. Klinck, E. L. Berson, B. Chabot and C. Rivolta (2011). "PRPF mutations are associated with generalized defects in spliceosome formation and pre-mRNA splicing in patients with retinitis pigmentosa." Hum Mol Genet **20**(11): 2116-2130.

Teo, G., G. Liu, J. Zhang, A. I. Nesvizhskii, A. C. Gingras and H. Choi (2014). "SAINTexpress: improvements and additional features in Significance Analysis of INTeractome software." J Proteomics **100**: 37-43.

Thomas, F. and U. Kutay (2003). "Biogenesis and nuclear export of ribosomal subunits in higher eukaryotes depend on the CRM1 export pathway." J Cell Sci **116**(Pt 12): 2409-2419.

Topisirovic, I., N. Siddiqui, V. L. Lapointe, M. Trost, P. Thibault, C. Bangeranye, S. Pinol-Roma and K. L. Borden (2009). "Molecular dissection of the eukaryotic initiation factor 4E (eIF4E) export-competent RNP." EMBO J **28**(8): 1087-1098.

Traynor, B. J., M. Alexander, B. Corr, E. Frost and O. Hardiman (2003). "An outcome study of riluzole in amyotrophic lateral sclerosis--a population-based study in Ireland, 1996-2000." J Neurol **250**: 473-479.

Valencia, C. A., W. Ju and R. Liu (2007). "Matrin 3 is a Ca2+/calmodulin-binding protein cleaved by caspases." Biochem Biophys Res Commun **361**(2): 281-286.
van Blitterswijk, M., E. T. Wang, B. A. Friedman, P. J. Keagle, P. Lowe, A. L. Leclerc, L. H. van den Berg, D. E. Housman, J. H. Veldink and J. E. Landers (2013). "Characterization of FUS mutations in amyotrophic lateral sclerosis using RNA-Seq." PLoS One **8**(4): e60788.

Viphakone, N., G. M. Hautbergue, M. Walsh, C. T. Chang, A. Holland, E. G. Folco, R. Reed and S. A. Wilson (2012). "TREX exposes the RNA-binding domain of Nxf1 to enable mRNA export." Nat Commun **3**: 1006.

Wang, P., P. J. Lou, S. Leu and P. Ouyang (2002). "Modulation of alternative pre-mRNA splicing in vivo by pinin." Biochem Biophys Res Commun **294**(2): 448-455.

Ward, M. E., A. Taubes, R. Chen, B. L. Miller, C. F. Sephton, J. M. Gelfand, S. Minami, J. Boscardin, L. H. Martens, W. W. Seeley, G. Yu, J. Herz, A. J. Filiano, A. E. Arrant, E. D. Roberson, T. W. Kraft, R. V. Farese, Jr., A. Green and L. Gan (2014). "Early retinal neurodegeneration and impaired Ran-mediated nuclear import of TDP-43 in progranulin-deficient FTLD." J Exp Med **211**(10): 1937-1945.

Watanabe, M., M. Fukuda, M. Yoshida, M. Yanagida and E. Nishida (1999). "Involvement of CRM1, a nuclear export receptor, in mRNA export in mammalian cells and fission yeast." Genes Cells **4**(5): 291-297.

Weihl, C. C., P. Temiz, S. E. Miller, G. Watts, C. Smith, M. Forman, P. I. Hanson, V. Kimonis and A. Pestronk (2008). "TDP-43 accumulation in inclusion body myopathy muscle suggests a common pathogenic mechanism with frontotemporal dementia." J Neurol Neurosurg Psychiatry **79**(10): 1186-1189.

Wickramasinghe, V. O., M. Stewart and R. A. Laskey (2010). "GANP enhances the efficiency of mRNA nuclear export in mammalian cells." Nucleus **1**(5): 393-396.
Wild, T., P. Horvath, E. Wyler, B. Widmann, L. Badertscher, I. Zemp, K. Kozak, G. Csucs, E. Lund and U. Kutay (2010). "A protein inventory of human ribosome biogenesis reveals an essential function of exportin 5 in 60S subunit export." PLoS Biol **8**(10): e1000522.

Woerner, A. C., F. Frottin, D. Hornburg, L. R. Feng, F. Meissner, M. Patra, J. Tatzelt, M. Mann, K. F. Winklhofer, F. U. Hartl and M. S. Hipp (2016). "Cytoplasmic protein aggregates interfere with nucleocytoplasmic transport of protein and RNA." Science **351**(6269): 173-176.

Writing, G. and A. L. S. S. G. Edaravone (2017). "Safety and efficacy of edaravone in well defined patients with amyotrophic lateral sclerosis: a randomised, double-blind, placebo-controlled trial." Lancet Neurol **16**(7): 505-512.

Xu, L., J. Li, L. Tang, N. Zhang and D. Fan (2016). "MATR3 mutation analysis in a Chinese cohort with sporadic amyotrophic lateral sclerosis." Neurobiol Aging **38**: 218 e213-214.

Xu, T.-R. and M. G. Rumsby (2004). "Phorbol ester-induced translocation of PKC epsilon to the nucleus in fibroblasts: identification of nuclear PKC epsilon-associating proteins." FEBS Letters **570**(1-3): 20-24.

Yamaguchi, A. and K. Takanashi (2016). "FUS interacts with nuclear matrix-associated protein SAFB1 as well as Matrin3 to regulate splicing and ligand-mediated transcription." Sci Rep **6**: 35195.

Yamashita, S., A. Mori, Y. Nishida, R. Kurisaki, N. Tawara, T. Nishikami, Y. Misumi, H. Ueyama, S. Imamura, Y. Higuchi, A. Hashiguchi, I. Higuchi, S. Morishita, J. Yoshimura, M. Uchino, H. Takashima, S. Tsuji and Y. Ando (2015). "Clinicopathological features of the first Asian family having vocal cord and pharyngeal weakness with distal myopathy due to a MATR3 mutation." Neuropathol Appl Neurobiol **41**(3): 391-398.

Yamazaki, F., H. Kim, P. Lau, C. K. Hwang, M. P. Iuvone, D. Klein and S. J. H. Clokie (2014). "pY RNA1-s2: A Highly Retina-Enriched Small RNA That Selectively Binds to Matrin 3 (Matr3)." PLoS ONE **9**(2).

Yang, J., H. P. Bogerd, P. J. Wang, D. C. Page and B. R. Cullen (2001). "Two closely related human nuclear export factors utilize entirely distinct export pathways." Mol Cell **8**(2): 397-406.

Yedavalli, V. S. R. K. and K.-T. Jeang (2011). "Matrin 3 is a co-factor for HIV-1 Rev in regulating post-transcriptional viral gene expression." Retrovirology **8**(61): doi:10.1186/1742-4690-1188-1161.

Yi, R., Y. Qin, I. G. Macara and B. R. Cullen (2003). "Exportin-5 mediates the nuclear export of pre-microRNAs and short hairpin RNAs." Genes Dev **17**(24): 3011-3016.

Zeitz, M. J., K. S. Malyavantham, B. Seifert and R. Berezney (2009). "Matrin 3: chromosomal distribution and protein interactions." J Cell Biochem **108**(1): 125-133.

Zhang, K., C. J. Donnelly, A. R. Haeusler, J. C. Grima, J. B. Machamer, P. Steinwald, E. L. Daley, S. J. Miller, K. M. Cunningham, S. Vidensky, S. Gupta, M. A. Thomas, I. Hong, S.-L. Chiu, R. L. Huganir, L. W. Ostrow, M. J. Matunis, J. Wang, R. Sattler, T. E. Lloyd and J. D. Rothstein (2015). "The C9orf72 repeat expansion disrupts nucleocytoplasmic transport." Nature **525**(7567): 56-61.

Zhang, Y. J., T. F. Gendron, J. C. Grima, H. Sasaguri, K. Jansen-West, Y. F. Xu, R. B. Katzman, J. Gass, M. E. Murray, M. Shinohara, W. L. Lin, A. Garrett, J. N. Stankowski, L. Daughrity, J. Tong, E. A. Perkerson, M. Yue, J. Chew, M. Castanedes-Casey, A. Kurti, Z. S. Wang, A. M. Liesinger, J. D. Baker, J. Jiang, C. Lagier-Tourenne, D. Edbauer, D. W. Cleveland, R. Rademakers, K. B. Boylan, G. Bu, C. D. Link, C. A. Dickey, J. D. Rothstein, D. W. Dickson, J. D. Fryer and L. Petrucelli (2016). "C9ORF72 poly(GA) aggregates sequester and impair HR23 and nucleocytoplasmic transport proteins." Nat Neurosci **19**(5): 668-677.

Zhang, Z. and G. G. Carmichael (2001). "The fate of dsRNA in the nucleus: a p54(nrb)-containing complex mediates the nuclear retention of promiscuously A-to-I edited RNAs." Cell **106**: 465-475.